FOSSIL ENERGY

DOE/BC/15108-6
(OSTI ID: 790184)

NOVEL CO_2-THICKENERS FOR IMPROVED MOBILITY CONTROL

Final Report
October 1, 1998-September 30, 2001

By:
Dr. Robert M. Enick, University of Pittsburgh
Dr. Eric J. Beckman, University of Pittsburgh
Dr. Andrew Hamilton, Yale University

Date Published: January 2002

Work Performed Under Contract No. DE-AC26-98BC15108

University of Pittsburgh
Pittsburgh, Pennsylvania

National Energy Technology Laboratory
National Petroleum Technology Office
U.S. DEPARTMENT OF ENERGY
Tulsa, Oklahoma

DOE/BC/15108-6
Distribution Category UC-122

Novel CO_2-Thickeners for Improved Mobility Control

By
Dr. Robert M. Enick
Dr. Erick J. Beckman
Dr. Andrew Hamilton

January 2002

Work Performed Under DE-AC26-98BC15108

Prepared for
U.S. Department of Energy
Assistant Secretary for Fossil Energy

Dan Ferguson, Project Manager
National Petroleum Technology Office
P.O. Box 3628
Tulsa, OK 74101

Prepared by
Department of Chemical and Petroleum Engineering
University of Pittsburgh
1249 Benedum Engineering Hall
Pittsburgh, PA 15261

Chemistry Department
Yale University
2250 Prospect Ave.
New Haven, CT 06520-8107

Table of Contents

Abstract

The first carbon dioxide thickeners have been successfully designed. Each thickener is characterized by a highly carbon dioxide-philic functionality that imparts CO_2-solubility and a carbon dioxide-phobic group that facilitates viscosity-enhancing intermolecular associations. The design of each thickener required that appropriate balance of these groups to yield a compound that was at least several weight percent soluble in CO_2 and capable of thickening the carbon dioxide by a factor of 2-20.

Four types of thickeners were identified, fluoroacrylate-styrene copolymers (polyFAST), fluorinated telechelic ionomers, semi-fluorinated trialkyltin fluorides and small, fluorinated hydrogen-bonding compounds. Although significant viscosity increases (e.g. doubling the viscosity) were evidenced for each thickener during falling cylinder viscometry analysis, the polyFAST thickener provided the most dramatic increases at dilute concentration.

PolyFAST is a bulk-polymerized, random copolymer of fluoroacrylate and styrene with a number-average molecular weight of about 500,000. It appears as a white, slightly waxy solid at ambient conditions. The fluoroacrylate enhances the CO_2 solubility, while the styrene promotes intermolecular stacking of the aromatic groups. Although concentrations between 20-29 mol% styrene yield a thickener, the optimal composition of polyFAST for thickening was 29mol% styrene and 71mol% fluoroacrylate. Mobility measurements with a Berea sandstone core indicated that at a superficial velocity of one foot per day, a 0.5wt% concentration of 29%styrene – 71%fluoroacrylate polyFAST tripled the viscosity. At concentrations of 1% and 1.5wt%, the CO_2 viscosity increased by a factor of 8 and 19, respectively. If lower proportions of styrene are used, the compound will dissolve more readily in carbon dioxide but the viscosity enhancement will diminish. At higher proportions of styrene, the CO_2 solubility decreases and the thickening capability also decreased, apparently due to the increased number of non-viscosity enhancing *intra*molecular interactions between the aromatic groups.

The high price, environmental persistence, and lack of availability of bulk amounts of the fluoroacrylate monomer guided our final efforts of this work (and all of our efforts in its continuation) toward the development of inexpensive non- fluorous compounds. We have therefore initiated the design highly CO_2 soluble polymers that can replace the fluoroacrylate. These hydrocarbon-based CO_2-philic compounds will then be incorporated into the structure of a compound that contains CO_2-phobic associating groups, yielding a commercial thickener.

Executive Summary

The objective of this contract was to design, synthesize, and characterize thickening agents for dense carbon dioxide and to evaluate their solubility and viscosity-enhancing potential in CO_2. The first carbon dioxide thickeners that were effective at concentrations of about 1wt% and did *not* require a co-solvent to attain *dissolution were successfully designed.* Solubility in carbon dioxide was determined using standard, non-sampling, high pressure phase behavior measurements in a windowed cell. Pressure required to achieve dissolution was comparable to the MMP as estimated by previously published correlations. Viscosity was determined using two techniques. Falling cylinder viscometry was used for all of the potential thickeners because these tests could be conducted rapidly in the same cell used for the phase behavior tests. Mobility measurements were also used to assess viscosity enhancement by measuring the pressure drop across a 100 md Berea sandstone for thickened CO_2 flowing at superficial velocities of 1-100 ft/day.

The fluoroacrylate-styrene copolymer, polyFAST, is the first associative thickener that has been identified for carbon dioxide. Fluoroacrylate is highly carbon dioxide-philic, enhancing the solubility of polyFAST in carbon dioxide. Styrene is relatively carbon dioxide-phobic, but promotes viscosity-enhancing, intermolecular associations. The polyFAST copolymer used in this study had a composition of 29 mol% styrene - 71 mol% fluoroacrylate, a number-average molecular weight of 540,000 and a polydispersity index of 1.63. Carbon dioxide density values of 0.65-0.85 g/cc were required to dissolve 0.25-2.0wt% polyFAST in the 298 – 373 K temperature range. Falling cylinder viscometry measurements at 298 K demonstrated that the viscosity enhancement of CO_2 associated with polyFAST increased with increasing polyFAST concentration, decreasing shear rate and decreasing temperature. The non-Newtonian falling cylinder viscometry results at 298 K were fit to a power law model with copolymer concentration-dependent coefficients. Mobility measurements of polyFAST-CO_2 solutions flowing through 80-200 md Berea sandstone cores at superficial velocities of 0.00035 – 0.028 m/s (1 - 80 ft/day) at 298 K also indicated that polyFAST was an effective thickener. At a superficial velocity of 0.00035m/s (1ft/day), 1.5wt% polyFAST increased the CO_2 viscosity by a factor of 19 relative to neat CO_2. Smaller increases in viscosity occurred at lower polyFAST concentrations and higher velocities.

Semi-fluorinated trialkyltin fluorides and fluorinated telechelic ionomers were soluble to at least several weight percent in dense liquid carbon dioxide without the use of a cosolvent. Increases in solution viscosity at 297 K were measured using falling cylinder viscometry. The viscosity of liquid carbon dioxide was increased by a factor of 2-3 at thickener concentrations of 2-4 wt%. These results demonstrated that carbon dioxide viscosity enhancement is possible without the need for a co-solvent by designing a compound with the appropriate balance of CO_2-philic groups for solubility and CO_2-phobic associating groups for macromolecular, viscosity-enhancing interactions. Neither compound, however, was as effective as the (29% styrene - 71% fluoroacrylate) copolymer we recently developed. More substantial increases in solution viscosity were not attained with the semi-fluorinated trialkyltin fluoride because the fluorinated alkyl chains disrupted the associations that formed viscosity-enhancing, weakly associating, linear polymers. The viscosity increases obtained with the telechelic ionomer were also less than expected due to the relatively low molecular weight of the carbon dioxide-soluble ionomers. Higher molecular weight ionomers would not be CO_2-soluble, however.

We evaluated the solubility and viscosity enhancing ability of both fluorinated aspartate bisureas and ureas. All samples were soluble in supercritical carbon dioxide at temperatures below 100^0C and at pressures below 7,000 psi. The fluoroether functionality was more CO_2-philic than fluoroalkyl

functionality, making the fluoroether bisureas and ureas more soluble in carbon dioxide. However, the much longer fluoroether chain greatly decreased the concentration of associative urea groups, leading to little solution viscosity increase. The ureas were less polar than the corresponding bisureas and were more soluble in carbon dioxide. By increasing the CO_2-philicity of the molecular structure other than the fluorinated tail, fluoroalkyl ureas became more soluble in carbon dioxide. The existence of phenyl group decreased the urea solubility, proving that aryl groups are CO_2-phobic. The relative solubility for our bisureas and ureas are generally: Fluoroether "tail" bisureas/ureas > Fluoroalkyl ureas > Fluoroalkyl bisureas and for fluoroalkyl "tail" urea series, the CO_2-philicity of R groups follows: 3,5-$(CF_3)_2$-phenyl > ethyl methacrylate > hexyl > *p*-CF_3-phenyl, *p*-F-phenyl, phenyl. The CO_2 solubility of the corresponding ureas follows the same trend. 3,5-$(CF_3)_2$-phenyl urea, ethyl methacrylate urea and hexyl urea were soluble in carbon dioxide at room temperature and pressure below 5,000 psi. Their solution viscosity was increased by 1.1~1.6 times at concentrations below 6.0wt%. Low-density microcellular materials can be generated from these fluorinated bisurea and urea solutions in carbon dioxide. Generally, the foamed networks exhibited cell sizes smaller than 10 μm with densities lower than 0.09 g/cm^3 except for the compact networks formed out of carbon dioxide solution. For both bisureas and ureas, there exists a threshold concentration, above which a monolith network can be formed that filled the whole sample cell (~25ml). The concentration of the hydrogen bonding urea groups is the key parameter that controls the formation of such network. Phenyl group may provide additional intermolecular association through π-π stacking, leading to more rigid network. Less CO_2-phobic R groups such as 3,5-$(CF_3)_2$-phenyl and ethyl methacrylate may promote interactions between the associated urea networks and carbon dioxide, resulting in more cells with smaller cell sizes.

Dr. Hamilton and co-workers in the Chemistry Dept. of Yale University synthesized small organic molecules that can gel a variety of solvents including CO_2, freons and perfluorinated solvents at low concentrations. The morphologies of these gels depend on concentration and molecular structure, but are in most cases fibrillar. In the case of the perfluorinated derivatives, upon removal of the CO_2, these gels produce free-standing foams with cells with an average diameter smaller than 1 micrometer and a bulk density reduction of 97% relative to the parent material. They believe the structures are held together by hydrogen bonding of the bis-urea groups. However, the hydrophobic interactions of the long alkyl chains are indispensable for gel formation. They will continue to make use of this class of compounds and study the hydrogen bonding interactions. Non- fluorous versions will also be made.

The effect of spacer length and number of aromatic rings in the copolymer of aromatic acrylates with fluoroacrylate on CO_2-solubility and viscosity enhancement was also studied in an attempt to understand and enhance the performance of these types of copolymer thickeners. The solubility of CO_2-phobic polymers was attained in CO_2 by incorporation of CO_2-philic fluoroacrylate monomer. Presence of a carbonyl group in the body of CO_2-phobic monomer affected the solubility in a favorable manner. Although they both are CO_2-phobic, the presence of aromatic rings instead of alkyl chain favors dissolution due to their strong quadrupole-quadrupole interactions with CO_2. Furthermore, location of phase behavior curve was a strong function of content of CO_2-phobic unit in the copolymer. Success in designing effective CO_2 thickeners in our work was arisen from discovering suitable polymer groups that have the ability to associate in CO_2 without being disturbed by the presence of CO_2 molecules, rather forming stable supramolecular structures. As mentioned before, some studies have also been done with the copolymer of fluoroacrylate with non-aromatic acrylates to verify the strength of association of aromatic rings by stacking. Results designated that some sorts of associations also exist between non-aromatic units, but with the results we have at this point, we are unable to draw the general conclusion.

A successful, commercial thickener must be inexpensive, available in bulk quantities and environmentally benign. Therefore we have initiated the study of non-fluorous thickeners, based only on carbon, hydrogen, oxygen and nitrogen. Our strategy for the development of a thickener involves three steps: the identification of a highly carbon dioxide soluble polymer, devising techniques for increasing the molecular weight of the polymer, and the incorporation of CO_2-phobic, viscosity enhancing groups. We had the opportunity to explore the first step during this research. Our continuation of this research will seek to successfully complete all three steps and design a commercial thickener.

Our preliminary results for the identification of a non-fluorous, CO_2-philic polymer focus on the identification of a CO_2-philic grouip that can replace the fluoroacrylate monomer. Previous investigators have established that homopolymer polypropyleneoxide, PPO, was highly carbon dioxide-soluble. We have found that polyvinylacetate, PVAc, appears to exhibit comparably high carbon dioxide solubility. A copolymer of glycidol and propylene oxide, with a structure that consists of a PPO backbone with pendant acetate groups, exhibited greater solubility in carbon dioxide than either PPO or PVAc. Although this polymer appears to be one of the most carbon dioxide-soluble, non-fluorous polymers yet identified, its CO_2 solubility is less than that of polyfluoroacrylate. Initial efforts to develop non-fluorous, small, hydrogen bonding compounds at the University of Pittsburgh were unsuccessful. Although carbon dioxide-philic tails of di(ethylene glycol), di(propylene glycol) and poly(propylene glycol) were used to replace the fluoroalkyl tails, the resultant triurea compounds was not soluble in carbon dioxide. Yale University is also developing non-fluorous, hydrocarbon-based, hydrogen bonding CO_2 thickeners. Currently, their efforts are focused on the incorporation of oligocarbonate tails in the structure, rather than fluoroalkyl groups.

Ch 1. Thickening Carbon Dioxide with the Fluoroacrylate-Styrene Copolymer

SPE 71497

Jianhang Xu, Robert M. Enick/Department of Chemical and Petroleum Engineering, University of Pittsburgh

This paper was prepared for presentation at the 2001 SPE Annual Technical Conference and Exhibition held in New Orleans, Louisiana, 30 September–3 October 2001.

Abstract

The fluoroacrylate-styrene copolymer, polyFAST, is the first associative thickener that has been identified for carbon dioxide. Fluoroacrylate is highly carbon dioxide-philic, enhancing the solubility of polyFAST in carbon dioxide. Styrene is relatively carbon dioxide-phobic, but promotes viscosity-enhancing, intermolecular associations. The polyFAST copolymer used in this study had a composition of 29 mol% styrene - 71 mol% fluoroacrylate, a number-average molecular weight of 540,000 and a polydispersity index of 1.63. Carbon dioxide density values of 0.65-0.85 g/cc were required to dissolve 0.25-2.0wt% polyFAST in the 298 – 373 K temperature range. Falling cylinder viscometry measurements at 298 K demonstrated that the viscosity enhancement of CO_2 associated with polyFAST increased with increasing polyFAST concentration, decreasing shear rate and decreasing temperature. The non-Newtonian falling cylinder viscometry results at 298 K were fit to a power law model with copolymer concentration-dependent coefficients. Mobility measurements of polyFAST-CO_2 solutions flowing through 80-200 md Berea sandstone cores at superficial velocities of 0.00035 – 0.028 m/s (1 - 80 ft/day) at 298 K also indicated that polyFAST was an effective thickener. At a superficial velocity of 0.00035m/s (1ft/day), 1.5wt% polyFAST increased the CO_2 viscosity by a factor of 19 relative to neat CO_2. Smaller increases in viscosity occurred at lower polyFAST concentrations and higher velocities.

Introduction

The mobility ratio of carbon dioxide floods is unfavorable because the viscosity of CO_2 is low relative to the oil being displaced. A more favorable mobility ratio would result in an increased amount of oil recovery prior to CO_2 breakthrough and increased rate of oil recovery thereafter. Water-alternating-gas

injection is typically used to improve the mobility ratio by decreasing the relative permeability of the carbon dioxide. Alternatively, the mobility ratio could be improved if the viscosity of carbon dioxide was increased. The use of "thickened" CO_2 would also eliminate the need for the co-injection of water.

The identification of a compound capable of dramatically increasing the viscosity of carbon dioxide when present in dilute solution has been an elusive goal, however. The primary obstacle has been the extremely low CO_2-solubility of candidate thickeners unless a substantial amount of co-solvent (e.g. 15% toluene) was added. DeSimone and coworkers were the first to demonstrate that poly(1,1-dihydro-perfluorooctylacrylate), PFOA, exhibited remarkably high CO_2 solubility[1]. Falling cylinder viscometry was used to demonstrate that PFOA could also increase the viscosity of CO_2. For example, at 323 K and 34 MPa, the addition of 6.7wt% PFOA to CO_2 resulted in an increase of viscosity from 0.2 mPas to 0.6 mPas. Although the level of viscosity enhancement was promising, the shear rate of the measurement was not provided and the concentration of PFOA was high[1].

Enick and coworkers designed, synthesized and evaluated several fluorinated associative thickeners. The fluoroalkyl, fluoroether and fluoracrylate functional groups in these compounds imparted CO_2-philicity to the candidate thickening agent. The hydrocarbon, polar or ionic groups in the thickener enhanced intermolecular associations. These intermolecular associations led to the formation of macromolecular structures in solution that are capable of inducing viscosity increases or gelation when present in dilute concentration. Candidates included small fluorinated hydrogen-bonding compounds[2], semifluorinated trialkyltin fluorides[3], fluorinated telechelic ionomers[3], fluoroacrylate homopolymers[3,4], fluoroacrylate-hydrocarbon copolymers[4] and partially sulfonated fluoroacrylate-styrene copolymers[4]. Modest increases in carbon dioxide viscosity at 298 K were detected via falling cylinder viscometry for the small hydrogen bonding compounds, semifluorinated trialkyltin fluorides and fluorinated telechelic ionomers. The fluorinated homopolymer and copolymers (PFOA, polyfluoroacrylate-hexylacrylate, polyfluoroacrylate-(2-(dimethylamino)ethylacrylate), and polyfluoroacrylate-hexylacrylate) also yielded modest increases in viscosity. The polyFAST copolymer and its slightly sulfonated analogs induced tremendous increases in viscosity, however[4]. Unlike all of the other polymers, polyFAST contained an aromatic component. It was postulated that the pendent phenyl groups associated with the styrene interacted with the phenyl group of a neighboring polyFAST via ð-ð stacking[5]. Stacking of aromatic rings is attributed to delocalization of electrons on the carbon atoms of ring and slight residual positive charge on the hydrogen atoms. The hydrogen atoms are attracted to the more electron rich carbon atoms to give T-shaped arrangement (the aromatic rings stack normal to one another, forming a "T" shape when viewed on edge)[5]. The optimal composition of polyFAST was 71mol%fluoroacrylate and 29mol%styrene. Compositions with greater amounts of styrene were more difficult to dissolve and caused smaller viscosity increases due to more intramolecular, rather than intermolecular, ð-ð stacking. Compositions with less styrene were more soluble in CO_2, but were somewhat less effective as thickeners.

Objective

The use of an associative thickener to reduce the mobility of carbon dioxide flowing through porous media has not previously been determined. Therefore the objective of the current work was to determine whether polyFAST would be sufficiently soluble in CO_2 in the 298 K – 373 K temperature range to decrease the mobility of carbon dioxide flowing through sandstone. Viscosity was initially estimated with a falling cylinder viscometer, and aluminum cylinders of varying diameter were used to

define the non-Newtonian characteristics of the thickened CO_2 over a wide range of shear rates. The mobility of thickened CO_2 flowing through Berea sandstone cores at superficial velocities of 0.00035 – 0.028m/s (1-80 ft/day) was then determined.

Experimental

PolyFAST Synthesis

Styrene [Aldrich, 99+%] was purified under vacuum distillation. 3,3,4,4,5,5,6,6,7,7,8,8,9,9,10,10,10-heptadecafluorodecyl acrylate [Aldrich, 97%] was used after the inhibitor, 100 ppm monomethyl ether hydroquinone, was removed by adding the monomer dropwise to an inhibitor removal column. Bulk, free radical polymerization, with AIBN as initiator, was used to obtain a random copolymer product, Figure 1.

In a typical synthesis of the 71%fluoroacrylate, 29% styrene copolymer, 0.82 g (0.007873 mol) styrene, 10.00 g (0.01929 mol) fluoroacrylate, and $8.93*10^{-3}$ g ($5.44*10^{5}$ mol) of AIBN were added to a 50 ml glass ampule under an inert N_2 atmosphere. The ampule was sealed and placed in an oil bath at 338 K for 12 hours to promote polymerization. The reaction products were then dissolved in 100 g 1,1,2-trichlorotrifluoroethane. The copolymer was then precipitated by washing with 300 g methanol, while the unreacted monomer remained in solution. The copolymer product, a white solid, was recovered by filtration. The copolymer was washed two additional times in a similar manner and dried under vacuum overnight. The yield was 85%.

Solubility Apparatus

The phase behavior studies of CO_2-polyFAST mixtures at 298 – 373 K were performed using the apparatus illustrated in Figure 2. Phase behavior measurements were conducted in a high pressure, variable-volume, windowed cell (D. B. Robinson Cell), rated to 69 MPa and 478 K. A thick-walled hollow quartz cylinder was inserted in the high pressure windowed cell. A floating piston in the hollow cylinder isolated the sample volume from the overburden fluid below the piston and surrounding the tube. Standard, non-sampling techniques were employed to determine copolymer solubility[2,3,4]. Specified amounts of the polyFAST and CO_2 were introduced to the sample volume. The mixture was then heated to the specified temperature and compressed to 45 MPa. Mixing was achieved by rocking the cell until a single, transparent phase was obtained. The sample volume was then slowly expanding by withdrawing the overburden fluid at a constant rate until the copolymer began to precipitate. This pressure corresponded to the cloud point pressure of the mixture of known overall composition. This procedure was repeated for polyFAST concentrations up to 5wt%.

Falling Cylinder Viscometry

The simplest test for estimating high-pressure fluid viscosity using the apparatus shown in Figure 2 was falling object viscometry[3,4]. Single phase solutions of polyFAST in CO_2 were prepared at 298 K and 34 MPa. An aluminum cylinder was placed within the sample volume of hollow quartz tube. Rapid inversion of the high pressure cell enabled the fall of the aluminum cylinder through the thickened CO_2 to be observed, Figure 3. Cylinders with an outer diameter slightly less than the inside diameter of the quartz tube were used, Table 1, thereby reducing the terminal velocity of the falling cylinder and minimizing the acceleration length required for the cylinder to attain its terminal velocity. The pressure

equilibration across the walls of the quartz tube eliminated the possibility of any change in the dimensions of the tube under high pressure conditions.

The viscosity and shear rate can be determined for Newtonian fluids given the geometry of the system, the density of the fluid and falling cylinder and the terminal velocity[6]. Multiple cylinders must be used to characterize non-Newtonian fluids[7]. Because the terminal velocity was sensitive to extremely small variations in the diameter of the falling cylinder or the piston, the viscometer was calibrated with neat CO_2.

The aluminum cylinder was introduced to the cell prior to the addition of the copolymer and the carbon dioxide.
The pressure was then increased above the cloud point, yielding a single, transparent phase within the sample volume. The entire high pressure cell was then rapidly inverted, Figure 3, causing the aluminum cylinder to fall through the neat or thickened carbon dioxide. The time required for the cylinder to fall a specified distance, 2-10cm, was then recorded. Each measurement was repeated five times. These measurements indicated that the cylinder attained its terminal velocity within several millimeters.

The falling cylinder results provided a convenient measure of the change in the fluid viscosity. During the initial screening of thickeners, the solution was assumed to be Newtonian.

$$\tau = -\mu \frac{dV_z}{dr} \qquad 1$$

Consider the aluminum cylinder falling through a dilute polymer solution that is considered to be a Newtonian fluid. The governing expression for a falling cylinder viscometer under these conditions is provided in equation 2.

$$\mu = C \frac{(\rho_c - \rho_f)}{V_c} \qquad 2$$

The viscometer constant, C, can be theoretically determined from the viscometer geometry[6] or experimentally determined by calibrating the viscometer with neat CO_2. The density of CO_2 was estimated with a precise equation of state[8]. The density of the thickened carbon dioxide was assumed to be comparable to the density of neat carbon dioxide because the concentration of the copolymer was relatively low, and the same cylinder was used when comparing neat CO_2 to thickened CO_2. Under these constraints for a Newtonian fluid, the ratio of the viscosity of thickened CO_2 to the viscosity of neat CO_2 was equal to the ratio of the terminal velocity in neat CO_2 to the terminal velocity in thickened CO_2.

$$\frac{\mu_{solution}}{\mu_{CO2}} = \frac{V_{c,CO2}}{V_{c,polyFASTsdution}} \qquad 3$$

The viscosity of the CO_2-polyFAST solutions was also modeled using a power law expression, providing a more accurate representation of the non-Newtonian nature of the solution. (Note that if non-Newtonian fluid approaches the Newtonian behavior, n approaches unity as m approaches ì.)

$$\tau = -m \left| \frac{dV_z}{dr} \right|^{n-1} \frac{dV_z}{dr} = -\eta \frac{dV_z}{dr} \qquad 4$$

The relative increase in the viscosity of carbon dioxide exhibited by the non-Newtonian polyFAST solution was defined as the following ratio[9]

$$\frac{\eta_{polyFASTsdution}}{\mu_{CO2}} \qquad 5$$

Flow Through Porous Media

The most accurate and relevant viscosity measurements were obtained by displacing the high pressure fluid through sandstone. A core holder rated to 100 MPa [Temco] was used to retain the 15.24 cm long, 2.54 cm diameter, clean, homogeneous Berea sandstone core [80-200md, American Stone]. The core sample was retained within a rubber sleeve, which had two pressure taps that permitted pressure measurements to be made 5.08 cm and 10.16 cm from the inlet face of the core. Neat CO_2 and thickened CO_2 were prepared in the Robinson cell at 298 K and 20 MPa to ensure a single phase of polyFAST-CO_2 solution at 298 K was attained. The radial overburden pressure of silicone oil was maintained at 23.5 MPa with a positive displacement pump [Ruska]. A dual positive-displacement proportioning pump [Ruska] was used to ensure that the fluid (CO_2 or thickened CO_2) was displaced into the core at the same rate that the volume for the effluent fluid from the core was expanded. High total pressure, low pressure drop differential pressure transducers [Validyne Engineering Co., DP303] were used to monitor the pressure drop along each third of the core.

Each core was initially saturated with neat carbon dioxide. Carbon dioxide was then displaced through the core, followed by 80-90 cm^3 of thickened carbon dioxide. Fluid viscosity was determined by rearranging Darcy's Law to solve for viscosity.

$$\mu = \frac{\Delta P}{L}\frac{K}{v} \qquad 6$$

The pressure drop measurement associated with the flow of neat carbon dioxide was used to determine the core permeability. Using this permeability value, the pressure drop associated with the flow of the thickened carbon dioxide was used to determine its viscosity. Because the same core was used for the experiments with neat CO_2 and thickened CO_2, the ratio of the viscosity of thickened CO_2 to neat CO_2 was estimated as the ratio of the respective pressure drops along the length of the core.

$$\frac{\mu_{polyFASTsdution}}{\mu_{CO2}} = \frac{(\Delta P/L)_{polyFASTsdution}}{(\Delta P/L)_{CO2}} \qquad 7$$

Results and Discussion

Polymer Characterization

The number-, weight- and Z-average molecular weights, M_n, M_w and M_z, respectively, were determined using gel permeation chromatography [American Polymer Standards Corporation]. These results are presented in Table 2, along with the polydispersity index, PDI, composition and melting point of polyFAST. The PDI is the ratio of M_w to M_n.

Solubility Results

The polyFAST copolymer is soluble in dense carbon dioxide at concentrations up to 5wt% at 298 K, 323 K, 348 K and 373 K, Figure 4. The cloud point curve shifted toward higher pressure with increasing concentration and temperature. The cloud point pressure at any given temperature must be contrasted

with the MMP at the same temperature to establish the solubility of polyFAST at reservoir conditions. One method of estimating the MMP was correlating the density of carbon dioxide with the (C_5-C_{30}) fraction of the crude oil[10]. For example, a CO_2 density of 0.75 g/cc was required to displace oil with a 55% (C_5-C_{30}) fraction, while a CO_2 density of 0.65 g/cc was needed to displace oil with an 67% (C_5-C_{30}) fraction[10]. The MMP was then estimated as the pressure required to attain that density at reservoir temperature.

Figure 5 illustrates isochores superimposed upon the solubility of polyFAST in carbon dioxide. This figure provides a guideline for the amount of polyFAST that can be dissolved at the MMP conditions as estimated by CO_2 density. For example, if the required CO_2 density is 0.75 g/cc and the reservoir temperature is 360 K, then up to 2 wt% polyFAST can be dissolved in the CO_2.

PolyFAST could be modified to become more soluble in CO_2 by reducing its molecular weight and/or reducing it styrene content. These modifications would reduce the thickening capability of the polyFAST, however. Future studies are directed at the design of inexpensive non-fluorous thickeners, rather than further optimizing polyFAST thickener.

Falling Cylinder Viscometer Results

The falling cylinder results for CO_2-rich solutions at 298 K and 34 MPa containing 0.2 – 5.0 wt% polyFAST are presented in Figure 6. Experimental data are provided along with curves that correspond to the power law correlation obtained using the parameters listed in Table 3. The plots of $\eta_{solution}/\mu_{CO2}$ as a function of shear rate illustrate that the polymer solutions are shear thinning in nature, and approach Newtonian behavior with diminishing polyFAST concentration. No discernible increase in viscosity was detected at polyFAST concentrations less than 0.2 wt%. This falling cylinder viscometer was not suited for the study of dilute polyFAST solutions at the very low shear rates associated with creeping flow through porous media (1-10s^{-1}). The results clearly indicate, however, that substantial increases in viscosity can be realized at extremely low shear rates with polyFAST at concentrations of 0.2 wt% or more.

Effect of Temperature on PolyFAST Thickening Capability

PolyFAST is capable of increasing the viscosity because of its high molecular weight and the intermolecular associations of the aromatic groups[5]. Although Figure 6 demonstrated effective thickening at 298 K, reservoir temperatures can be much higher. An increase in temperature may influence the strength and geometry of the stacking of the phenyl groups, which may result in the change of local molecular environment, thereby effecting the π-π stacking of the aromatic groups and the thickening capability of polyFAST. The aluminum cylinder with a diameter of 3.157 cm was used to estimate viscosity. Figure 7 demonstrates that the effectiveness of polyFAST as a thickener at concentrations of 1 and 0.5wt% decreased slightly with increasing temperature in the 298 – 373 K range at 34 MPa.

Measurement of Thickened CO_2 Mobility in Sandstone

The pressure drops along each third of the core were uniform and invariant after the thickened carbon dioxide had saturated the core. Therefore, the pressure drops of the neat and thickened CO_2 in each core

were used to estimate the increase in CO_2 viscosity. This increase in viscosity at 298 K and 20MPa is presented as a function of polyFAST concentration for a constant superficial velocity, Figure 8. These mobility results demonstrate for the first time that it is possible to design a direct carbon dioxide thickening agent. PolyFAST concentrations as low as 0.25wt% were capable of thickening CO_2. Higher polyFAST concentration at a constant superficial velocity led to remarkable increases in viscosity at low superficial velocities. The 1.0 and 1.5wt% polyFAST solutions were 8 and 19 times more viscous than neat CO_2, respectively, at a velocity of 0.00035 m/s (1 ft/day). Because of the shear-thinning nature of polyFAST, increases in superficial velocity led to diminished thickening. For example, the addition of 1.5wt% polyFAST increased the CO_2 viscosity by a factor of only 2 at a superficial velocity of 0.028 m/s (80 ft/day).

Next-Generation Thickeners

Although silicone polymers have been previously used to thicken carbon dioxide, substantial amounts of an organic cosolvent were required[11]. PolyFAST is a *direct* thickener in that it does *not* require a cosolvent. Nonetheless, polyFAST is a highly fluorinated copolymer that is expensive, unavailable in large quantities and environmentally persistent. Rather than continuing to enhance the properties of polyFAST (e.g. adjusting the composition and Mn to attain higher solubility of polyFAST at a specified pressure), a new generation of CO_2 thickeners will be designed. Specifically, our future studies will focus on inexpensive, biodegradable, *non-fluorous* direct thickeners that can be produced in large amounts and do *not* require an organic cosolvent to achieve dissolution. The same strategy used in the development of polyFAST will be employed in the development of the non- fluorous thickener. Novel copolymers composed of carbon, hydrogen, oxygen and nitrogen will be designed to exhibit high CO_2 solubility[12]. CO_2-phobic, associating groups will then be incorporated into the copolymer to impart thickening capabilities. The associating group content of the thickener composition will be adjusted to attain a reasonable balance of CO_2 solubility and thickening capability.

Conclusions

PolyFAST, a 71mol% fluoroacrylate-29mol% styrene random copolymer was synthesized via bulk, free-radical polymerization. This copolymer had a number-average molecular weight of 540,000 and a polydispersity index of 1.63. PolyFAST exhibited remarkably high solubility in dense carbon dioxide, which was attributed to the high fluoroacrylate content of the copolymer. The thickening capability of polyFAST over the 298 – 373 K temperature range was attributed to intermolecular stacking of the aromatic rings associated with the styrene monomer. Falling cylinder viscometry results were used to develop a power law model of the pseudoplastic solutions of polyFAST in CO_2. Pressure drop measurements of polyFAST-CO_2 solutions flowing through Berea sandstone demonstrated that polyFAST could effectively reduce the mobility of carbon dioxide at superficial velocities up to 0.0035m/s (10ft/day). Higher velocities resulted in much smaller reductions in mobility.

Although the composition and MW of polyFAST could be modified to enhance its thickening ability, fluorinated polymers are expensive, unavailable in bulk quantities and environmentally persistent. Therefore, we are currently investigating *non-fluorous* thickeners, which are composed of carbon, hydrogen, oxygen and nitrogen.

Nomenclature

C falling cylinder viscometer constant
K permeability, md
L length, m
m power law model constant
MMP minimum miscibility pressure, Pa
Mn number-average molecular weight, g/mol
Mw weight-average molecular weight, g/mol
Mz Z-average molecular weight, g/mol
n power law model constant
P pressure, Pa
PDI polydispersity index
r r coordinate, m
Tm melting point, K
v superficial velocity, m/s
Vc falling cylinder terminal velocity, m/s
Vz velocity fraction in z direction, m/s
x mole fraction styrene in polyFAST
y mole fraction fluoracrylate in polyFAST
z z coordinate, m
η non-Newtonian fluid viscosity, Pa-sec
μ Newtonian fluid viscosity, Pa-sec
ρ_c cylinder density, g/cm^3
ρ_f fluid density, g/cm^3
τ shear stress, N/m^2

Acknowledgments

The authors would like to express their appreciation to the US DOE National Energy Technology Center for their support of this program through National Petroleum Technology Office contracts DOE-RA26-98BC15108 and DE-FC26-01BC15315. We would also like to thank Bayer, Cabot Oil and Gas and Air Products for their financial support.

References

1. McClain, J.B., Betts, D.E., Canelas, D.A., Samulski, E.T., DeSimone, J.M.: "Characterization of Polymers and Amphiphiles in Supercritical CO_2 using Small Angle Neutron Scattering and Viscometry", Spring Meeting of the ACS, Division of Polymeric Materials Science and Engineering, New Orleans, LA, (1996) 234-235.
2. Shi, C., Huang, Z., Kilic, S., Xu, J., Enick, R., Beckman, E., Carr, A., Melendez, R., Hamilton. A.: " The Gelation of CO_2: A Sustainable Route to the Formation of Microcellular Materials," Science (19 Nov. 1999), **286**, 1540-1543.
3. Shi, C., Huang, Z., Beckman, E., Enick, R., Kim, S. Y., and Curran, D.: "Semi-Fluorinated Trialkyltin Fluorides and Fluorinated Telechelic Ionomers as Viscosity-Enhancing Agents for Carbon Dioxide", Industrial & Engineering Chemistry Research (2001), **40**(3), 908-913.
4. Huang, Z., Shi, C., Xu, J., Kilic, S., Enick, R., Beckman, E.: "Enhancement of the Viscosity of Carbon Dioxide Using Styrene/Fluoroacrylate Copolymers", Macromolecules (2000), **33**, 5437-5442.
5. Weber, E.: *Topics in Current Chemistry: Design of Organic Solids*, Springer, Germany, 1998.
6. Iezzi, A.: M.S. Thesis, University of Pittsburgh, 1989.
7. Ashare, E., Bird, R.B.: "Falling Cylinder Viscometer for non-Newtonian Fluids", AIChEJ (1965), **11**(5), 910-916.
8. Span, R., Wagner, W.: "A New Equation of State for Carbon Dioxide Covering the Fluid Region from the Trile-Point Temperature to 1100 K at Pressures up to 800 MPa," J. Phys. Chem. Ref. Data (1996), **25**(6), 1509-1596.
9. Enick, R., Beckman, E., Hamilton, A.: "Novel CO_2-Thickeners for Improved Mobility Control, Quarterly Report, April 1 – June 30, 2000, DOE-RA26-98BC15018, July, 2000.
10. Holm, L.W. and Josendal, V.A.: "Effect of Oil Composition on Miscible Type Displacement by Carbon Dioxide," SPEJ (Feb. 1982) 87-98.
11. Bae, J., Irani, C.: "A Laboratory Investigation of Thickened CO_2 Process," paper SPE 20467, Sept. 1990.
12. Sarbu, T., Styranec, T., and Beckman E. J.: "Non-fluorous Polymers with Very High Solubility in Supercritical CO_2 Down to Low Pressures", Nature (May 2000), **405**, 165-168.

Table 1. Falling Cylinder Viscometry

Cylinder material	Aluminum
Cylinder specific gravity	2.7 g/cm^3
Cylinder length	2.192 cm
Cylinder #1 diameter	3.162 cm
Cylinder #2 diameter	3.159 cm
Cylinder #3 diameter	3.157 cm
Cylinder #4 diameter	3.149 cm
Cylinder #5 diameter	3.134 cm
Cylinder #6 diameter	3.127 cm
Cylinder #7 diameter	3.122 cm
Cylinder #8 diameter	3.116 cm
Quartz hollow cylinder ID	3.175 cm
Distance traveled by falling cylinder	5~12 cm
Fluid	Neat CO_2 or thickened CO_2

Table 2. Molecular Weight Analysis of PolyFAST

Polymer	PolyFAST (copolymer)
x	0.29
y	0.71
M_n	539600
M_w	880200
M_z	1265000
PDI=M_w/M_n	1.63
T_m (K)	345

Table 3. m and n Values for the PolyFAST-CO_2 Solutions

Wt% of PolyFAST in CO_2	m	N
5	0.272	0.625
3	0.026	0.833
1	0.034	0.714
0.2	0.003	0.909

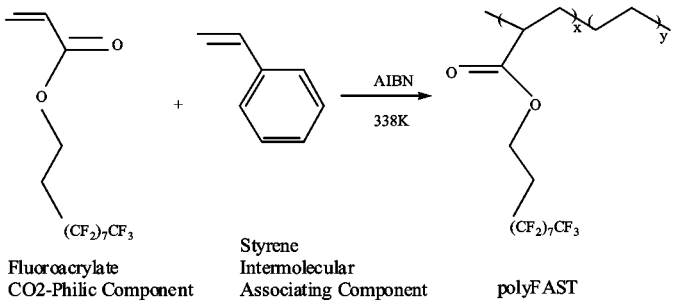

Figure 1. Synthesis of PolyFAST Random Copolymer

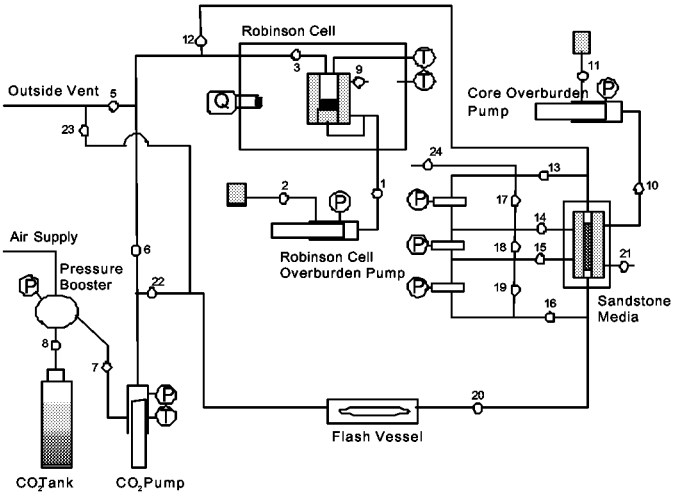

Figure 2. Apparatus for Phase Behavior, Falling Cylinder Viscometry and Mobility Measurements

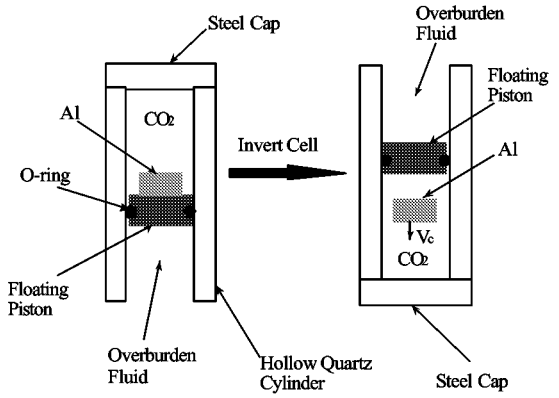

Figure 3. Falling Cylinder Viscometry

Figure 4. Effect of Temperature on the Solubility of polyFAST in Carbon Dioxide

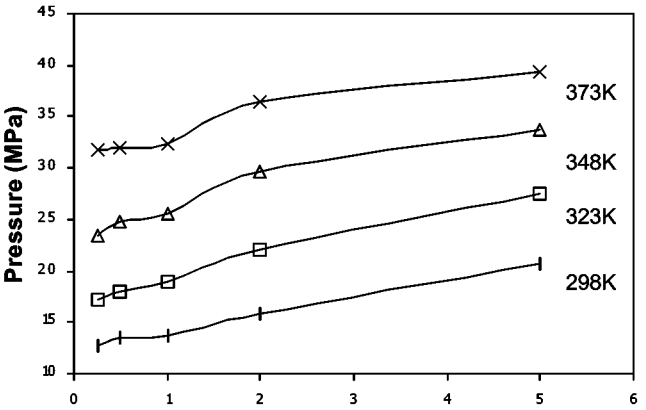

Figure 5. CO2 Density Required to Dissolve PolyFAST

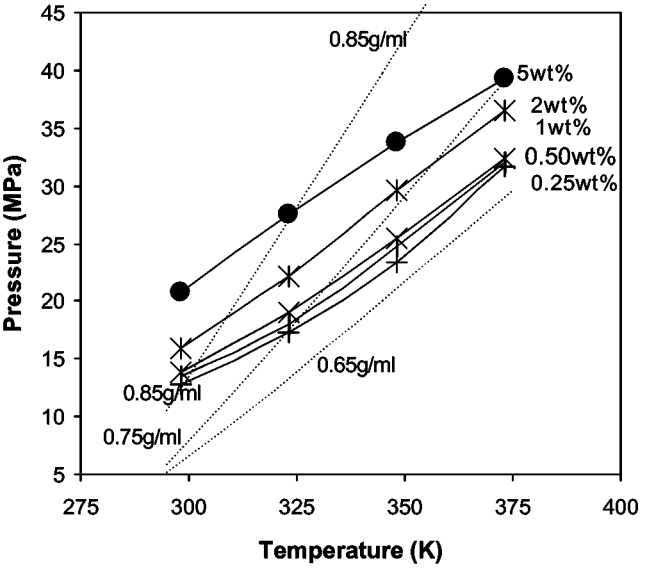

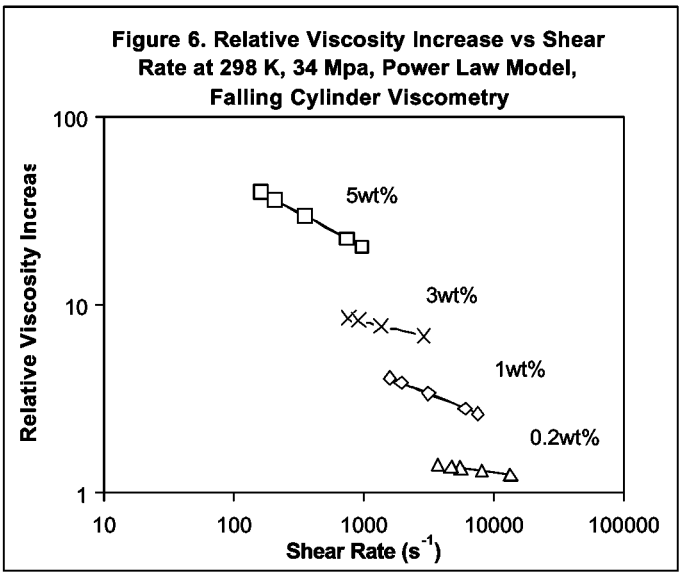
Figure 6. Relative Viscosity Increase vs Shear Rate at 298 K, 34 Mpa, Power Law Model, Falling Cylinder Viscometry
Relative Viscosity Increas
100
10
1
5wt%
3wt%
1wt%
0.2wt%
10
100
1000
10000
100000
Shear Rate (s-1)

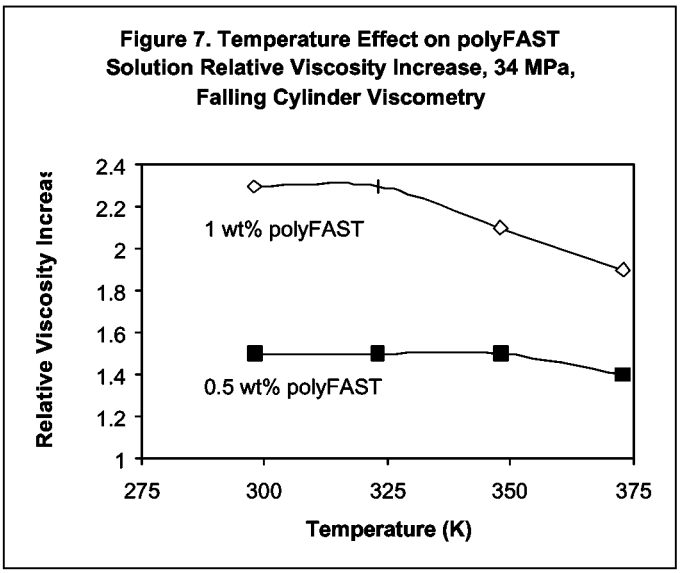
Figure 7. Temperature Effect on polyFAST Solution Relative Viscosity Increase, 34 MPa, Falling Cylinder Viscometry
Relative Viscosity Increas
2.4
2.2
2
1.8
1.6
1.4
1.2
1
1 wt% polyFAST
0.5 wt% polyFAST
275
300
325
350
375
Temperature (K)

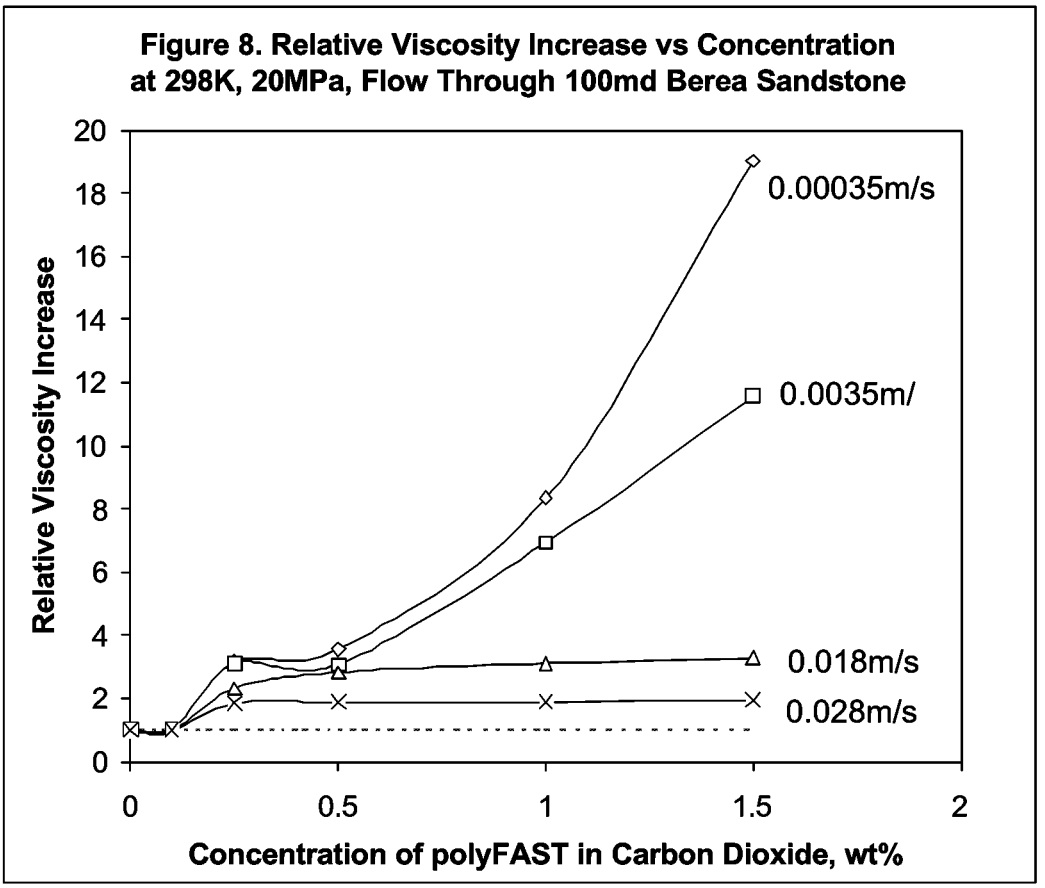
Figure 8. Relative Viscosity Increase vs Concentration
at 298K, 20MPa, Flow Through 100md Berea Sandstone
Relative Viscosity Increase
20
18
16
14
12
10
8
6
4
2
0
0
0.5
1
1.5
2
Concentration of polyFAST in Carbon Dioxide, wt%
0.00035m/s
0.0035m/
0.018m/s
0.028m/s

Ch. 2. Semi-Fluorinated Trialkyltin Fluorides and Fluorinated Telechelic Ionomers as Viscosity-Enhancing Agents for Carbon Dioxide

Chunmei Shi, Zhihua Huang, Eric J. Beckman, Robert M. Enick*

Department of Chemical and Petroleum Engineering
Sun-Young Kim, Dennis P. Curran

Department of Chemistry and Center for Combinatorial Chemistry

University of Pittsburgh, Pittsburgh, PA 15261, U.S.A.

E-mail: enick@engrng.pitt.edu,Fax: (412) 624-9639

Abstract

Direct thickeners for dense carbon dioxide were designed and synthesized. Each thickener contained "CO_2-philic" fluorinated groups to impart solubility in carbon dioxide and "CO_2-phobic" functionalities to promote intermolecular associations for viscosity enhancement. Semi-fluorinated trialkyltin fluorides and fluorinated telechelic ionomers were soluble to at least several weight percent in dense liquid carbon dioxide without the use of a cosolvent. Increases in solution viscosity at 297 K were measured using falling cylinder viscometry. The viscosity of liquid carbon dioxide was increased by a factor of 2-3 at thickener concentrations of 2-4 wt%. These results demonstrated that carbon dioxide viscosity enhancement is possible without the need for a co-solvent by designing a compound with the appropriate balance of CO_2-philic groups for solubility and CO_2-phobic associating groups for macromolecular, viscosity-enhancing interactions. Neither compound, however, was as effective as the (29% styrene - 71% fluoroacrylate) copolymer we recently developed. More substantial increases in solution viscosity were not attained with the semi-fluorinated trialkyltin fluoride because the fluorinated alkyl chains disrupted the associations that formed viscosity-enhancing, weakly associating,

linear polymers. The viscosity increases obtained with the telechelic ionomer were also less than expected due to the relatively low molecular weight of the carbon dioxide-soluble ionomers. Higher molecular weight ionomers would not be CO_2-soluble, however.

Introduction

Carbon Dioxide for Enhanced Oil Recovery After waterflooding a petroleum reservoir, dense CO_2 can be injected into the sandstone or limestone to maintain the reservoir pressure and to displace additional petroleum. During a CO_2 flood, carbon dioxide can dynamically develop effective miscibility with petroleum and can therefore displace oil left behind by waterflooding. The CO_2 is typically introduced at a pressure that yields a carbon dioxide density of about 0.5-0.7 g/cm^3 at a reservoir temperature of 300-400 K. At the production well, CO_2 can be readily separated from the oil by pressure reduction. Other favorable properties of CO_2 such as natural abundance, low cost, non-flammability, low toxicity, and classification as a non-VOC also contribute to make CO_2-flooding an attractive sustainable oil recovery procedure. The foremost disadvantage of CO_2 as an oil displacement fluid is its low viscosity, 0.03-0.10 mPa s (cp) at the reservoir conditions[1]. The oil has a viscosity that varies from 0.1 cp to 50 cp. This results in a much higher CO_2 mobility (the ratio of fluid permeability in porous media to fluid viscosity) than oil mobility. The mobility ratio (CO_2 mobility/oil mobility) is therefore greater than unity, resulting in unfavorable macroscopic flow patterns. CO_2 "fingers" towards the production well, bypassing much of the oil in the reservoir[2], lowering oil production rates and prolonging the life of the oil recovery project. Water is commonly

injected along with carbon dioxide in order to reduce the relative permeability of the carbon dioxide in the porous media, thereby decreasing its mobility. However, this water-alternating-gas strategy extends the duration of the injection of a specified amount of carbon dioxide. Further, the contact of the carbon dioxide and oil more difficult to achieve due to the "shielding" of the oil from the carbon dioxide.

If the CO_2 viscosity could be elevated to a level comparable with the oil it is displacing, the mobility ratio would approach or become less than unity and there would be requirement to inject slugs of water along with the thickened carbon dioxide. Substantial improvements in oil recovery efficiency and production rate could result. The US Department of Energy has estimated that if the viscosity of CO_2 could be tripled or quadrupled, the domestic production rate of oil achieved using CO_2 flooding would increase from 180,000 barrels per day to 400,000 barrels of oil per day (US DOE 2000).

Thickening Carbon Dioxide Most of the previously evaluated CO_2 thickeners were known to thicken or gel hydrocarbon liquids. These compounds included small molecules such as trialkyltin fluorides[3,4], hydroxystearic acid[5], aluminum disoaps[6], and low molecular weight telechelic ionomers[7]. The unique molecular structures of these compounds promoted intermolecular associations in solution and hence significantly increased solution viscosity. High molecular weight polymers, known to increase solution viscosity by chain entanglement[8,9], were also considered as potential CO_2 thickeners. However, due to the extremely low solubility of conventional hydrocarbon thickeners in

CO_2, none rendered a viscosity increase for dense CO_2 unless a substantial amount of organic co-solvent, such as toluene, was introduced.

Research associated with the use of dense CO_2 for sustainable reaction and separation processes resulted in the identification of highly CO_2-soluble molecular structures. These structures were referred to as "CO_2-philic" functional groups, and included fluoroacrylates, fluoroethers, fluoroalkanes and silicones[10-12]. One of these studies reported a significant increase in CO2-rich solution viscosity at a relatively dilute polymer concentration. DeSimone and coworkers observed that poly(1,1-dihydroperfluorooctyl acrylate) (PFOA, MW = $1.4x10^6$) could be polymerized homogeneously in supercritical CO_2. The resultant polymer remained soluble without the need for a cosolvent[13] and at concentrations of 5-10 wt%, the viscosity of CO_2 was increased by a factor of 3-8 at 323 K and a pressure of 200-350 bar.

Polymers with aromatic groups can associate and form regular structures both in solid state and in solution[19]. We recently evaluated a series of fluoroacrylate-styrene copolymers and adjusted the copolymer composition in an attempt to develop a CO_2 thickener. Copolymers of fluoroacrylate and styrene were previously used as stabilizers for dispersion polymerization of styrene in CO_2[20], but we designed a high molecular weight copolymer of optimal composition for thickening carbon dioxide. Some of the copolymer thickeners were sulfonated at the pendant phenyl groups and their solubility and thickening capability were evaluated[21]. The fluoroacrylate-styrene copolymers were

capable of increasing the viscosity of carbon dioxide, as determined with a falling cylinder viscometer, by a factor of 5-400 at a concentration of 1-5 wt%[21].

The objective of this study was to design and synthesize novel direct thickeners for carbon dioxide. We intended to demonstrate that carbon dioxide thickening agents could be developed by balancing CO_2-philic functional groups that promoted CO_2-solubility with CO_2-phobic groups that induced intermolecular associating leading to viscosity enhancement. These associations resulted in the formation of pseudo-polymeric structures in solution, which were capable of causing increases in solution viscosity that would be difficult to attain with random coil polymers[14]. The direct CO_2 thickeners considered in this study were semi-fluorinated trialkyltin fluorides and fluorinated telechelic disulfates.

We recognized that the expense and environmental persistence of these fluorinated thickeners made them impractical for enhanced oil recovery. Yet if were successful in the design of a fluorinated CO_2-thickening agent, we could then attempt to synthesize an inexpensive, non-fluorous, environmentally benign analog that could be used in the oilfield. Therefore this study was not intended to evaluate all of the aspects of a commercial CO_2 thickener, such as water solubility, wettability alterations, near-wellbore formation damage, phase behavior over a wide range of temperature, relative permeability in porous media, mobility in porous media, displacement efficiency and volumetric sweep efficiency. We only desired to identify the types of thickening agents that had the potential to induce very large changes in solution viscosity at dilute

concentrations. (Our future work will focus on the development and evaluation of non-fluorous analogs of these fluorinated thickeners.)

Semi-fluorinated Trialkyltin Fluorides

Tributyltin fluoride has been reported to slowly dissolve in n-hexane. It can increase the solvent viscosity by three orders of magnitude at a concentration of 10 g/L[3]. These remarkable viscosity increases were attributed to transient polymeric chain formation through intermolecular Sn-F bridging. This bridging was caused by the interactions of the electropositive tin atom and the electronegative fluorine atom, as shown in Figure 1[15]. Heller and coworkers systematically studied the solubility and viscosity behavior of various trialkyltin fluorides in Liquefied Petroleum Gas (LPG) and dense CO_2. Despite viscosity enhancement observed for the light alkanes, the solubility of the trialkyltin fluorides in CO_2 did not exceed 0.17 g/100ml and no viscosity increase resulted[16]. Therefore, we designed and synthesized trialkyltin fluorides with fluorinated carbons at each chain end to enhance their solubility in CO_2. These semi-fluorinated trialkyltin fluorides included tris(2-perfluorobutyl ethyl)tin fluoride $(F(CF_2)_4(CH_2)_2)_3SnF$ and tris(3-perfluoromethyl propyl)tin fluoride $(F(CF_2)(CH_2)_3)_3SnF$.

Fluorinated Telechelic Disulfates

Telechelic ionomers, polymers of relatively low molecular weight (<50,000) with end-functionalized ionic groups, have been used to thicken or gel non-polar organic solvents at dilute concentrations (< 5 wt%). Rheological behavior and light scattering studies have indicated that the gel and significant solution viscosity increase of telechelic

ionomers in non-polar solvents resulted from the strong dipolar interactions between the ionic end groups[17,18]. For linear di-functional telechelic ionomers, the ionic groups can aggregate into pairs, multiplets of a few ion pairs or clusters consisting of 30-100 ion pairs. The aggregates form a macromolecular structure in solution, which is manifested as the apparent viscosity increase in solution or gel formation. Heller and coworkers also studied the possibility of using hydrocarbon-based telechelic ionomer as a thickener for dense CO_2 in their evaluation of sulfonated polyisobutylene[7]. This ionomer exhibited extremely low solubility in CO_2, however. Therefore, we synthesized relatively low molecular weight telechelic disulfates from a CO_2-philic fluoroether diol. The molecular weight of the telechelic disulfates were changed by extending the diol with diisocyanates to give a mostly fluorinated CO_2-soluble polyurethane backbone.

Experimental

Synthesis

Samples of each thickener were prepared on a 1-5 gram scale following the procedures described below. Purity was estimated at 96-99% based on characterization results.

The detailed synthesis procedures for tris(2-perfluorobutyl ethyl)tin fluoride and tris(3-perfluoromethyl propyl)tin fluoride were previously described by Kim and Curran[22].

Figure 2 describes the synthesis route of fluorinated telechelic disulfates. The reaction stoichiometric ratios for 1,6-bis(diisocyanato hexane) (HDI) extended diols and the molecular weight of the telechelic disulfates obtained are shown in Table 1. Detailed synthesis procedures were described elsewhere by Shi[23].

Solubility and Phase Behavior of Thickener-CO_2 systems

The solubility of each thickener in CO_2 was studied in a high pressure, variable volume, windowed cell [D.B. Robinson], Figure 3[11,12,21,23]. The sample volume (0-100 cm^3) was confined within a thick-walled hollow quartz cylinder (3.175 mm ID, 5.715 cm OD, 20.32 cm length). The sample (carbon dioxide and thickener mixture) resided above a "floating" cylindrical piston that fit within the hollow quartz cylinder. The floating cylinder held an O-ring for sealing the sample volume from the overburden fluid. The silicone oil overburden fluid was below the floating piston. The oil also surrounded the outside of the hollow cylinder, thereby eliminating any pressure drop across the thick wall of the hollow Pyrex cylinder. The hollow cylinder, floating piston and the overburden fluid were housed within a high-pressure windowed vessel rated to 458 K and 70 MPa that also provided a seal for the top of the sample volume.

The phase boundary of mixtures of specified overall composition was determined using isothermal compressions and expansions of a mixture of known overall composition at 297 K. In a typical experiment, a known amount of thickener was charged into the sample volume of the high pressure cell. Liquid carbon dioxide was then

metered into the sample volume at the exact same rate that the sample volume was expanded using a 28-speed dual positive displacement pump [Ruska] rated to 70 MPa. The CO_2-thickener mixture was then isolated and subsequently compressed and mixed until a transparent single phase was achieved. The system was then slowly expanded until the solution became cloudy, indicating the appearance of a second phase. The pressure was subsequently increased again and the cell rocked until a single phase was attained. The expansion was repeated at a slower rate and the cloud point pressure determined. This procedure was repeated several times and an average cloud point pressure (P_c) was recorded. The solubility of the thickeners in CO_2 is typically evaluated up to 5wt% at 297 K and below 48.3 MPa.

Viscosity of CO_2-Thickener Solutions

The viscosity of single-phase thickener-CO_2 solution was determined with a falling cylinder viscometer. The viscosity tests were conducted in the same apparatus used for the phase behavior experiments, thereby enabling us to determine phase behavior and solution viscosity using the same CO_2-thickener mixture. This technique was selected because of its simplicity in monitoring large viscosity increases in fluids as indicated by reductions in the terminal velocity of a falling object. Visual observations enabled the verification that the reduced terminal velocity, u_c, was caused by an increase in the solution viscosity. It was easy to detect if the fall of the cylinder was impeded by small amounts of thickener (that had not dissolved) lodged in the annulus between the falling cylinder and the hollow cylinder. The objective of this study was to determine which of the proposed thickeners could induce substantial viscosity increase (at least a 2-

fold increase), rather than precise measurements of very small increases in viscosity. The falling cylinder viscometer was used because it enabled the rapid detection of substantial increases in solution viscosity immediately after performing solubility measurements. The most appropriate measure of viscosity for enhanced oil recovery processes was considered to be the measurement of the pressure drop associated with flow of neat CO_2 and thickened CO_2 through porous media, such as sandstone and limestone. These tests can take days to perform, however, and were not used during this initial screening of thickener candidates. (In our future work, flow-through-porous media viscosity tests will be conducted on the most promising fluorinated thickener and on the non- fluorous thickeners.)

The governing equation for the viscometer, shown as equation (1), relates the fluid viscosity ¡ to the product of the calibration constant, K and the density difference between the aluminum cylinder and the fluid (ρ_c - ρ_f), divided by the terminal velocity of the cylinder, u_c .

$$\mu = \frac{K(\rho_c - \rho_f)}{u_c} \qquad (1)$$

Based on the diameter of the aluminum cylinder, 3.159 cm, and the inside diameter of the hollow tube, 3.175 cm, the calibration constant K was calculated[24] as 2.2 E-4 cm^3s^{-2}. The calibration constant was determined experimentally using neat liquid CO_2 at 297 K to be 3.3 E-4 cm^3s^{-2}. Although this equation is only valid for Newtonian fluids, it can also be used for estimating the viscosity of non-Newtonian fluids when the shear rate is low and

shear dependence is not considered[24-26]. The shear rate that corresponded to each viscosity measurement was also determined[24]. The objective of this study was not to quantify the non-Newtonian nature of CO_2-thickener mixtures, but rather to identify which of the candidate thickeners could induce an extremely large increase in solution viscosity at dilute concentration. Therefore a study of the solution viscosity over a wide range of shear rates using aluminum cylinders of varying diameter was not conducted.

In a typical viscosity measurement, a precisely machined aluminum cylinder was placed into the cylindrical sample volume before the thickener was added. The aluminum cylinder was designed such that the ratio of its radius to the hollow quartz tube radius was 0.995, thereby minimizing the magnitude of error caused by non-coaxial fall of the cylinder[26]. The length of the cylinder, 2.54 cm, corresponded to the length of the flow path of the solution in the annulus. This distance was about 400 times greater than the annular gap, 0.008 cm, minimizing entrance end effects as the fluid flowed into and out of the annular gap below and above the falling cylinder, respectively. After equilibration of the system and the single phase was achieved at 297 K and 34 MPa, the cell was inverted in one second and the terminal velocity of the cylinder was then measured (Fig. 4.). The distance associated with the fall of the cylinder was 10-15 cm, and the duration of the fall was as high as 0.15 cm/s, with lower velocities for the thickened solution. Measurements at different positions were made to verify that the cylinder reached its terminal velocity. The falling cylinder reached its terminal velocity within the first 10% of the length of its fall. Five terminal velocity measurements were made during each fall of the cylinder. We assumed that the change in solution density due to the thickener was

not significant. Therefore the solution relative viscosity (the ratio of thickened solution viscosity to neat carbon dioxide viscosity) was equated to the ratio of the terminal velocity in neat CO_2 to the terminal velocity in the thickened solution. These ratios were equated to the ratio of falling time in thickened solution, $t_{solution}$, to falling time in neat carbon dioxide, t_{CO2}, for a specified distance, equation (2).

$$\frac{\mu_{solution}}{\mu_{CO_2}} = \frac{u_{c,CO_2}}{u_{c,solution}} = \frac{t_{solution}}{t_{CO_2}} \qquad (2)$$

Terminal velocity experiments were repeated at least six times at each concentration and the average relative viscosity results were reported together with the measurement shear rate range.

Results and Discussion

Semi-fluorinated Trialkyltin Fluorides

Phase Behavior

Tris(2-perfluorobutyl ethyl)tin fluoride is soluble in liquid CO_2 at room temperature and at pressures below 18 MPa. However, tris(3-perfluoromethyl propyl)tin fluoride is not soluble in liquid CO_2, even at a pressure of 48 MPa. The cloud point pressure vs. composition curve (P-x diagram) for tris(2-perfluorobutyl ethyl)tin fluoride is shown in Figure 5. The incorporation of fluoroalkyl end groups has greatly enhanced the solubility of the trialkyltin fluoride in carbon dioxide. At a pressure as low as 18 MPa, Tris(2-perfluorobutyl ethyl)tin fluoride is miscible with CO_2 up to a concentration of 4 wt% at pressures below 18 MPa. We believe that the fluoroalkyl content of tris(3-

perfluoromethyl propyl)tin fluoride is not adequate to impart CO_2-solubility to the trialkyltin fluoride.

Solution Viscosity

The relative solution viscosity results for tris(2-perfluorobutyl ethyl)tin fluoride are also presented in Figure 5. Tris(2-perfluorobutyl ethyl)tin fluoride can increase the solution viscosity by 3.3 times at a concentration as low as 4 wt%. The increase of solution relative viscosity tends to reach a maximum at higher concentrations. A dramatic increase in viscosity (several orders of magnitude) due to imminent gel formation, commonly reported in trialkyltin fluoride-alkane solutions, was not observed. The absence of gel formation may be attributed to the fluorine atoms at chain ends. Although these chain-end fluorines are not as electronegative as those adjacent to the tin, they are sufficiently electronegative to compete for the association with the tin atom of the neighboring molecule. This disrupts the formation of a linear, pseudo-polymer chain that is responsible for dramatic increases in viscosity.

Fluorinated Telechelic Disulfates

Phase Behavior

The phase behavior of HDI extended fluorinated telechelic disulfates is presented in Figure 6. The disulfate with MW of 13,800 is the lowest MW sample in the series that is soluble in liquid CO_2 below 48 MPa at 297 K. As the molecular weight increases from 13,800 to 15,400 and then to 18,700, the cloud point pressure decreases significantly. The increased miscibility with increasing molecular weight can be attributed to the enhanced CO_2-philicity of the ionomer. As the molecular weight increases from 13,800 to 18,700,

the increase of CO_2-philic fluorinated polyurethane content dominates, rendering the whole molecule greater solubility in CO_2 despite the molecular weight increase. Above the optimal molecular weight (for CO_2-solubility), however, the unfavorable entropy of mixing associated with high molecular weight polymer in CO_2 system dominates. Therefore the disulfate becomes less soluble in CO_2 and the pressure needed for solubilization at a certain concentration increases as illustrated by the results for the ionomer with a MW of 29,900. There exists an optimal molecular weight, 18,700, where the two effects are balanced for greatest solubility. Optimal molecular weights of carbon dioxide-soluble amphiphiles have been previously reported[27].

The solubility of a polyfluoroacrylate is also presented in Figure 6. Poly(heptadecafluorodecyl acrylate) (PHFDA), polymerized in trifluorotoluene, is very soluble in liquid CO_2 as indicated by the low cloud point pressure (below 10 MPa) up to a concentration of 5 wt%. This solubility result is in agreement with the results of DeSimone *et. al*[13]. The presence of ionic end groups and the lower CO_2-philicity of fluoroethers relative to fluoroacrylate make these ionomers less CO_2 soluble than the fluoroacrylate homopolymer.

Solution Viscosity

The CO_2 solution relative viscosity results of the fluorinated telechelic disulfate, MW = 29,900, in carbon dioxide at concentrations up to 4 wt% are shown in Figure 7 to 4 wt%. This ionomer was selected because previous studies have shown that the viscosity-enhancing capability of telechelic ionomers increases with molecular weight. Below 1

wt%, the ionomer-CO_2 solution relative viscosity is quite close to that of neat carbon dioxide. However, there is a marked viscosity increase at concentrations between 2-4 wt%, leading to relative viscosity of 2.7 at 4 wt%. The viscosity results indicate that the CO_2-soluble fluorinated telechelic disulfate is capable of increasing the viscosity of CO_2 at relatively low concentrations.

The relative viscosity of poly(heptadecafluorodecyl acrylate) (polymerized in trifluorotoluene) in CO_2 solution is also presented in Figure 7. Although the polymer molecular weight, estimated at 10^5, is much higher than the telechelic disulfate molecular weight, the degree of solution viscosity increase is less than that achieved with the disulfate at an equivalent concentration. This illustrates that although high molecular weight polymers can increase liquid CO_2 viscosity by chain entanglement, fluorinated telechelic disulfates are more effective thickeners because they have CO_2-phobic disulfate groups that tend to associate in CO_2 solution.

The viscosity-enhancements achieved with the fluorinated telechelic disulfate and the semi-fluorinated trialkyltin fluoride were comparable. This increase was quite modest compared to that attained with fluoroacrylate-styrene copolymers[21]. Once again, no dramatic increases in viscosity were observed for the telechelic ionomers, as has been reported for hydrocarbon-based telechelic ionomers used to thicken organic solvents[28]. For example, non-functionalized polystyrene, MW = 80,000, increased the viscosity of cumene by a factor greater than 10 at a concentrations of several wt%, and a polystyrene disulfonate of equivalent molecular weight increased the viscosity by a

factor of 100 or more at the same concentrations[28]. The ability of the polymer and the ionomer to enhance the viscosity was greatly diminished as the molecular weight decreased to 20,000. Non- functionalized fluorinated polyurethane polymers (with molecular weights comparable to the disulfates used in the present study) were not capable of inducing a detectable viscosity increase in carbon dioxide at concentrations up to 4 wt%[29]. The fluorinated disulfate tested in this study increased the viscosity by a factor of 2-3 at the same concentration. Therefore, it appears that the molecular weight of about 30,000 is insufficient for viscosity enhancement. Increases in the molecular weight of the disulfate would result in carbon dioxide-insolubility, however.

Conclusions

Two types of direct CO_2 thickeners, a semi-fluorinated trialkyltin fluoride and a fluorinated telechelic ionomer, have been developed. Their viscosity-enhancing capability has been determined at 297 K and 34 MPa. Tris(2-perfluorobutyl ethyl)tin fluoride was soluble in carbon dioxide up to 4 wt% at pressures below 18 MPa. The solution viscosity increased by a factor of 3.3 (relative to neat carbon dioxide) at 4wt%. This increase was much less than expected, possibly due to the disruptive effect of the side chain fluorine atoms on the Sn-F associations that led to the formation of linear, weakly associating, transient polymers. Fluorinated telechelic disulfates were soluble in carbon dioxide within the molecular weight range of 13,800 and 29,900. The optimal molecular weight for solubility in carbon dioxide was 18,700. The highest molecular weight disulfate that could be dissolved in dense carbon dioxide at pressures below 25 MPa (MW = 29,900) increased the solution viscosity by a factor of 2.7 at a concentration

of 4 wt%. The increase was also less than expected due to the low molecular weight of this ionomer.

Both of these thickeners were slightly more effective in thickening CO_2 than the solution polymerized fluoroacrylate homopolymer at equivalent concentration (wt%), due to the intermolecular associations between the "CO_2-phobic' ionic groups. Neither compound was as soluble in carbon dioxide or as effective in thickening carbon dioxide as the fluoroacrylate-styrene copolymers[21]. This was evidenced by lower pressure requirements required to dissolve the fluoroacrylate-styrene copolymer and viscosity increases that were approximately 2 orders of magnitude greater at the same concentration (wt%). The fluoroacrylate functionality used in the fluoroacrylate-styrene copolymer was more CO_2-philic than either the fluoroether or fluoroalkyl groups incorporated in the trialkytin fluorides or telechelic ionomers, respectively. The CO_2-phobicity of the styrene groups was less pronounced than the CO_2-phobicity of the tin-fluoride or sulfate groups, yet the ð-ð stacking of these phenyls led to significant increases in solution viscosity.

Acknowledgements

We would like to express our appreciation of the financial support of the US DOE National Petroleum Technology Office under contract DOE-RA26-98BC15108. We also would like to thank Air Products, Cabot Oil and Gas, and Universal Well Services for their support.

References

(1) Stalkup, F. *Miscible Displacement, SPE Monograph No.8.*, SPE: New York, 1983.

(2) Habermann, B. The Efficiency if Miscible Displacement as a Function of Mobility Ratio, *Trans. AIME*, **1965**, *219*, 264.

(3) Heller, J., Dandge, D. Topical Viscosity Control for Light Hydrocarbon Displacing Fluids in Petroleum Recovery and in Fracturing Fluids for Well Stimulation, U.S. Patent 4,607,696, 1986.

(4) Taylor, C., Dandge, D., Heller, J. Review of the Literature on Trialkyltin Fluorides. PRRC 86-5 , Petroleum Recovery Research Center: Socorro, NM,1986.

(5) Gullapalli, P., Tsau, J., Heller, J. Gelling Behavior of 12-Hydroxystearic Acid in Organic Fluids and Dense CO_2. SPE International Symposium on Oilfield Chemistry, San Antonio, TX, Feb., 14-17, 1995; SPE 28979

(6) Cohen, L., Gregory, W. Aluminum Soap Thickeners with Surface Active Agents. US. Patent 3,539,311, 1970.

(7) Martin, F., Heller, J. Improvement of CO_2 Flood Performance, PRRC 90-34, Petroleum Recovery Research Center: Socorro, NM, 1990.

(8) Heller, J., Dandge, D. Direct Thickeners for Mobility Control of CO_2 Floods, *SPEJ*, **1985**, 679.

(9) Harris, T., Irani, C., Pretzer, W. Enhanced Oil Recovery Using CO_2 Flooding. U.S. Patent 4,913,235, 1990.

(10) Mistele, C., Thorp, H., DeSimone, J. The Ring-Opening Metathesis Polymerization of Norbornene in Supercritical Carbon Dioxide. *Polymer Preprints*, **1995,** *36(1),* 507.

(11) Yazdi, A., Beckman, E. Design of Highly CO_2-Soluble Chelating Agents for Carbon Dioxide Extraction of Heavy Metals. *J. Material Research*, **1995,** *10(3),* 530.

(12) Parks, K., Beckman, E. Generation of Microcellular Polyurethane Foams Via Polymerization in Carbon Dioxide. I: Phase Behavior of Polyurethane Precursors. *Polymer Engineering and Science*, **1996,** *36(19),* 2404.

(13) McClain, J., Betts, J., Canelas, D., Samulski, E., DeSimone, J., Landona, J., Winall, G. Characterization of Polymers and Amphiphiles in Supercritical CO2 using Small Angle Neutron Scattering and Viscometry. *Proceedings of the 1996 Spring Meeting of the ACS, Division of Polymeric Materials: Science and Engineering*, New Orleans, LA, **1996**, *74*,234

(14) Rudin, A. *The Elements of Polymer Science and Engineering*, Academic Press, New York, 1998.

(15) Dunn, P., Oldfield, D. Tri-n-butyltin Fluoride, A Novel Coordination Polymer in Solution. *J. Macromol. Sci. Chem.*, **1970,** *A4(5),* 1157.

(16) Heller, J., Kovarik, F., Improvement of CO_2 Flood Performance, PRRC Report 86-18, Petroleum Recovery Research Center: Socorro, NM, 1986.

(17) Hegedus, R., Lenz, R. Telechelic Sulfate Ionomers. I. Preparation and Solution and Thermal Properties, Journal of Polymer Science: Part A: Polymer Chemistry. **1988**, *26*, 367.

(18) Tant, M., Wilkes, G. Sulfonated Polyisobutylene Telechelic Ionomers. XIII. Viscosity Behavior in Nonpolar Solvents and Nonpolar-Polar Solvent Mixtures. *Journal of Applied Polymer Science*, **1989,** *37*, 2873.
(19) Dagani, R. Intelligent Gels. *Chemical and Engineering News*, **1997,** *June 9*, 26.
(20) Guan, Z., DeSimone, J. Fluorocarbon-Based Heterophase Polymeric Materials. 1. Block Copolymer Surfactants for Carbon Dioxide Applications. *Macromolecules*, **1994**, *27*, 5527.
(21) Huang, Z., Xu, J., Shi, C., Kilic, S., Enick, R., Beckman, E. Enhancement of the Viscosity of Carbon Dioxide Using Styrene/Fluoroacrylate Copolymers. *Macromolecules* **2000,** *33 (15),* 5437.
(22) Curran, D., Hadida, S., Kim, S.-Y., Luo, Z. Fluorous Tin Hydrides: A New Family of Reagents for Use and Reuse in Radical Reactions, *Journal of the American Chemical Society*, **1999,** *121(28),* 6607.
(23) Shi, C. Formation of Macromolecules in Carbon Dioxide for Enhanced Oil Recovery and Foam Generation. PhD. Dissertation, University of Pittsburgh, Pittsburgh, PA, 1999.
(24) Barrage, T. A High Pressure Visual Viscometer Used in the Evaluation of the Direct Viscosity Enhancement of High Pressure Carbon Dioxide. MS. Thesis, University of Pittsburgh, Pittsburgh, PA, 1987.
(25) Eeichstadt, F., Swift, G. Theoretical Analysis of the Falling Cylinder Viscometer for Power Law and Bingham Plastic Fluids. *AIChE Journal*, **1966,** *12*, 1179.
(26) Sen, Y., Kiran, E. A New Experimental System to Study the Temperature and Pressure Dependence of Viscosity, Density, and Phase Behavior of Pure Fluids and Solutions, *The Journal of Supercritical Fluids*. **1990,** *3*, 91.
(27) Lepilleur, C., Beckman, E. Dispersion Polymerization of Methyl Methacrylate in Supercritical CO_2. *Macromolecules,* **1997,** *30*(4), 745.
(28) Moller, M., Omeis, J., Muhleisen, E. Association and Gelation of Polystyrenes via Terminal Sulfonate Groups. In *ACS Symposium*; Russo, P. Ed.; Americal Chemical Society: Washington, DC, 1987, Vol. 350, p. 87.
(29) Enick, R., Beckman, E., Shi, C., Karmana, E., Formation of Fluoroether Polyurethanes in CO_2. *The Journal of Supercritical Fluids* **1998,** *13*, 127.

N_{OH}, mmol	N_{NCO}, mmol	N_{NCO}/ N_{OH}	MW^{cal}	MW^{exp}
5	3.735	0.747	15,200	13,800
5	3.895	0.779	17,700	15,400
5	3.980	0.796	19,300	18,700
5	4.865	0.873	32,500	29,900

Table 1. Stoichiometric ratios of HDI extended diols with different molecular weight.

$MW^{cal}=M_0X_n + M_{eg}$, where $M_0=2196$, $M_{eg}=0$, $X_n=(1+r)/(1-r)$. Here $r = N_{NCO}/N_{OH}$.

MW^{cal} was estimated by assuming conversion p=1.

MW^{exp} was determined by diol end-group titration.

Figure 1. Association between trialkyltin fluoride molecules.

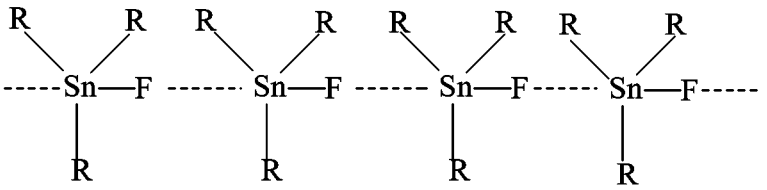

Figure 2. Synthetic route forfluorinated telechelic disulfates.

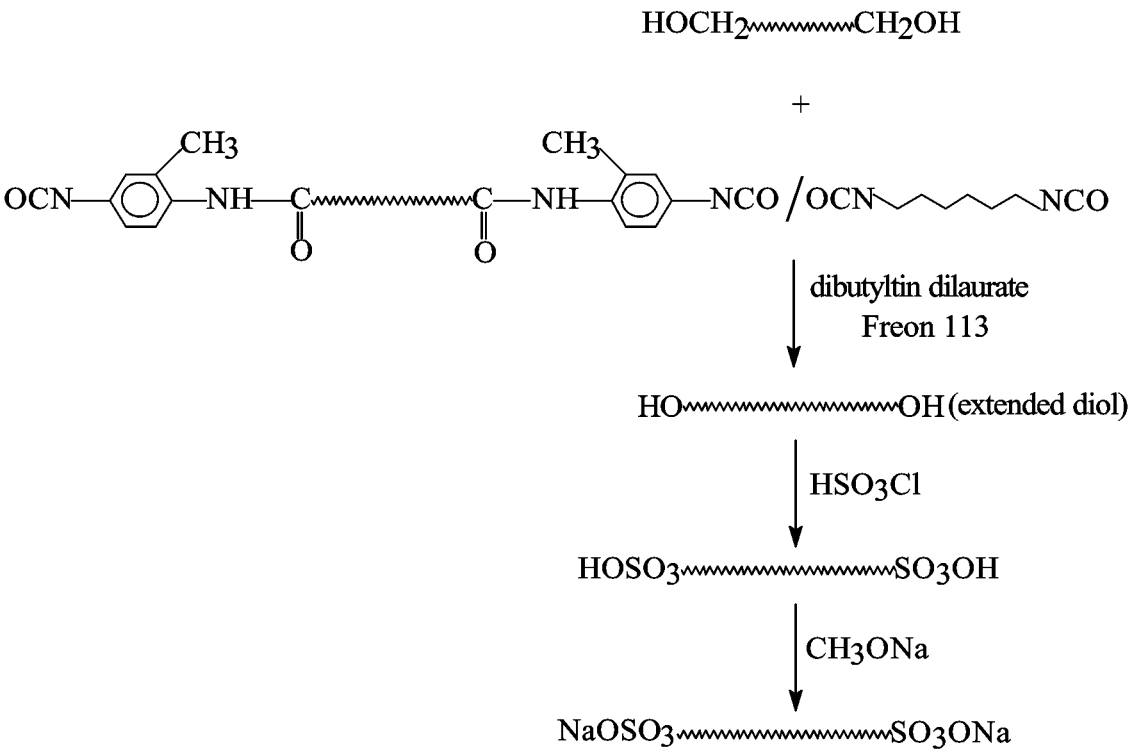

Figure 3. Experimental apparatus for solubility measurements in a high pressure, variable volume, windowed cell.

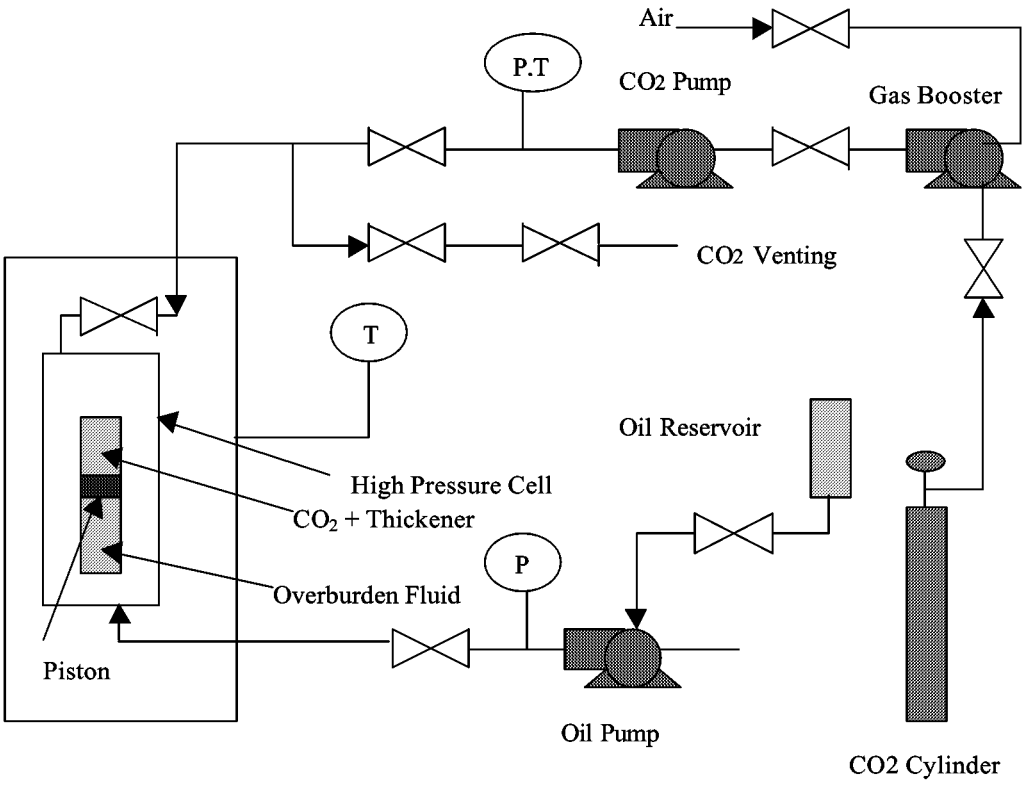

Figure 4. Schematic diagram for viscosity measurements with a high pressure falling cylinder viscometer.

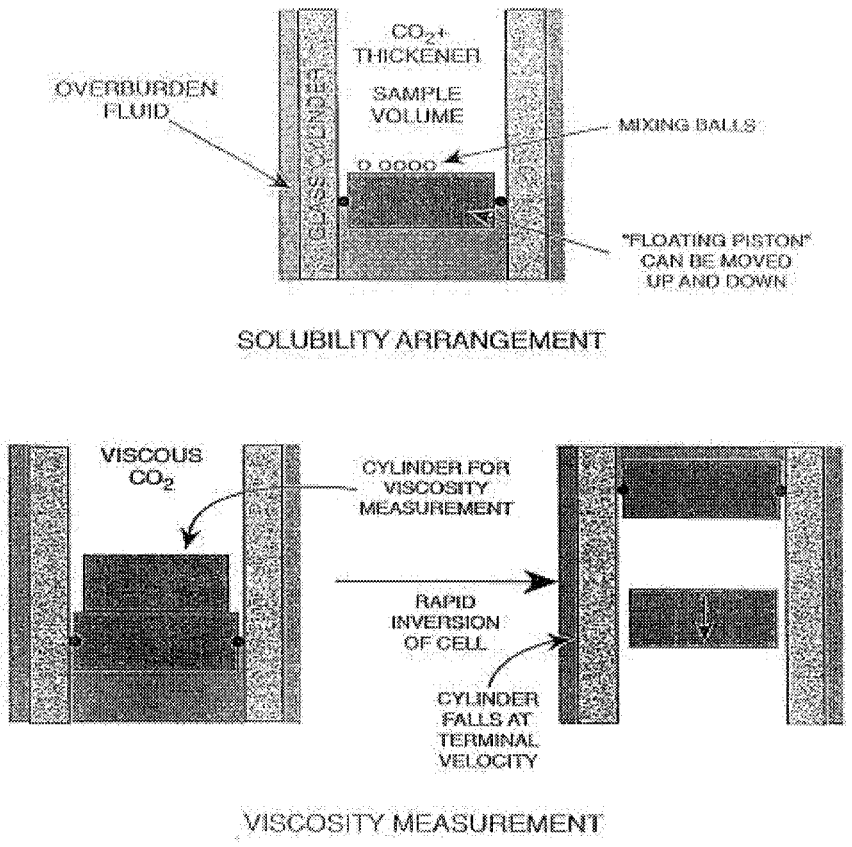

Figure 5. Solubility and solution relative viscosity of tris(2-perfluorobutyl ethyl)tin fluoride in liquid carbon dioxide; shear rate range for viscosity measurements 2300-6500 s^{-1}, T=297 K

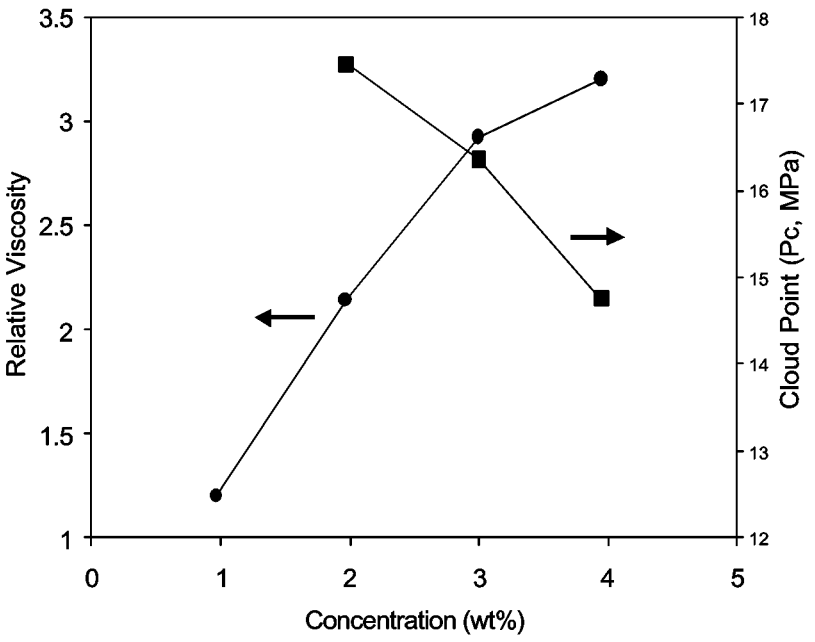

Figure 6. Phase behavior of fluorinated telechelic disulfates in liquid carbon dioxide, T=297 K.

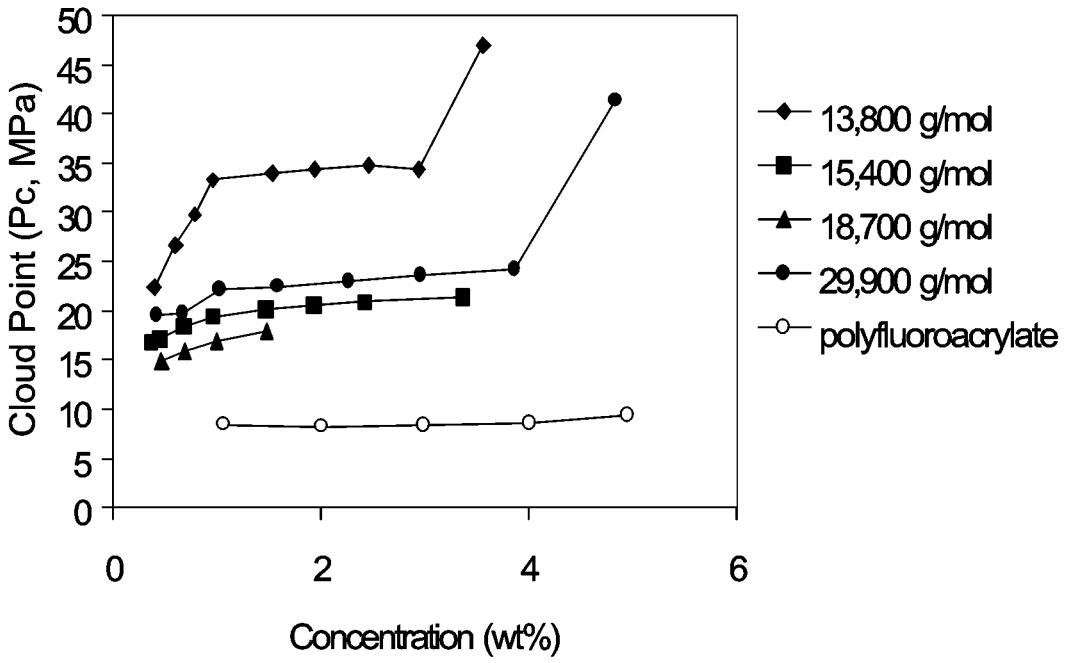

Figure 7. Solution relative viscosity results for fluorinated telechelic disulfates; The relative

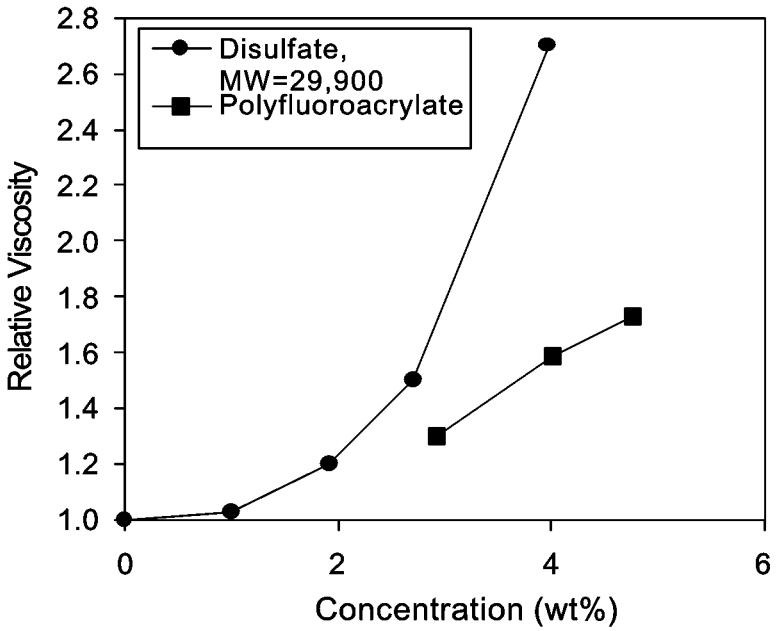

Ch. 3. EVALUATION OF FLUOROALKYL ASPARTATE BISUREAS AND UREAS FOR CARBON DIOXIDE THICKENING AND MICROCELLULAR FOAM GENERATION

6.1 Synthesis and Characterization

6.1.1 Materials

N-t-BOC protected aspartic acid (N-t-BOC-L-Asp) and N-CBZ protected aspartic acid (N-CBZ-L-Asp) were obtained from Sigma and stored below 0 ^{0}C in the fridge before use. 1H,1H,2H,2H-Perfluorodecanol (97%) was purchased from Lancaster Synthesis. Hexafluoropropylene oxide homopolymer alcohol (MW=1200 g/mol, fluoroether monofunctional alcohol, DuPont product, brand name Krytox, 95%) was purchased from Miller-Stephenson; 1-[3-(Dimethylamino)propyl]-3-ethylcarbondiimide hydrochloride (EDCI, 98+%) and 4-(Dimethylamino)pyridine (DMAP, 99+%) were both ordered from Aldrich; Palladium hydroxide, 20 wt% Pd (dry basis) on carbon (Pearlman's catalyst) was obtained from Aldrich; Diisocyanates and isocyanates used in our synthesis were purchased from Aldrich. All other chemicals and solvents were obtained from Aldrich and used as received.

6.1.2 Reactions

The reaction routes for the synthesis of fluorinated aspartate bisureas and ureas were generalized in Fig. 16 [109]. To synthesize a bisurea, a diisocyanate was reacted with the deprotected aspartate; To synthesize a urea, an isocyanate was the reactant instead.

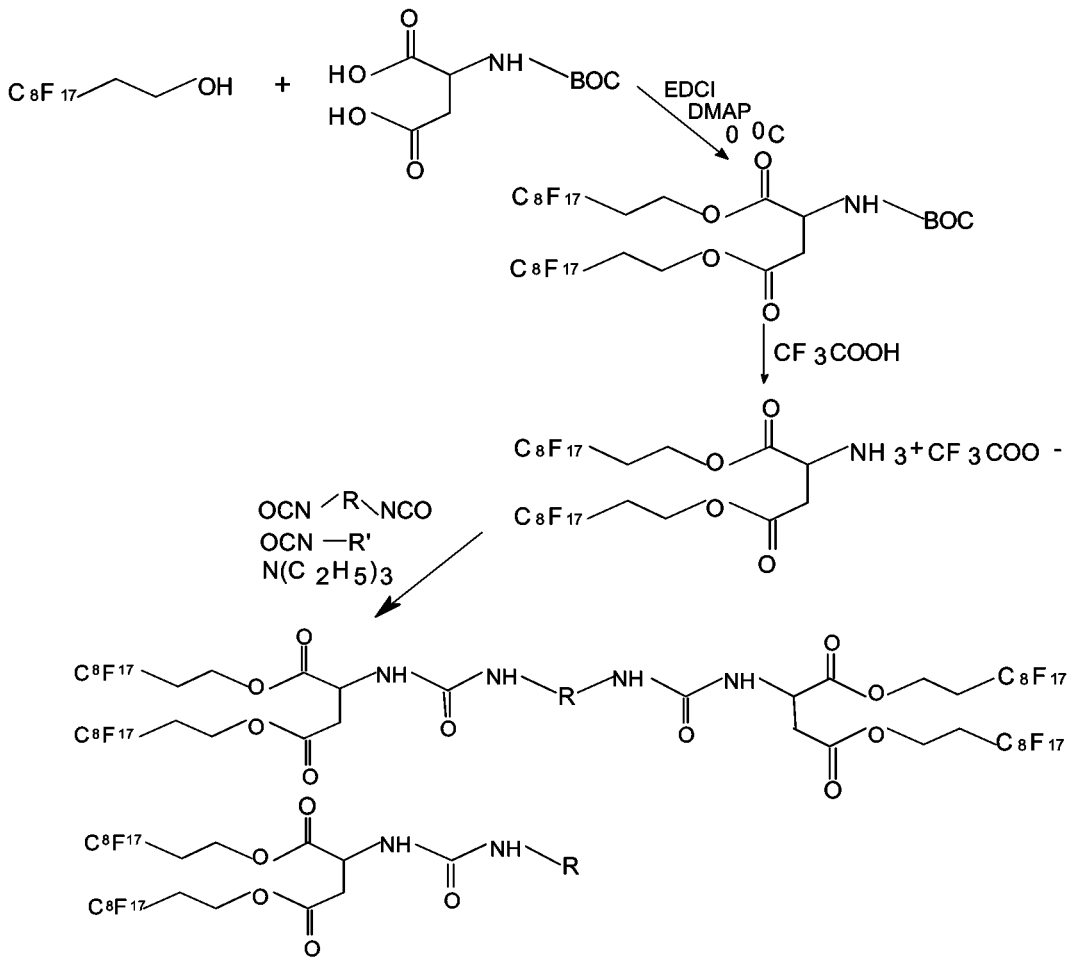

Fig.23 Synthetic routes for fluorinated aspartate bisureas and ureas

In our synthesis, both short chain (FW = 464g/mol) fluoroalkyl alcohol and long chain (MW = 1,200) fluoroether alcohol were used to introduce the CO_2-philic functionalities into the bisurea and urea structures. Different diisocyanates and isocyanates were also

used to give various CO_2-phobic structures. The synthesized bisureas were listed in Table 4. The synthesized ureas were listed in Table 5.

CO_2-phile	R group	Melting Point, ^0C	Freon 113		PFDMCH	
			Soluble?	Gel?	Soluble?	Gel?
$CF_3(CH_2)_7(CH_2)_2$	$(CH_2)_6$	120.7	no	no	no	yes
$CF_3(CH_2)_7(CH_2)_2$	$(CH_2)_{12}$	113.7	no	no	no	yes
$CF_3(CH_2)_7(CH_2)_2$	1,4-phenyl	198.6	no	no	no	yes
$CF_3(CH_2)_7(CH_2)_2$	1,4-xylyl	166.6	no	no	no	yes
$CF_3(CH_2)_7(CH_2)_2$	fluoroether[b]	135.4	no	no	no	loose fibers
fluoroether[a]	$(CH_2)_6$	--------	yes	no	yes	no

Table 4 Fluorinated aspartate bisureas synthesized; The solubility and gelling behavior at 1wt% concentrations of theses biureas in freon 113 and PFDMCH (perfluoro-1,3 dimethyl cyclohexane) were also listed as a screening test before evaluation in carbon dioxide.

a. Hexafluoropropylene oxide homopolymer alcohol, MW=1200

b. Fluorolink B, as described in Chapter 5.1.1., MW=3000

CO_2-phile	R group	Melting Point, ^0C	Freon 113		PFDMCH	
			Soluble?	Gel?	Soluble?	Gel?
$CF_3(CH_2)_7(CH_2)_2$	*p*-fluoro-phenyl	137.4	no	yes	no	yes
$CF_3(CH_2)_7(CH_2)_2$	*p*-CF_3-phenyl	127.1	no	no	no	no
$CF_3(CH_2)_7(CH_2)_2$	3,5-$(CF_3)_2$-phenyl	96.7	no	yes	no	yes
$CF_3(CH_2)_7(CH_2)_2$	$CH_3(CH_2)_5$	87.3	yes	yes	no	yes
$CF_3(CH_2)_7(CH_2)_2$	phenyl	133.2	no	yes	no	yes
$CF_3(CH_2)_7(CH_2)_2$	Ethyl methacrylate	72.7	no	no	no	yes
fluoroether[a]	3,5-$(CF_3)_2$-phenyl	--------	yes	no	yes	no
fluoroether[a]	$CH_3(CH_2)_5$	--------	yes	no	yes	no

Table 5 Fluorinated aspartate ureas synthesized; The solubility and gelling behavior at 1wt% concentrations of theses biureas in freon 113 and PFDMCH (perfluoro-1,3 dimethyl cyclohexane) were also listed as a screening test before evaluation in carbon dioxide.

a. Hexafluoropropylene oxide homopolymer alcohol, MW=1200

6.1.3 Procedures

(1) Synthesis of Deprotected Fluoroalkyl Aspartate Amine

Typically, in a 250ml 3-neck flask equipped with a stirring bar, charge 100ml dichloromethane. 7.88g 1H,1H,2H,2H-perfluorodecanol (0.017mol) was added and the

flask was cooled in an ice bath. 2g N-Boc-Asp (0.0086mol) and 3.28g (0.017mol) EDCI were subsequently charged to the reaction mixture. Start stirring until most of the reactants were dissolved. 1.05g DMAP (0.0086mol) was then introduced. The reaction mixture was kept in the ice bath for 30 min, then the ice bath was removed and reaction was kept at room temperature overnight.

The reaction mixture was then diluted with 100ml chloroform and transferred to a separation funnel. The organic layer was washed with 50ml 1% HCl twice, and 50ml brine once and dried over sodium sulfate. Solvents were later removed under vacuum to yield a pale yellow solid. The solid was then dissolved in a minimal amount of dichloromethane (Freon was added if necessary). The obtained solution was transferred to a silica column and washed with chloroform. Solvent was subsequently removed under vacuum and a white solid aspartate product was obtained with 80% yield.

The obtained aspartate diester was subject to deprotection with trifluoroacetic acid. Typically, 5g aspartate was deprotected with 10ml trifluoroaceticacid in 20ml dichloromethane for 4 hours. The solvent was removed under reduced pressure. Chloroform was added and removed under vacuum until a white solid was formed. The solid was then recrystallized from 200ml ethanol and cooled to room temperature and stored in a fridge for 3 hours. The solid was collected and dried under reduced pressure. The deprotected aspartate amine was a needle-shaped white solid with 78% yield.

^{1}H NMR spectra taken from a Bruker 300 MHz NMR showed 4.87ppm (O=C(C**H**)CH_2NH in aspartate residue), 4.58ppm (O=C(C$\mathbf{H_2}$)CH in aspartate residue),

4.40ppm ($C_8F_{17}CH_2(C\mathbf{H_2})O$ in fluorodecanol residue), and 2.48ppm ($C_8F_{17}(C\mathbf{H_2})CH_2$ in fluorodecanol residue). See Appendix C.

(2) Synthesis of Deprotected Fluoroether Aspartate Amine

Similar to the synthesis of fluoroalkyl aspartate, fluoroether aspartate was synthesized in 100ml cooled ethyl acetate-1,1,2-trichlorotrifluoroethane (called in the following freon 113 or freon) mixture (1:1 v/v) with fluoroether alcohol and N-CBZ-Asp as the reactants. After reaction, most solvents were removed and the concentrated oil was washed with 50ml ethyl acetate twice, 50ml ethanol once, and 100ml 1% HCl twice. The residue was then diluted with 50ml freon and dried over sodium sulfate. Evaporate most freon 113 under vacuum until the residue reached a volume of 20-30ml. The yellow-colored solution was then purified over a silica column and washed down with 1:1 ethyl acetate-freon mixture. Solvents were later evaporated and yield a colorless oil.

The fluoroether aspartate diester was then deprotected by hydrogenation with $Pd(OH)_2/C$ as the catalyst. Typically, 5.0g fluoroether aspartate diester was dissolved in 20ml perfluoro1,3-dimethyl cyclohexane, 0.25g palladium hydroxide on carbon catalyst was added. Start stirring vigorously. N_2 was passed through the reaction flask to displace air before hydrogen was introduced. The diester was deprotected with hydrogen for 12 hours, then the catalyst was removed first by filtration (Whatman #1 filter), then the residual fine catalyst particles were removed by Millipore membrane filter (0.45μm). The solvent was removed under vacuum and residue washed with ether. Yellowish oil sample was then dried under vacuum.

^{1}H NMR spectra for fluoroether CBZ-Aspartate showed peaks at 7.22ppm ($C_6\mathbf{H_5}CH_2$ in CBZ-Asp residue), 5.99ppm ($CF_2(C\mathbf{H_2})O$ from fluoroether alcohol residue), 5.00ppm ($O{=}C(C\mathbf{H_2})CH$ in aspartate residue), 4.34ppm ($O{=}C(C\mathbf{H})CH_2NH$ in aspartate residue), 4.69ppm ($CH(N\mathbf{H})C{=}O$ from aspartate residue), and 2.93ppm ($O(C\mathbf{H_2})C_6H_5$ from CBZ-Asp residue). See Appendix C.

(3) Synthesis of Bisureas and Ureas

The deprotected fluoroalkyl or fluoroether aspartate amines were than reacted with stoichiometric amounts of commercially available diisocyanates and isocyanates to yield bisureas and ureas of different structures.

Typically, the reactions between deprotected fluoroalkyl aspartate amine and diisocyanates/isocyanates were carried out in 50ml dichloromethane with triethylamine as the catalyst. The product fluoroalkyl bisureas/ureas are white solids and collected by filtration and washed with 1% HCl and hexanes and then dried under vacuum. The fluoroether bisureas/ureas were obtained by reacting the deprotected fluoroether amine with different diisocyanates/isocyanates in 50ml freon 113, with triethylamine as the catalyst. After reactions, solvent was removed by reduced pressure and the oily product was washed with 1% HCl and hexanes and dried.

The synthesized bisureas/ureas were characterized by taking IR spectra on a Mattson Polaris FT-IR. Solid samples were mixed with KBr and compressed into pellets before

taking the spectra. Liquid samples were prepared in the form of thin films between NaCl windows.

The IR spectra for fluoroalkyl bisureas/ureas are similar, showing N-H streching absorbance at 3350-3360 cm^{-1}, C-H stretching at 2940-2990 cm^{-1}, carbonyl absorbance around 1735-1745 cm^{-1}, N-H scissoring absorbances at 1630 and 1570 cm^{-1} respectively.

The IR spectra for fluoroether bisureas/ureas usually show N-H streching absorbances at 3340-3350 cm^{-1}, C-H strecthing at 2940-2980 cm^{-1}, carbonyl absorbance around 1760-1770 cm^{-1}, and two N-H scissoring absorbances at 1650 and 1570 cm^{-1}. See Appendix C. for spectra.

The melting point for each solid bisurea/urea sample was measured in a TA Instrument DSC 2910 with indium as the reference and nitrogen as the purging gas. The heating rate was 10 ^{0}C/min. The melting points were listed in Table. 4 for bisureas and in Table. 5 for ureas respectively. The DSC curves were listed in Appendix D.

6.2 Phase Behaviors of Fluorinated Aspartate Bisureas and Ureas in Carbon Dioxide

6.2.1 Experimental

The experimental set-up is the same as described in Chapter 4.2.1. The solubility of every fluorinated aspartate bisurea or urea was first evaluated at room temperature and below system maximum pressure 7,000 psi. If the sample was not completely soluble at room temperature, the high pressure cell was then heated to 80 ^{0}C or higher while keeping the pressure between 5,000 ~ 6,800 psi by expanding the sample volume until the sample was dissolved in supercritical carbon dioxide. The resulted solution was subsequently cooled down to room temperature by keeping the pressure above 5000 psi and the behavior was recorded.

CO_2-phile	R group	behavior in carbon dioxide	
		Soluble?	behavior after cooling
$CF_3(CH_2)_7(CH_2)_2$	$(CH_2)_6$	yes, at 90 ^{0}C, 6000 psi	monolith at 3.0-4.9wt%, collapsed network at 2.2wt%
$CF_3(CH_2)_7(CH_2)_2$	$(CH_2)_{12}$	yes, at 90 ^{0}C, 6000 psi	collapsed network at 4.0wt%
$CF_3(CH_2)_7(CH_2)_2$	1,4-phenyl	yes, at 100 ^{0}C, 6000 psi	precipitated powder at 2.0wt%
$CF_3(CH_2)_7(CH_2)_2$	1,4-xylyl	yes, at 100 ^{0}C, 6000 psi	precipitated powder at 3.4wt%
$CF_3(CH_2)_7(CH_2)_2$	fluoroether[b]	yes, at 90 ^{0}C, 6000 psi	loose floating fibers at 2.5wt%
fluoroether[a]	$(CH_2)_6$	Yes, up to 5.0wt% at 25 ^{0}C, 2000 psi	stay as a solution at 25 ^{0}C, no significant viscosity increase

Table 6 Phase behavior of fluorinated aspartate bisureas in carbon dioxide

a. Hexafluoropropylene oxide homopolymer alcohol, MW=1200

b. Fluorolink B, as described in Chapter 5.1.1., MW=3000

CO_2-phile	R group	behavior in carbon dioxide	
		Soluble?	behavior after cooling
$CF_3(CH_2)_7(CH_2)_2$	*p*-fluoro-phenyl	yes, at 90 ^{0}C, 6000 psi	collapsed network at 4.5wt%
$CF_3(CH_2)_7(CH_2)_2$	*p*-CF_3-phenyl	yes, at 90 ^{0}C, 6000 psi	precipitated powder at 2.5wt%
$CF_3(CH_2)_7(CH_2)_2$	3,5-$(CF_3)_2$-phenyl	yes, up to 6.0wt% at 25^{0}C, 2000 psi	collapsed network at 2.0-6.0wt%
$CF_3(CH_2)_7(CH_2)_2$	$CH_3(CH_2)_5$	yes, up to 5.0wt% at 25^{0}C, 5000psi	collapsed network at 3.7-5.0wt%
$CF_3(CH_2)_7(CH_2)_2$	phenyl	yes, up to 5.1wt% at 90^{0}C, 6000 psi	monolith at 4.8-5.1wt%, collapsed network at 1.5wt%
$CF_3(CH_2)_7(CH_2)_2$	Ethyl methacrylate	yes, up to 4.7wt% at 25^{0}C, 2000 psi	collapsed network at 4.7wt%
fluoroether[a]	3,5-$(CF_3)_2$-phenyl	yes, up to 5wt% at 25^{0}C, 2000psi	stay as a solution at 25 ^{0}C, no significant viscosity increase
fluoroether[a]	$CH_3(CH_2)_5$	yes, up to 5wt% at 25^{0}C, 2000psi	stay as a solution at 25 ^{0}C, no significant viscosity increase

Table 7 Phase behavior of fluorinated aspartate ureas in carbon dioxide

a. Hexafluoropropylene oxide homopolymer alcohol, MW=1200

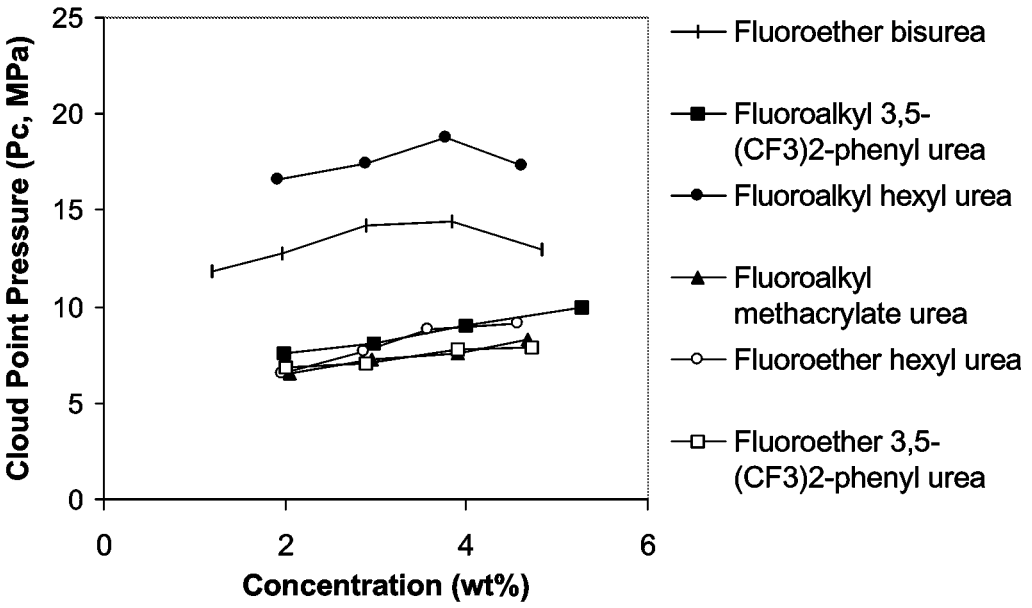

Fig. 24 Phase behavior of CO_2-soluble fluorinated aspartate biureas and ureas at 298 K

6.2.2 Results and Discussions

The solubility of bisureas in carbon dioxide was listed in Table 6. The solubility of ureas in carbon dioxide was summarized in Table 7. The behaviors after cooling were also recorded in Table 6. and Table 7. for bisureas and ureas respectively. As can be seen from the tables, all of the bisureas and ureas that we evaluated can be dissolved in carbon dioxide below 48.3 MPa (7,000 psi) and at room temperature or elevated temperature. The P-x phase diagram for bisureas and ureas that were soluble in carbon dioxide at room temperature was presented in Fig. 24.

Of all these fluorinated aspartate bisureas tested, only the bisurea with fluoroether tails and HDI backbone was soluble in liquid carbon dioxide at room temperature. We believe that although both fluoroalkyl and fluoroether are CO_2-philic, fluoroether functionality is more CO_2-philic and therefore is able to impart higher solubility in carbon dioxide if the other molecular structures are the same. This was obvious when we compare the solubility of fluoroether 1,6-hexyl bisurea and fluoroalkyl 1,6-hexyl bisurea. The fluoroether version was readily soluble in carbon dioxide at room temperature with a cloud point pressure below 15 MPa, while the fluoroalkyl version was not soluble at 41.4 MPa (6,000 psi) until heated to 90 ^{0}C.

Comparison among the bisureas that have the same CO_2-philic tail also revealed the CO_2-phobic trend for different backbone structures. Among them, the aryl groups such as phenyl and xylyl were more CO_2-phobic than the alkyl structures, as indicated by the higher cloud point pressure after sample solubilization (data not shown). We tried to enhance the bisurea solubility by introducing fluoroether backbone into the molecular structure, but the solubility of thus synthesized bisurea was not changed much. We believe this may be due to the lower solubility of the longer chain fluoroether. The fluoroether diisocyanate were tested to require higher pressure to dissolve in carbon dioxide at room temperature. For example, at 5wt%, the cloud point pressure for Fluorolink B was 25 MPa. Apart from that, the existence of CO_2-phobic aromatic groups in the fluorolink B diisocyanate prepolymer may further decrease the product solubility in carbon dioxide.

Because most fluorinated aspartate bisureas showed poor carbon dioxide solubility, we synthesized fluorinated asparate ureas, reducing the number of CO_2-phobic urea functionality from two to one. Generally, the ureas exhibited enhanced solubility in carbon dioxide as we expected (compare Table 6 and Table 7). Hexyl urea was able to dissolve in carbon dioxide at room temperature below 20 MPa, whereas 1,6-hexyl bisurea had to be heated to 90 ^{0}C to dissolve at 41.4 MPa (6,000 psi).

The apparently different solubility of ureas with different R groups followed the trend of different degrees of carbon dioxide phobicity. The phenyl urea showed poor carbon dioxide solubility due to the existence of CO_2-phobic aryl group. The

incorporation of a fluorine atom or a CF_3 group at the *para*-position did not enhance the solubility of the corresponding urea. The incorporation of two CF_3 groups at the 3,5 position, however, significantly enhanced the urea solubility in carbon dioxide. This again proved that fluoroalkyl (in this case fluoromethyl) groups are indeed CO_2-philic, and the introduction of "enough" number of such CO_2-philic functionality could make the molecule as a whole more CO_2-philic.

The solubility data for fluoroalkyl ureas in carbon dioxide also revealed the same trend of relative CO_2-phobicity as for fluoroalkyl bisureas. That is, the aryl groups are more CO_2-phobic than the alkyl groups, making the hexyl urea much more soluble than the phenyl urea. We also discovered that the ethyl methacrylate, among others, was the least CO_2-phobic. In effect, the acrylate functionality was believed by some researchers to be CO_2-philic and may have favorable specific interactions with carbon dioxide.

The fluoroether proved to be more efficient than fluoroalkyl functionality in enhancing the urea solubility in carbon dioxide, therefore, the fluoroether was the more CO_2-philic functionality. The phase behavior data showed that the fluoroether ureas that we evaluated were miscible with carbon dioxide up to 5wt% at room temperature and a pressure slightly higher than the critical pressure of CO_2.

6.3 Viscosity Enhancement by Fluorinated Aspartate Bisureas and Ureas

6.3.1 Experimental

The experimental set-up and mechanism for solution relative viscosity measurements were described in Chapter 4.3.1. In our series of fluorinated bisureas and ureas, only those that were soluble in carbon dioxide at room temperature were subsequently evaluated for their viscosity enhancement ability.

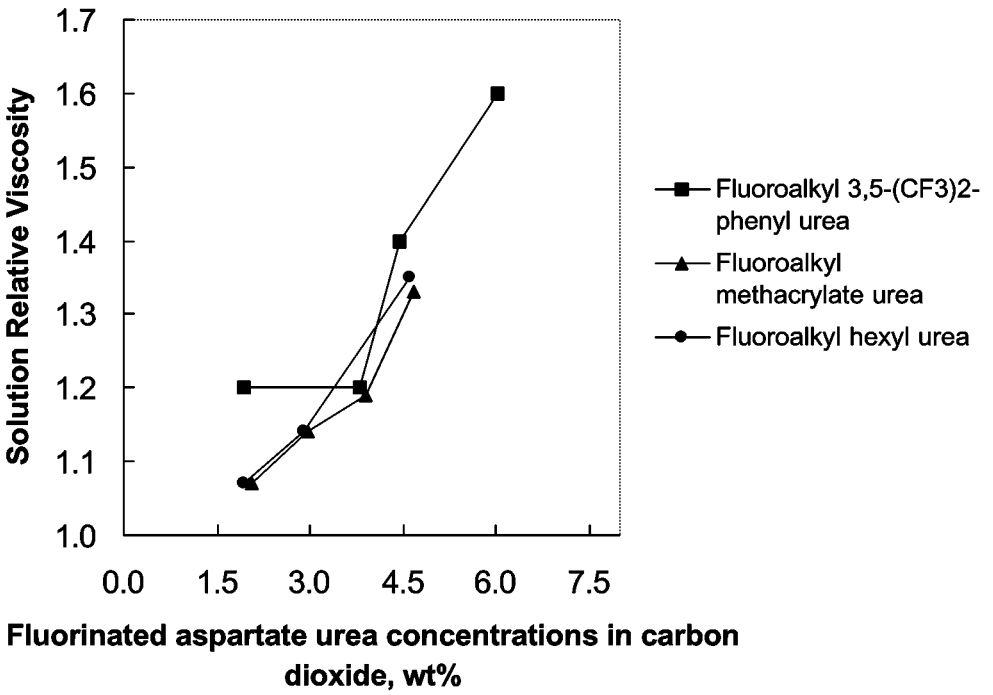

Fig.25 Solution relative viscosity of bisurea/urea in carbon dioxide,

T=298 K, P=5000 psi; Shear rate range: 4400-6800 s^{-1};

6.3.2 Results and Discussions

The solution relative viscosity was presented in Fig. 25. Of the CO_2-soluble bisureas and ureas, fluoroether bisurea and ureas did not exhibit measurable viscosity enhacement as detected by our high pressure falling cylinder viscometer. Or rather, the solution viscosity was almost the same as neat carbon dioxide at the same temperature and pressure. The solution viscosity for CO_2-soluble fluoroalkyl ureas was measured at 5,000 psi to ensure solubility of all three samples.

Overall, the fluoroalkyl ureas exhibited better viscosity enhancing capabilities than the fluoroether versions at low concentrations (< 6wt%). This is probably because the concentration of hydrogen bonding urea functionality in the fluoroalkyl version was higher than the fluoroether version owing to the much shorter fluoroalkyl group. For this reason, the fluoroalkyl ureas may have a greater chance to associate through intermolecular hydrogen bonding, leading to greater solution viscosity.

Among the three fluoroalkyl ureas, 3,5-$(CF_3)_2$-phenyl urea gave the highest solution viscosity increase, followed by hexyl urea, and the ethyl methacrylate urea gave the lowest. A possible reason for the observed greater solution viscosity for 3,5-$(CF_3)_2$-phenyl urea may be attributed to the enhanced intermolecular association through π-π stacking of the CO_2-phobic phenyl rings. The relatively longer hydrocarbon chain in a hexyl urea molecule may be another factor that leads to solution viscosity increase by intermolecular association. The long hydrocarbon chain was CO_2-phobic, and may

promote intermolecular association through Van der Waals interactions in a carbon dioxide environment. This result proved the importance of long chain associations apart from hydrogen bonding in network formation and was consistent with the findings with similar organic solvent gelling agents.

6.4 Conclusions and Speculations

We evaluated the solubility and viscosity enhancing ability of both fluorinated aspartate bisureas and ureas. All samples were soluble in supercritical carbon dioxide at temperatures below 100^0C and at pressures below 7,000 psi. The fluoroether functionality was more CO_2-philic than fluoroalkyl functionality, making the fluoroether bisureas and ureas more soluble in carbon dioxide. However, the much longer fluoroether chain greatly decreased the concentration of associative urea groups, leading to little solution viscosity increase. The ureas were less polar than the corresponding bisureas and were more soluble in carbon dioxide.

By increasing the CO_2-philicity of the molecular structure other than the fluorinated tail, fluoroalkyl ureas became more soluble in carbon dioxide. The existence of phenyl group decreased the urea solubility, proving that aryl groups are CO_2-phobic. The relative solubility for our bisureas and ureas are generally:

Fluoroether "tail" bisureas/ureas > Fluoroalkyl ureas > Fluoroalkyl bisureas and for fluoroalkyl "tail" urea series, the CO_2-philicity of R groups follows:

3,5-$(CF_3)_2$-phenyl > ethyl methacrylate > hexyl > *p*-CF_3-phenyl, *p*-F-phenyl, phenyl

The CO_2 solubility of the corresponding ureas follows the same trend. 3,5-$(CF_3)_2$-phenyl urea, ethyl methacrylate urea and hexyl urea were soluble in carbon dioxide at room temperature and pressure below 5,000 psi. Their solution viscosity was increased by 1.1~1.6 times at concentrations below 6.0wt%.

Low-density microcellular materials can be generated from these fluorinated bisurea and urea solutions in carbon dioxide. Generally, the foamed networks exhibited cell sizes smaller than 10 μm with densities lower than 0.09 g/cm^3 except for the compact networks formed out of carbon dioxide solution. For both bisureas and ureas, there exists a threshold concentration, above which a monolith network can be formed that filled the whole sample cell (~25ml). The concentration of the hydrogen bonding urea groups is the key parameter that controls the formation of such network. Phenyl group may provide additional intermolecular association through π-π stacking, leading to more rigid network. Less CO_2-phobic R groups such as 3,5-$(CF_3)_2$-phenyl and ethyl methacrylate may promote interactions between the associated urea networks and carbon dioxide, resulting in more cells with smaller cell sizes.

Ch. 4. The Design of Organogelators – Yale University Subcontract

We have previously shown that bis-urea derivatives such as **1** form strong complexes with bis-carboxylates in polar organic solvents (Figure 1).[i] However, the poor solubility of bis-ureas in less polar solvents suggested that in the solid state significant intermolecular interactions are present.

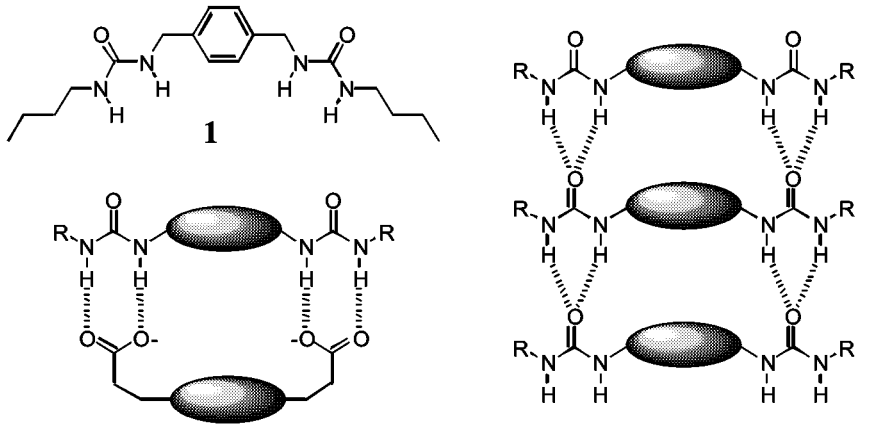

Figure 1 Schematic representation of a 1:1 complex formation and aggregation behavior of bis-ureas.

Since gelation depends upon initial dissolution followed by aggregation and network formation, we reasoned that a modest increase in the solubility of the bis-ureas might lead to a new family of gelling agents. The use of different amino acid esters gave us access to a range of solubilizing and potentially interacting functionalities. These self-complementary components were prepared by reaction of xylylene-1,4-bis-isocyanate with the *t*-butyl esters of L-alanine, L-phenylalanine and L-valine to give **2**, **3** and **4**. The bis-ureas were synthesized by preparing the isocyanate of the amino acid and then reacting it with *para*-xylylendiamine. The amino acid isocyanates were synthesized following Nowick's protocol, which uses equimolar amounts of phosgene.[ii]

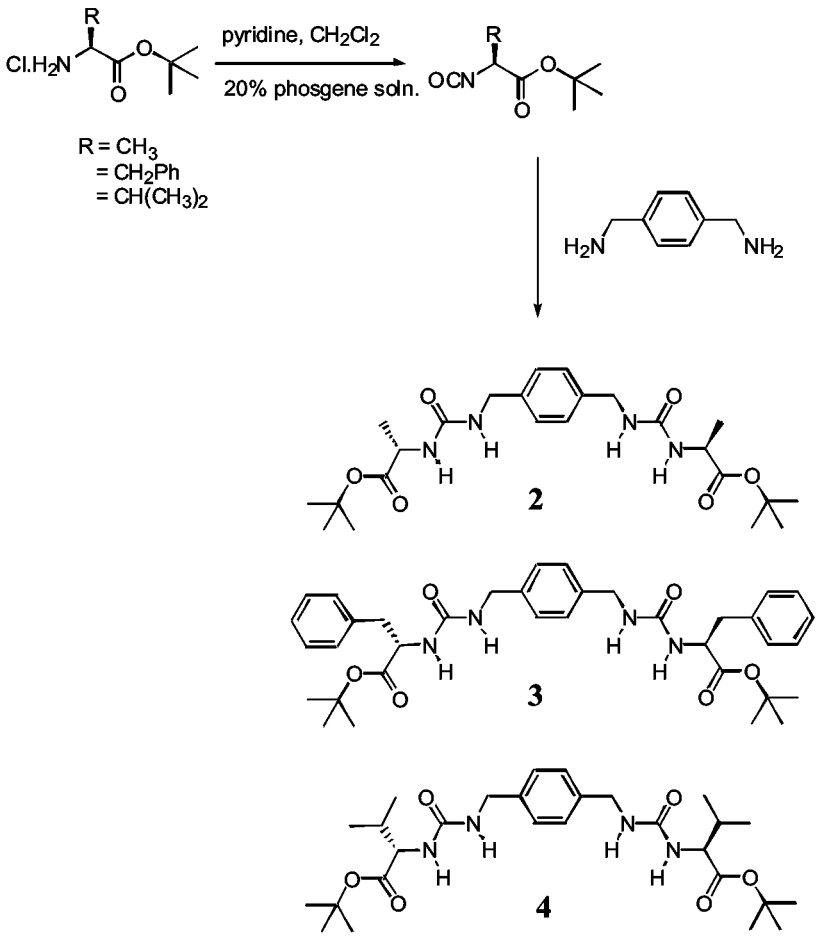

Scheme 1 Synthesis of bis-ureas with a p-xylyl spacer.

We had observed that during the purification of bis-ureas **2**, **3** and **4** they gelled mixtures of ethyl acetate and hexanes. The gelation properties of the *t*-butyl esters were measured in a range of organic solvents and the results are collected in Table 1. In all cases (unless otherwise noted) the compound was dissolved in a solvent at a concentration of 56 mM. The solution was then cooled to 5°C for thirty minutes and the presence of a gel was assessed by inverting the vial and observing the flow of the sample. Bis-urea **2** was able to gel THF and acetone at 5°C but the gel melted on warming to room temperature. The bis-phenylalanine analog **3** showed enhanced solubility but without improved network formation and no gelation properties were observed in any solvent. The best gelling agent in this series of bis-ureas was bis-valine **4**, which appears to combine good solubility with side chain functionality that can interact effectively to form a gel matrix. A particularly stable gel was formed by **4** in ethyl acetate which retained its form at room temperature for hours. The compound also gels mixed solvents of hexanes with acetone and ethyl acetate. But these gels are less stable than those in ethyl acetate, either melting or crystallizing upon standing at room temperature.

Table 1 Gelation results of bis-urea derivatives **4**, **2** and **3**.

Solvent	4	2	3
$CHCl_3$	Sol.-Cryst.	Sol.	Sol.
CH_2Cl_2	Sol.	Sol.-Cryst.	Sol.
DMSO	Sol.	Sol.	Sol.
Ether	Insol.	Insol.	Insol.
Hexanes	Insol.	Insol.	Insol.
Hexanes/25% Acetone	Gel 5°C (10 mM) Cryst. (56 mM)	Insol.	Insol.
Hexanes/50% Ethyl Acetate	Gel 5°C (10 mM)	Cryst.	Cryst.
Ethyl Acetate	Gel – stable at RT	Sol.	Gel 5°C (98 mM)
Acetone	Sol.	Gel 5°C	Sol.
Tetrahydrofuran	Sol.	Gel 5°C	Sol.
Ethanol	Sol.	Sol.	Sol.
Acetonitrile		Sol.	Insol.

Sol. = soluble with no gel formation. Insol. = insoluble.

Gel 5°C = gel formed when solution of compound was cooled to 5°C for 30 minutes.

X-ray quality crystals of **4** were grown from hexanes and acetone. The crystal structure of **4** showed the formation of one-dimensional hydrogen bonds. Each molecule forms four hydrogen bonds to the adjacent molecule from both N-H urea groups to the carbonyl with distances of N…O of 2.18 and 2.23 Å. Molecules are related to each other in the strands by 2_1 screw symmetry. Because of this symmetry there is no π–π stacking. Instead, the *tert*-butyl group from one of the ester groups is oriented close to the phenyl ring, making what seems to be a π–alkyl interaction (C…ring centroid, d=3.69 Å. Similar effects have been seen in solution and in the solid state by us and Andreetti.[iii] The other *tert*-butyl group is in an extended conformation to form van der Waals interactions with the corresponding adjacent tert-butyl groups on the adjacent strands (C…C, d= 2.49 Å). The bis-urea molecules are oriented in the same direction and therefore form polar hydrogen bonded strands. It should also be noted that all strands are pointing in the same direction, which makes the crystal polar.

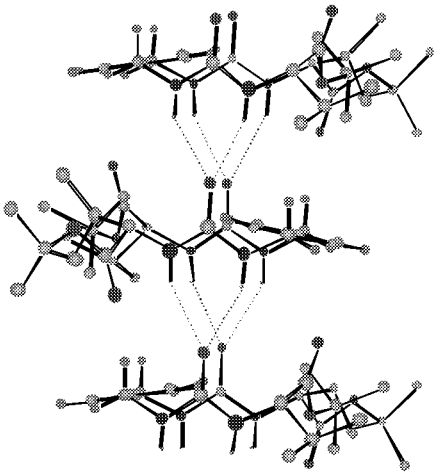

a

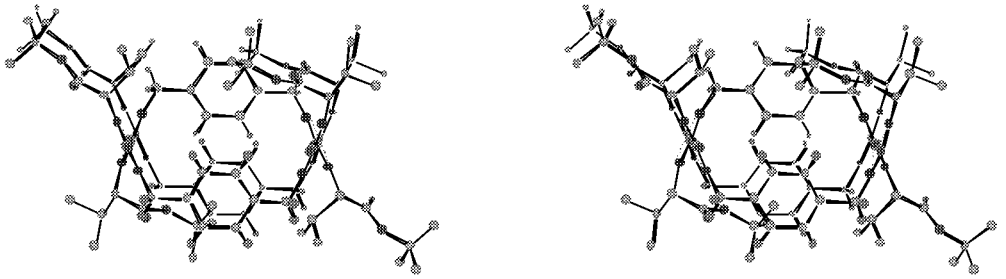

b

Figure 2 Crystal structure of **4**. (**a**) side view of the hydrogen bonding strands, (**b**) top view shown the phenyl-methyl interactions.

Although these bis-urea molecules show some gelation in organic solvents, there is improvement to be made. Many of the reported organogelators in the literature show the presence of long alkyl chains, presumably for solubility purposes. In our attempt to improve the design of these gelators we divided the molecule in three parts: the spacer, the hydrogen bonding group and the alkyl substituents (See Figure 3). The spacers can be varied in length and can be aliphatic or aromatic. The hydrogen bonding groups can be, for example amines, urethanes or ureas. The alkyl substituents can be also varied in length and nature. This design allows us to modify the gelators for a variety of purposes that we will cover through out this section.

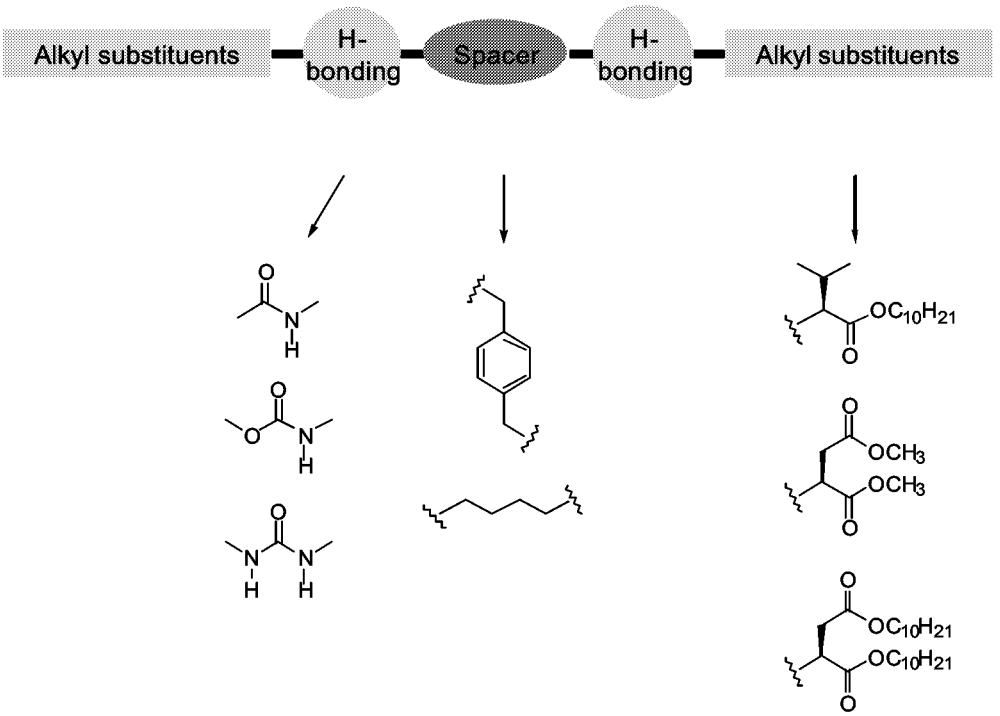

Figure 3 Molecular design of organogelators

Early developments of this project directed us to the use of bis-ureas as the best hydrogen bonding functional group for our molecules.[iv] We also discovered that long alkyl chains are very important for good gelation results. The synthesis of these molecules is straight forward and allows us to use commercially available bis-isocyanates of various lengths. In terms of the reacting amine to form the urea, we can use amino acid esters. The use of aspartic acid also allows us to introduce two ester groups into our molecule (See Scheme 2)

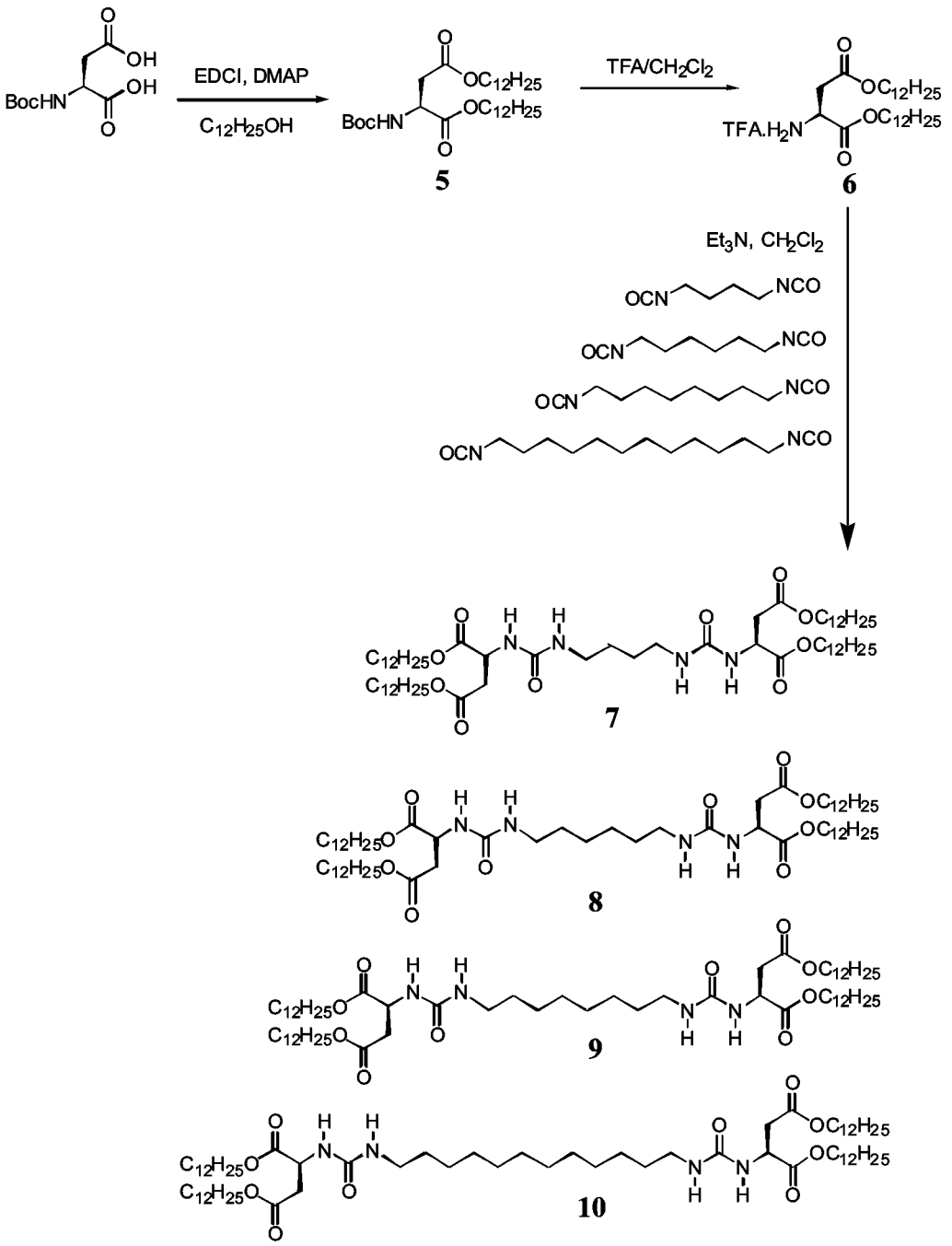

Scheme 2 Synthesis of bis-urea aspartic acid derivatives.

The synthesis of decyl ester derivatives was also carried out to test for gelation. The two derivatives, **13** and **14** were synthesized by following the same protocol as for the previous gelators (see Scheme 3)

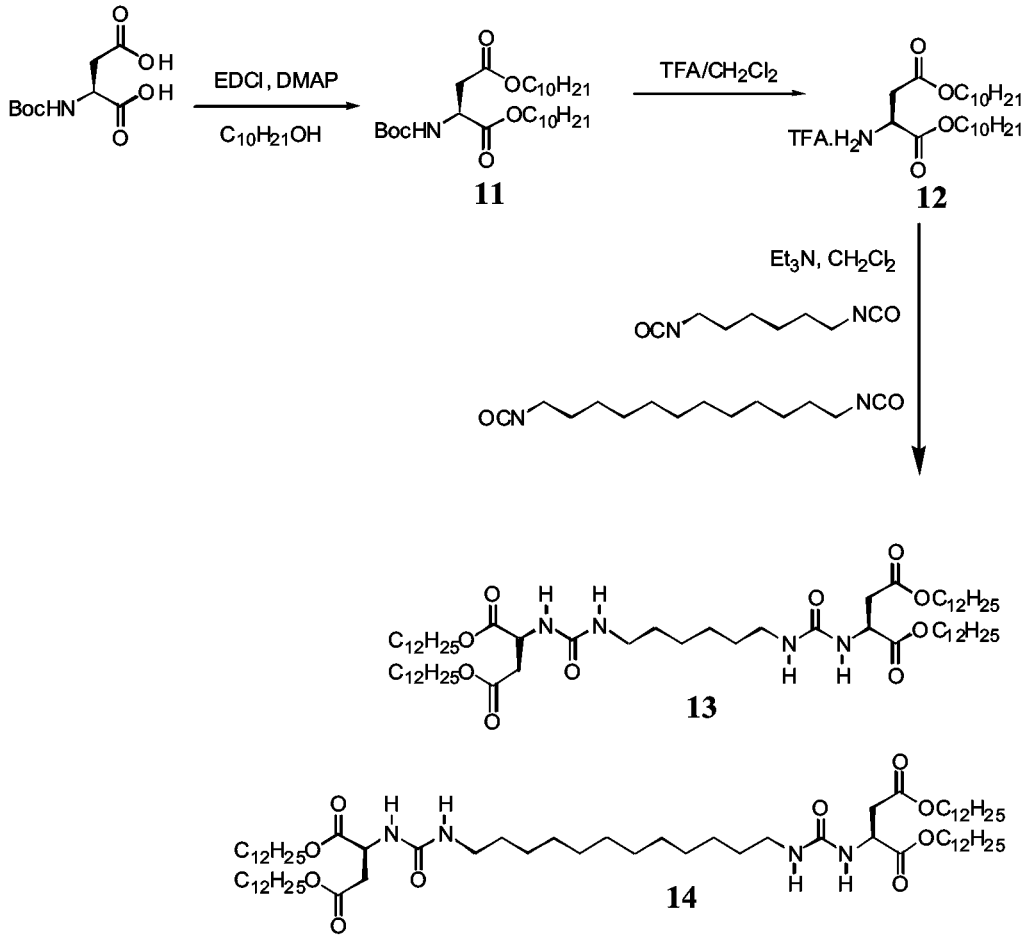

Scheme 3 Synthesis of decyl ester aspartic acid gelators.

Gelation tests were conducted by dissolving 2mg of the compound in the appropriate solvent. The solution was heated to the boiling point and then allowed to cool to room temperature for 1 hour. The test tube was inverted to observe for gelation or increased viscosity of the solution. If the compound showed gelation in the solvent, the minimum concentration was determined by dilution. Interestingly, these molecules gel DMSO (polar solvent) and hexanes (non-polar solvent) at very low concentrations. In particular, they are excellent gelators for hexanes at concentrations ranging from 3.5-6.5 mM. Compounds **9** and **10** also gel diethyl ether. Gelation results are summarized in Table 2.

Table 2 Gelation results for bis-ureas aspartic acid derivatives.

Solvents	Minimum gelation concentration (mM)					
	7	**8**	**9**	**10**	**13**	**14**
$CHCl_3$	Sol.	Sol.	Sol.	Sol.	Sol.	Sol.
CH_2Cl_2	Sol.	Sol.	Sol.	Sol.	Sol.	Sol.
THF	Sol.	Sol.	Sol.	Sol.	Sol.	Sol.
Ether	Insol.	Insol.	Gel 5.0	Cl. G 10.4	Insol.	Insol.
Hexanes	Ppt	Gel 3.5	Gel 4.1	Cl. G 6.5	Gel 4.1	Cl. G 6.2
DMSO	Ppt	Gel 8.3	Viscous 8.1	Cl. G 12.4	Gel 9.6	Ppt
Ethanol	Ppt	Ppt	Ppt	Ppt	Ppt	Ppt
Acetone	Ppt	Ppt	Ppt	Ppt	Ppt	Ppt
Ethyl acetate	Ppt	Ppt	Ppt	Ppt	Ppt	Ppt
Acetonitrile	Ppt	Ppt	Ppt	Ppt	Ppt	Ppt

Sol.= Soluble Insol.= Insoluble Ppt.= Precipitate

Gel= Clear Gel Cl. G= Cloudy Gel

The gel of compound **13** was studied by ^{1}H NMR to observe hydrogen bonding. A 10 mM gel of 127 in DMSO-d^6 was prepared and heated in 10°C increments from 25°C to 125°C. Figure 4 shows the spectra from 7.0-2.0 ppm at 25, 55 and 95°C. Upon heating the urea protons shift upfield by 0.213 ppm, which indicates that intermolecular hydrogen bonding in the gel state is being weakened by increasing temperature.

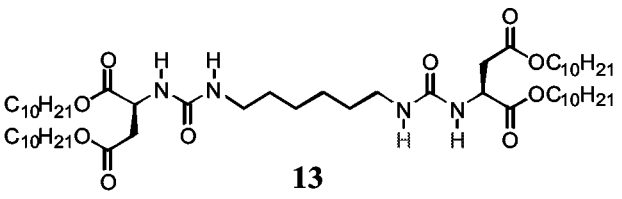

13

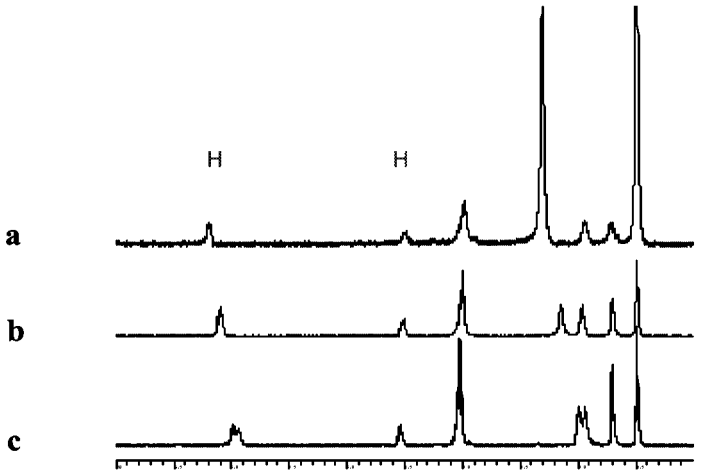

Figure 4 ^{1}H NMR of **127** in DMSO-d^6 at variable temperatures (**a**) 25°C, (**b**) 55°C, (**c**) 95°C.

Perfluorinated compounds, including freons are known as the third medium for organic synthesis and supramolecular chemistry. In synthetic applications, perfluorinated catalysts have the advantage of easily being removed from the reaction media by extraction in perfluorinated solvents.[139] Perfluorinated compounds are also known to be soluble in supercritical CO_2, which has been termed "the green solvent", due to its environmental acceptance.[140] Supercritical CO_2 is also readily available, inexpensive, nonflammable, nontoxic and chemically inert. Another application of supercritical CO_2 is in enhanced oil recovery. However, its foremost disadvantage is its low viscosity. We have synthesized a variety of perfluoro organogelators making use of different amino acids in order to incorporate long perfluoro alkyl esters (see Scheme 4 and 5).

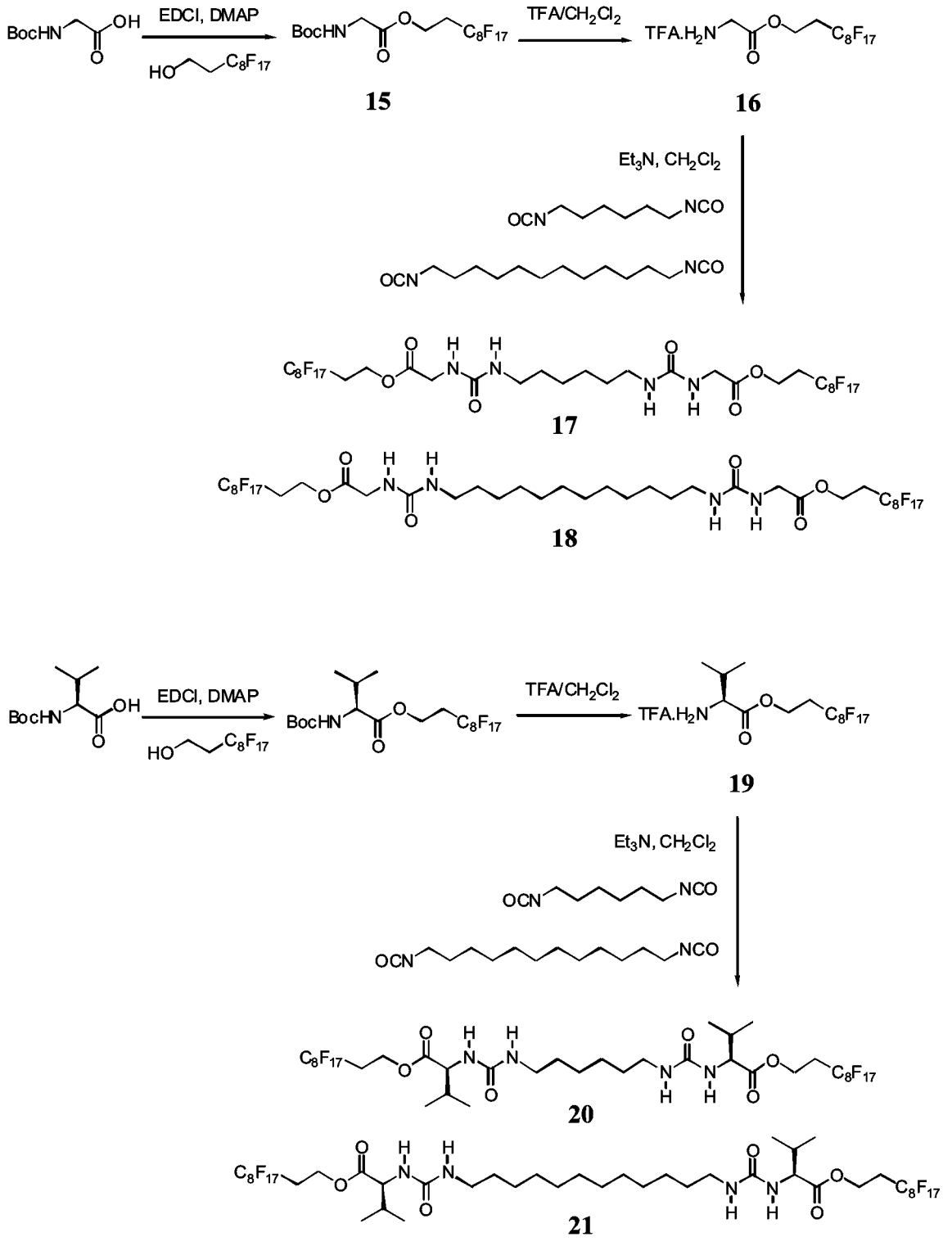

Scheme 4 Synthesis of perfluorinated bis-urea gelators.

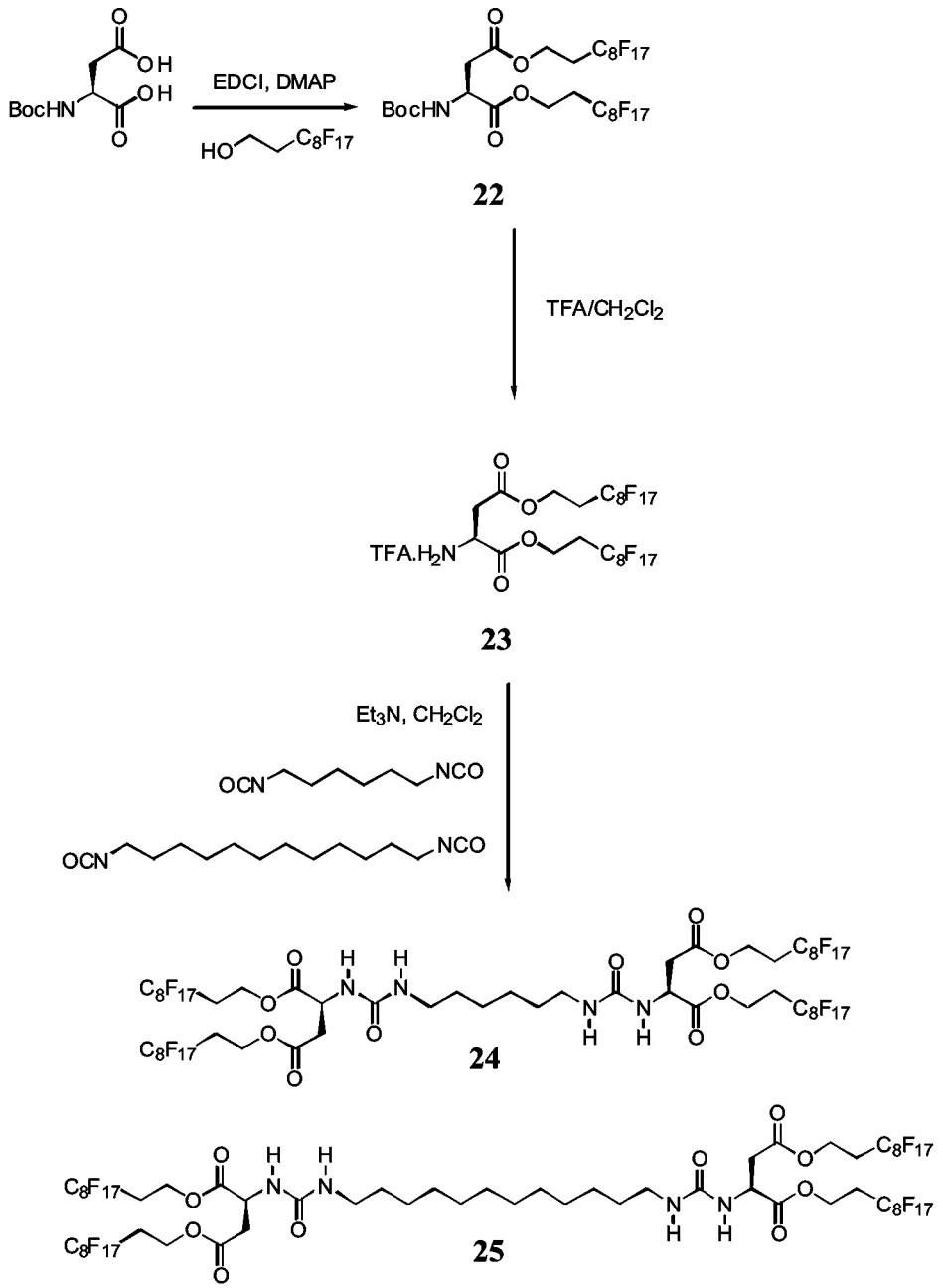

Scheme 5 Syntheis of perfluorinated bis-urea gelators.

In an attempt to make the isocyanate of the aspartic acid perfluoroderivative, using Nowick's protocol, we isolated compound **26**, which is a mono urea with no spacer (See Scheme 6).

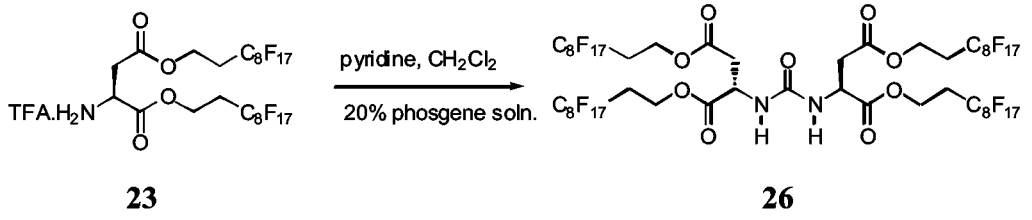

Scheme 6 Synthesis of monourea aspartic acid derivative **26**.

There have been no reports on gelation of low-molecular weight compounds in perfluorohydrocarbons and halofluorocarbons (CFCs or freons). Freons have been linked to the destruction of the Earth's ozone layer. There is no single alternative to freons and new technology, chemicals and working practices play an important role in the replacement of these substances. Many organogelators have been used for environmental cleaning of oil spills and in general for trapping solvents. We have tested our molecules as freon gelators and found very interesting results. In freons and organic solvents such as benzene and chloroform, the perfluorinated compounds are mostly insoluble or precipitate at room temperature. The hydrocarbon analogs of the aspartic acid derivatives form gels in methylcyclohexane. This indicates that miscibility of the side chain with the solvent medium is required for gel formation. Interestingly, hydrocarbon analogs of the aspartic acid series form gels in freons however, the perfluorinated derivatives do not. To our knowledge these are the first freon gelators reported. Gelation tests were conducted by dissolving the gelators in glass tubes which were heated to 120-130°C in an oil bath. The resulting solution was allowed to stand for 1 hour at room temperature. Table 3 summarizes gelation results in perfluorohydrocabons (PFH's), CFC's, and less polar organic solvents. Glycine derivatives **17** and **18** were insoluble in all organic solvents, PMCH (perfluoromethylcyclohexane) and freons. Heating 1 mg of compound in 50 μL of PMCH to the boiling point in a sealed tube resulted in the disperion of the compound in the solvent. The solid settled to the bottom of the tube upon removal of heat. These compounds were soluble in 3% TFA in chloroform, but showed no gelation. The valine derivatives **20** and **21** showed no solubility in organic solvents and freons. However, they show some solubility in perfluorinated solvents and gelation in PMCH at concentrations of 5.8 and 6.7 g/L respectively (5.2 and 5.5 mM). The best gelation results in perfluorinated solvents were obtained with **24** and **25**. Compounds **24** and **25** formed gels of concentrations of 2.3 and 3.9 mM respectively, in PMCH. Organogelators **13** and **14** do not dissolve in perfluorinated solvents. However, **14** gels freons at 5.2 and 9.6 mM concentrations. Interestingly, mono-perfluorinated urea **26** gels both PMCH and freons, the latter at very low concentrations (4.4 mM). These values indicate that they are so-called 'supergelators' in perfluorinated solvents.

Table 3 Gelation results in freons, perfluorinated and organic solvents.

Compound	Minimum gelation concentration (g/L)							
	PMCH	PFN	PFH	PFB	111-TriCl-F	112-TriCl-F	MCH	benzene
17	Insoluble	Insoluble	Insoluble	Insoluble	Insoluble	Insoluble	Insoluble	Insoluble
18	Insoluble	Insoluble	Insoluble	Insoluble	Insoluble	Insoluble	Ppt	Ppt
20	Gel (5.8)	Ppt	Ppt	soluble	Ppt	Ppt	Ppt	Ppt
21	Gel (6.7)	Ppt	Insoluble	soluble	Ppt	Ppt	Ppt	Ppt
24	Gel (5.1)	Gel (5.2)	Gel (6.4)	viscous	Insoluble	Ppt	Ppt	Ppt
25	Gel (9.1)	Gel (10.3>)	Insoluble	Gel (2.9)	Insoluble	Insoluble	Insoluble	Insoluble
13	Insoluble	Insoluble	Insoluble	Ppt	Viscous	viscous	Cloudy Gel	soluble
14	Insoluble	Insoluble	Insoluble	Ppt	Gel (5.7)	Gel (10.4)	Cloudy Gel	soluble
26	Gel (19.8)	Cloudy Gel (10.2)		Ppt	Gel (8.2)	Gel (8.2)	Insoluble	Insoluble

PMCH= perfluoromethylcyclohexane PFN= perfluorononane PFH= perfluorohexane PFB= perfluorobenzene
111-TriCl-F= 1,1,1-trichloroperfluoroethane 112-TriCl-F= 1,1,2-trichloroperfluoroethane
MCH= methylcyclohexane Ppt= precipitate

In the FT-IR spectra of the gel state in perfluoromethylcyclohexane, the amide I and II bands of **24**, were observed at 1626 and 1559 cm-1 and the ester carbonyl was at 1741 cm-1. This indicates that the bis-urea group is participating in hydrogen bonding to contribute in the formation of, what we believe are, one-dimensional aggregates.

Compounds **24** and **25** exhibit solubility in CO_2 at 90°C at 300 atm. Upon cooling the solutions to room temperature at constant pressure, the solution exhibits a sharp phase separation (sudden complete opacity of the mixture). Removal of the CO_2 by gradual depressurization yielded a monolithic cellular or fibrillar material that was stable and could be handled and examined by SEM (Figures 5 - 6). We have reported these and other perfluorinated organogelators that not only slightly increase the viscosity of supercritical CO_2, but form gels which upon removal of solvent leave self-sustained foams.[141] This work was carried out in collaboration with the research groups of Prof. Eric Beckmann and Prof. Robert Enick in the Department of Chemical and Petroleum Engineering at the University of Pittsburgh.

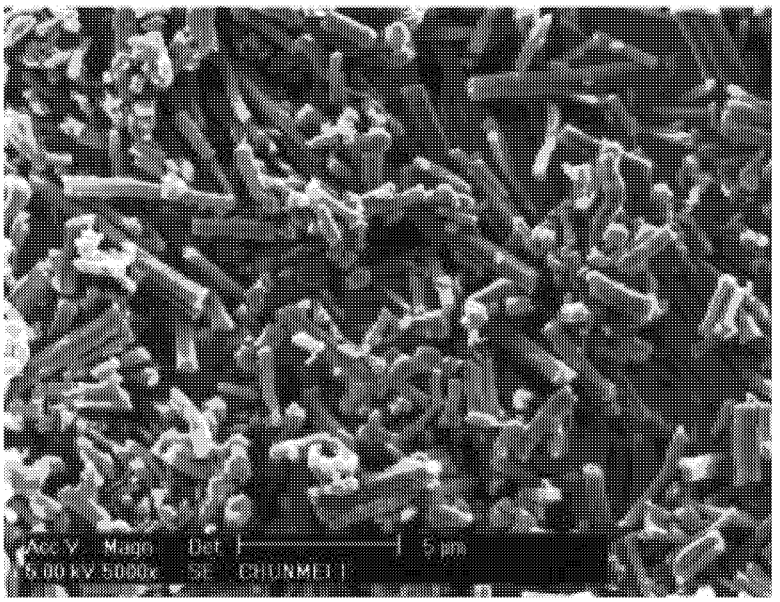

Figure 5 SEM photograph of foam produced by 4 wt % of **24** in supercritical CO_2 (magnification 5000x)

Figure 6 SEM photographs of foams formed from 2 wt % of **24** in supercritical CO_2

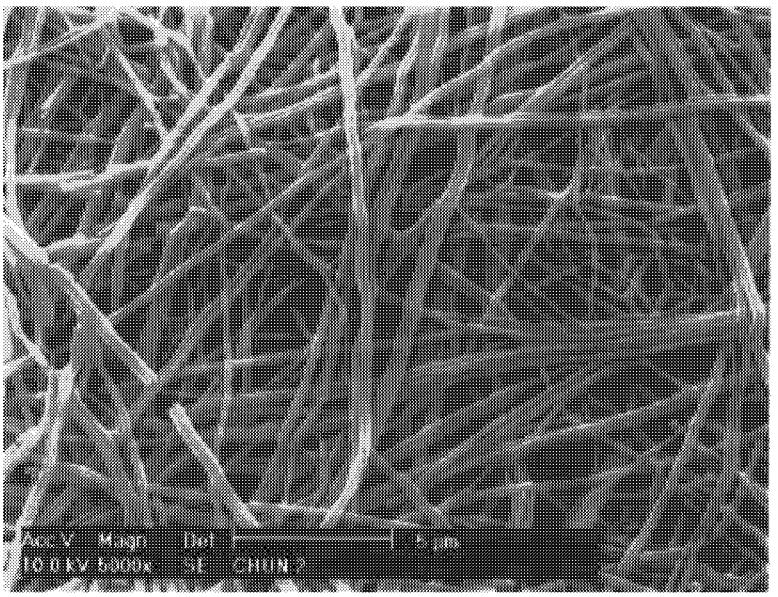

(magnification 5000x)

We found that variations in the structure of the molecules led to changes in the morphology of the foams. When 24 is dissolved in CO_2 at slightly less than 5% weight, a cellular material that exhibits the morphology of "stacks" of small parallelograms is produced. Despite the dense appearance of this material, its bulk density is reduced by 97% relative to the parent material. As can be seen in Figure 5, the pores (the spaces between the parallelograms) are submicrometer in size. Lengthening the spacer from hexyl to dodecyl (25) produces a foam with a more conventional porous structure, larger cells, and a slightly higher bulk density. Changing the concentration of the agents in solution resulted in striking changes in the morphology of the foams. Lowering the concentration of 24 in CO_2 to <2.5 weight % (all other conditions the same) produces a material with submicrometer pores and fibrillar in morphology (Figure 6). The fibrillar morphology is the one most familiar to us and is observed in many organogels studied by SEM. A number of issues remain to be explored, including understanding the mechanism for morphology development in the foams and hence why we have observed such striking changes in morphology upon changing either molecular structure or concentration.

These structures show promise in their development as microcellular materials. The process is a one-step, CO_2-based route for generation of low bulk density organic analogs to silicate aerogels. Some applications of such materials are catalyst and separation supports, low-dielectric materials, insulation, tissue engineering scaffolds. Current methods to generate these materials (organic and inorganic) involve multiple process steps and large volumes of solvent. Commercial foaming processes using CO_2 are by contrast "greener" but they do not generate the combination of low bulk density and submicrometer pore size.

We also wanted to explore if the morphology of the organogelators was similar to the perfluorinated analogs. We removed the solvent from the gel making use of freeze-drying methods. We have also removed the solvent out of the gel matrix of **14** by freeze-drying from 1,1,1-trichloroperfluoroethane gel and from a benzene solution. Scanning electron micrographs show formation of a porous sheet matrix from the freon solution and fibers from the benzene solution (Figure 7). The fibers formed by **14** from the benzene solution are not as well defined as its perfluorinated analog.

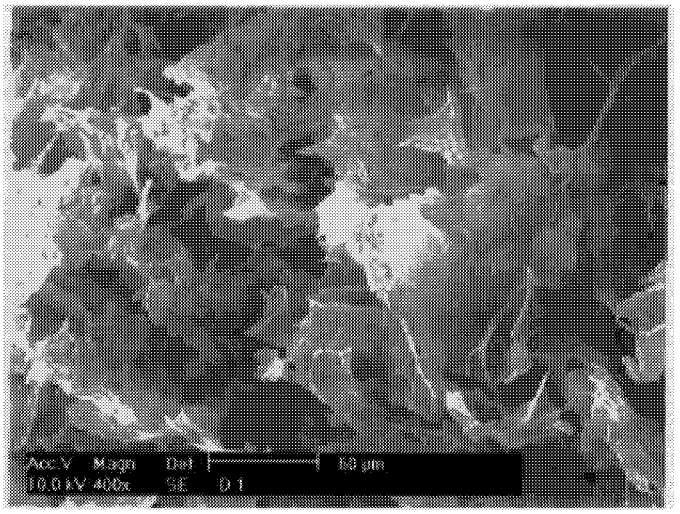

(a)

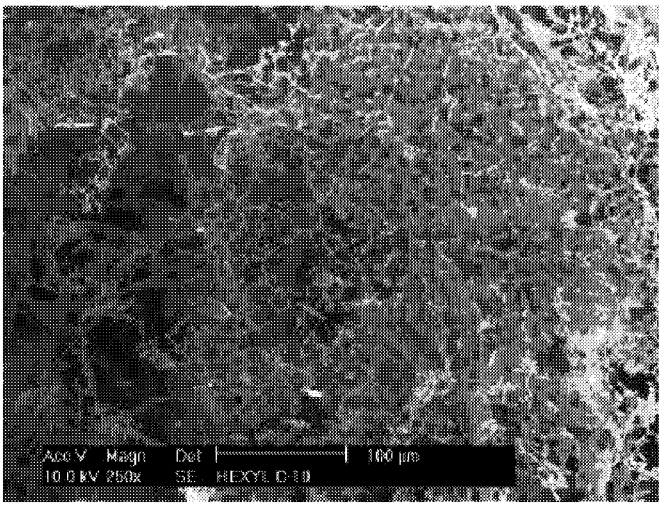

(b)

Figure 7 SEM of **14** after the solvent has been removed by freeze drying methods from a solution of 1,1,1-trichloroperfluroethane (**a**) and benzene (**b**) at 5.2 mM concentration

We synthesized a family of aspartate methyl esters (**27-30**) with the main purpose of growing X-ray quality crystals (See Scheme 7). However, these compounds can also be used as controls for studying the aggregation of these bis-ureas in solution.

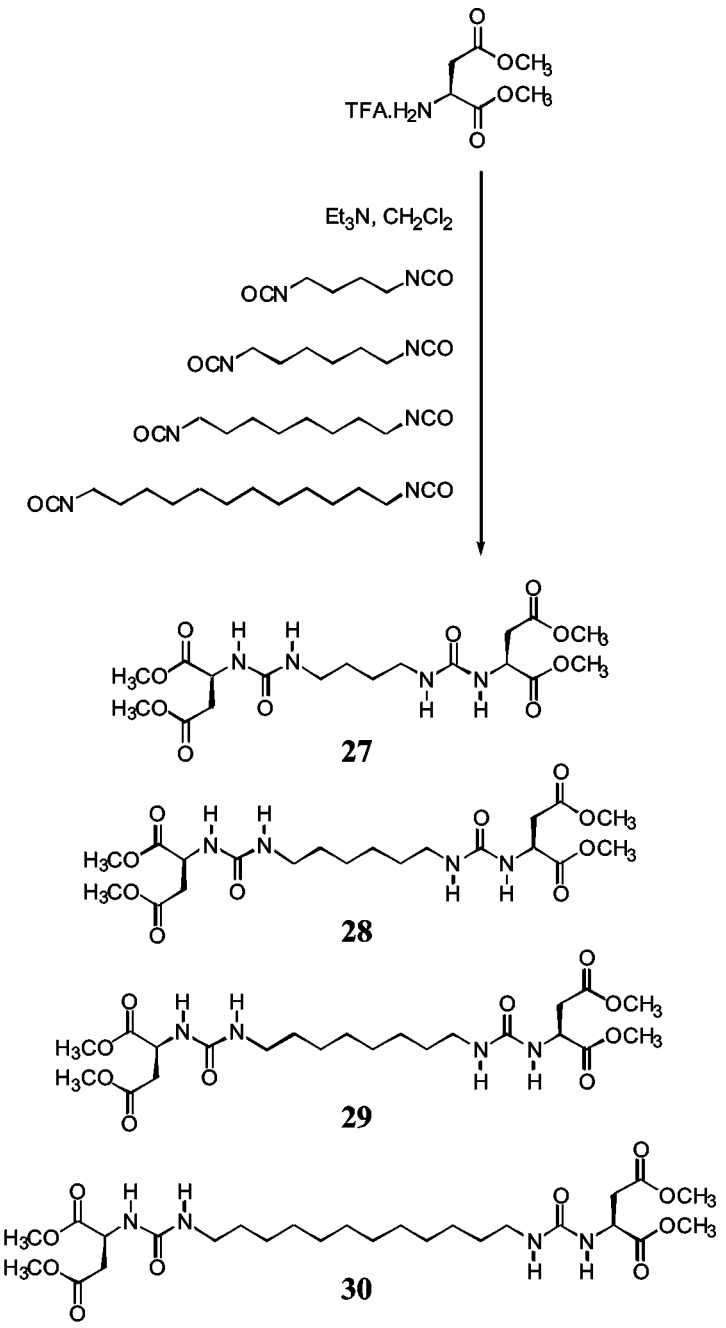

Scheme 7 Synthesis of methyl ester aspartate derivatives **27-30**.

Attempts to grow X-ray quality crystals from any of these compounds was not successful. Interestingly, although none of these compounds exhibit any gelation properties, upon evaporation of the solvent a white solid was left from a 30 mM solution of **28** in CH_2Cl_2. The solid resembled the foams observed from perfluorinated compounds and was examined by SEM. To our surprise the morphology of the solid is fibrillar as shown in Figure 8

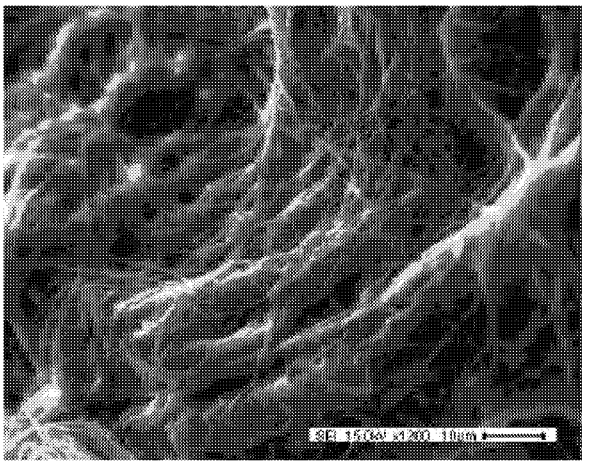

(a)

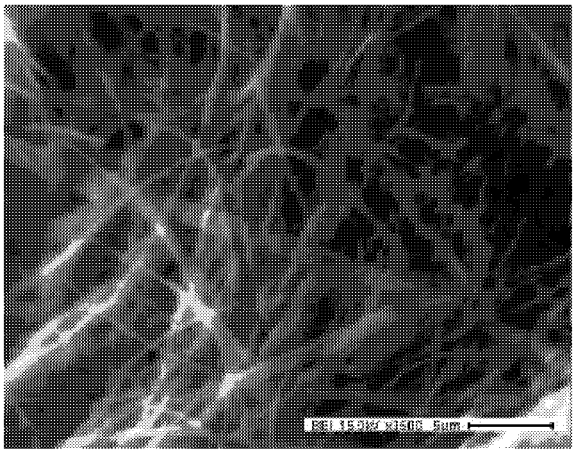

(b)

Figure 8 Fibrillar morphology is observed when CH_2Cl_2 is allowed to evaporate from a solution of 30 mM of **28**. (**a**) magnification 1200x (**b**) magnification 3500x

Conclusions

We have synthesized small organic molecules that can gel a variety of solvents including CO_2, freons and perfluorinated solvents at low concentrations. The morphologies of these gels depend on concentration and molecular structure, but are in most cases fibrillar. In the case of the perfluorinated derivatives, upon removal of the CO_2, these gels produce free-standing foams with cells with an average diameter smaller than 1 micrometer and a bulk density reduction of 97% relative to the parent material. We believe the structures are held together by hydrogen bonding of the bis-urea groups. However, the hydrophobic interactions of the long alkyl chains are indispensable for gel formation. In the next Chapter we will present new ideas to make use of this class of compounds and study the hydrogen bonding interactions.

Ch. 5. Non-Fluorous Copolymers and Hydrogen Bonding Triureas

In this report, several non- fluorous polymers have been synthesized and tested to see if they are CO_2-soluble. These polymers were designed based on introduction of carbonyl group, which has specific interaction (Lewis acid -base nature) with CO_2, and the group which shows low cohesive energy density. Poly(propylene glycol) was the first polymer we considered, because it has low flexible chain, Tg, and actually low molecular weight poly(propylene glycol) has been proved to be CO_2-soluble. However, poly(propylene glycol) becomes CO2-insoluble when the molecular weight is higher than 2000. So, the carbonyl-modified poly(propylene glycol) was designed and synthesized to improve the solubility in CO_2. Secondly, because methyl group may reduce the cohesive energy of the compound, we designed the poly(vinyl esters) series. This work has not been finished yet, but the poly(vinyl acetate)s with different molecular weight have been synthesized and tested in CO_2, the results shows they are CO_2-soluble. Finally, a hydroxyl-end polycarbonate was designed and synthesized based on the CO_2-soluble Propylene oxide/CO_2 copolymer.

RESULTS:

1. Poly(propylene glycol) with acetate groups on the side chain

(1) Synthesis

Copolymers of glycidol and propylene oxide were synthesized by cationic polymerization using BF_3 as initiator. The obtained polymers were then reacted with acetyl chloride to cap the hydroxyl groups on the side chain.

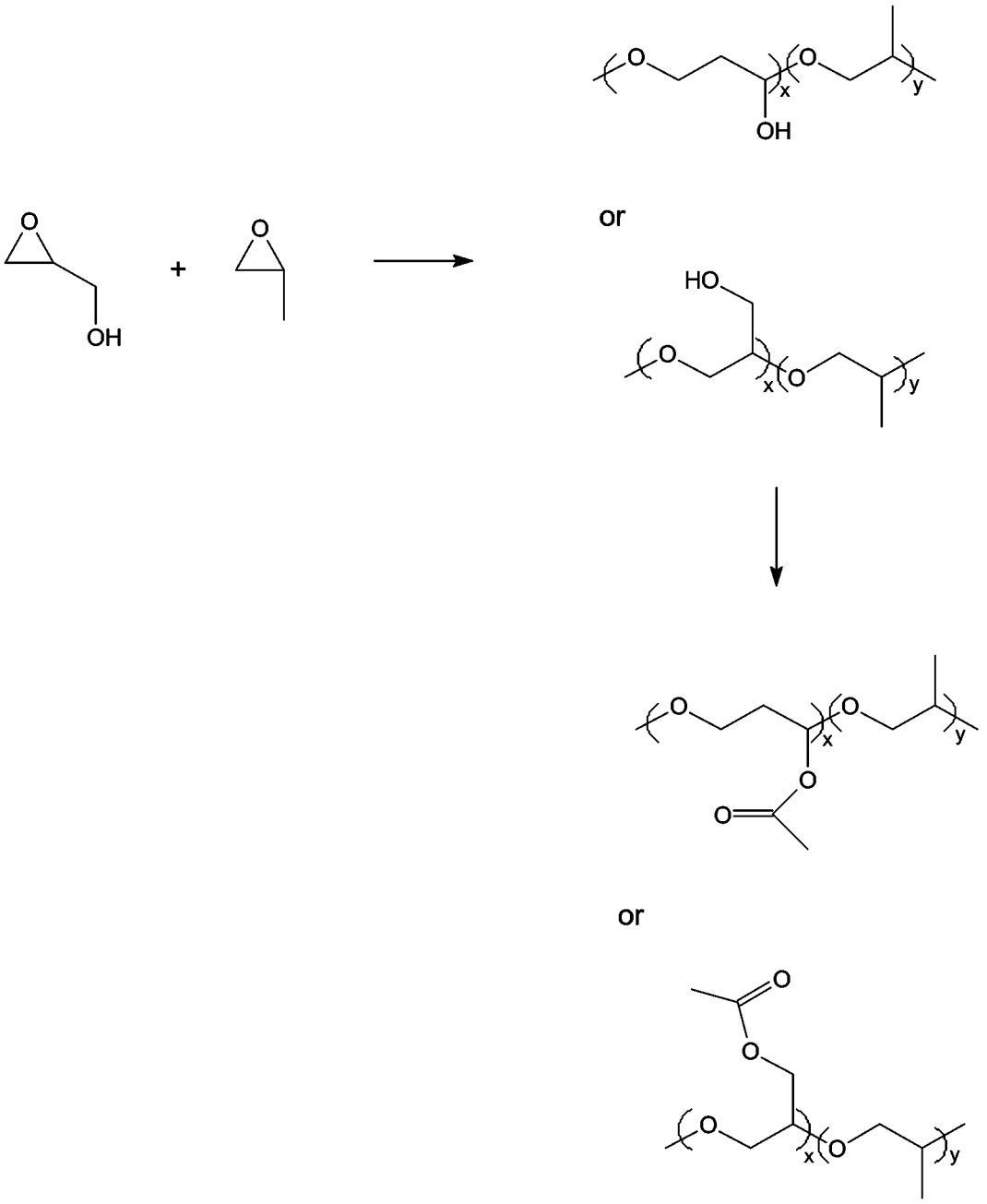
O
OH
+
O
or
HO
x
y
O
O
or

(2) Cloud point in CO_2

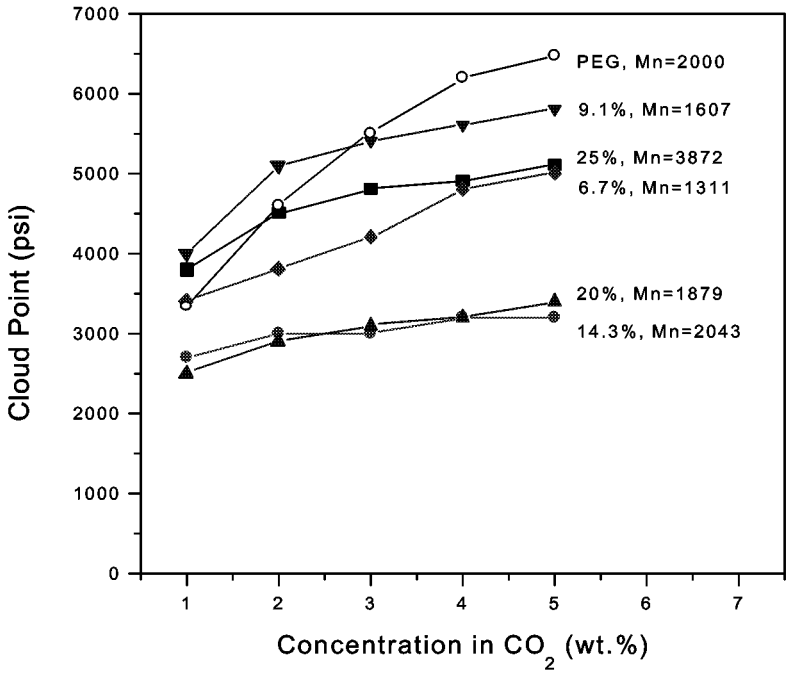

Fig. 1. Cloud point of acetyl-capped PO-Glycidol copolymer. (content of acetyl group is calculated by using propylene oxide and glycidol feeding mole ratio, and shown as percentage in the figure.)

2. Poly(vinyl esters)

(1) Synthesis

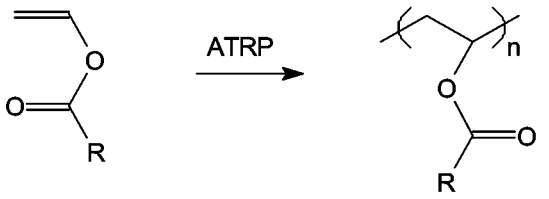

R= CH_3, or $C(CH_3)_3$

Poly(vinyl acetate) (PVAc) and poly(vinyl pivalate) (PVPi) were synthesized by Atomic Transfer Radical Polymerization (ATRP) using CCl_4 as initiator and Iron(II) acetate as ligand.

(2) Cloud point in CO_2

The cloud point of poly(vinyl ester)s was shown below. Poly(vinyl acetate)s with Mn of 7700 and 13000 can dissolve in CO_2 at room temperature. And they have flat cloud point curve from concentration of 0.5 wt.% to 5 wt.%. The Poly(vinyl pivalate) (PVPi) with Mn 8500 and Mw/Mn=1.68 did not dissolve in CO_2 at low concentration with pressure lower than 7000 psi.

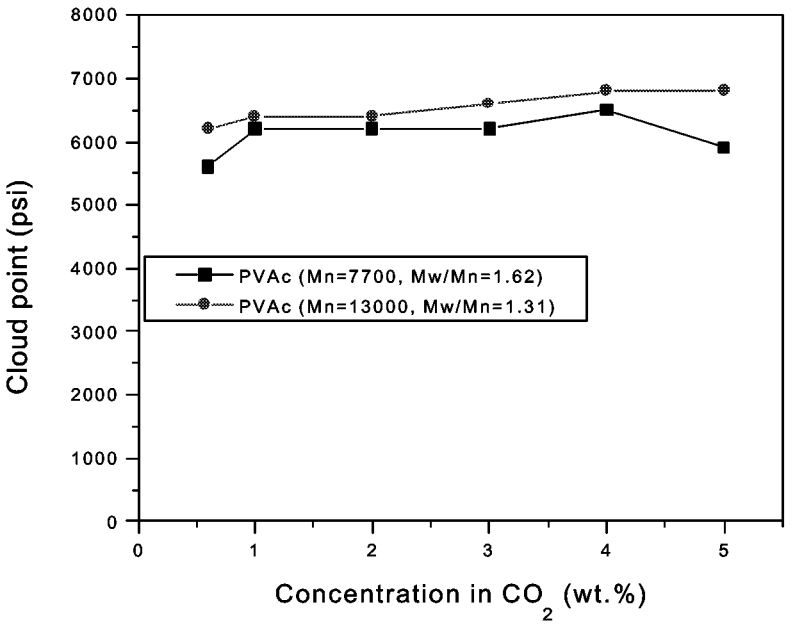

Figure 2. Cloud point of Poly(vinyl acetate)s in CO_2.

3. Polycarbonate

(1) Synthesis

Polycarbonate shown below was synthesized by ring opening polymerization of ethylene carbonate under Sn catalyst (dibutyltin dilaurate) at 160 °C. This polymer has about 48 mol.% carbonate in the structure according to NMR result.

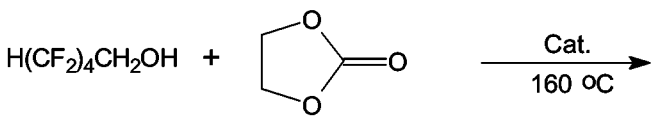

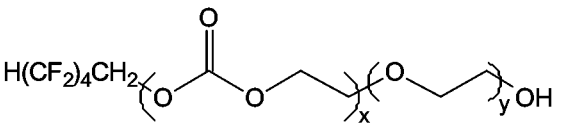

(2) Solubility in CO_2

The polymer doesn't dissolve in CO_2 at room temperature and 7000psi with concentration from 3.0 wt.% to 0.6 wt.%.

4. Small hydrogen bonding compounds

(1) Triurea with Di(ethylene glycol) n-butyl ether tails

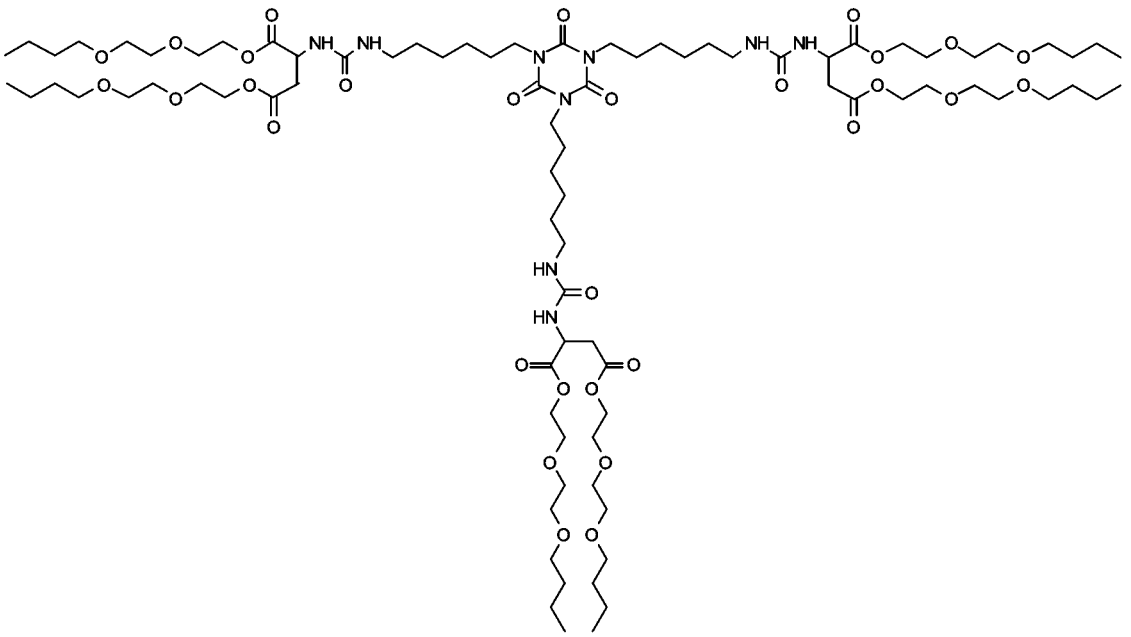

The compound with poly(ethylene glycol) repeat units is CO_2-soluble. However, the triurea shown above does not dissolve in CO_2 at 100 °C and pressure of 7000 psi.

(2) Triurea with Di(propylene glycol) methyl ether tails

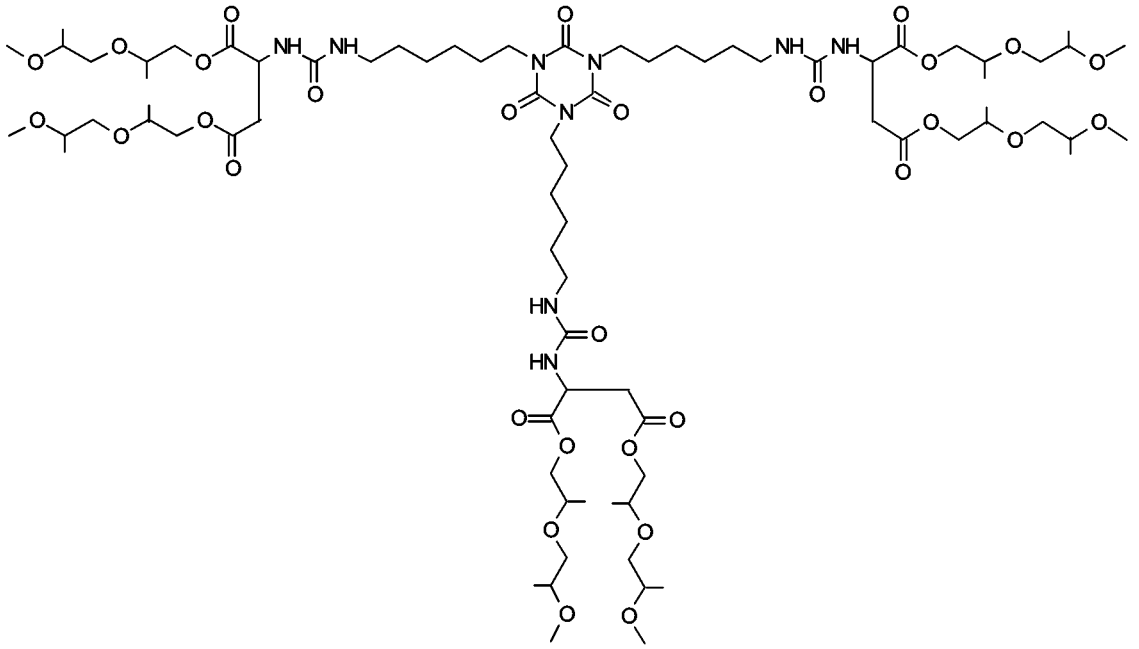

This sample does not dissolve in CO_2 at 100 °C and pressure of 7000 psi.

(3) Triurea with poly(propylene glycol) methyl ether tails

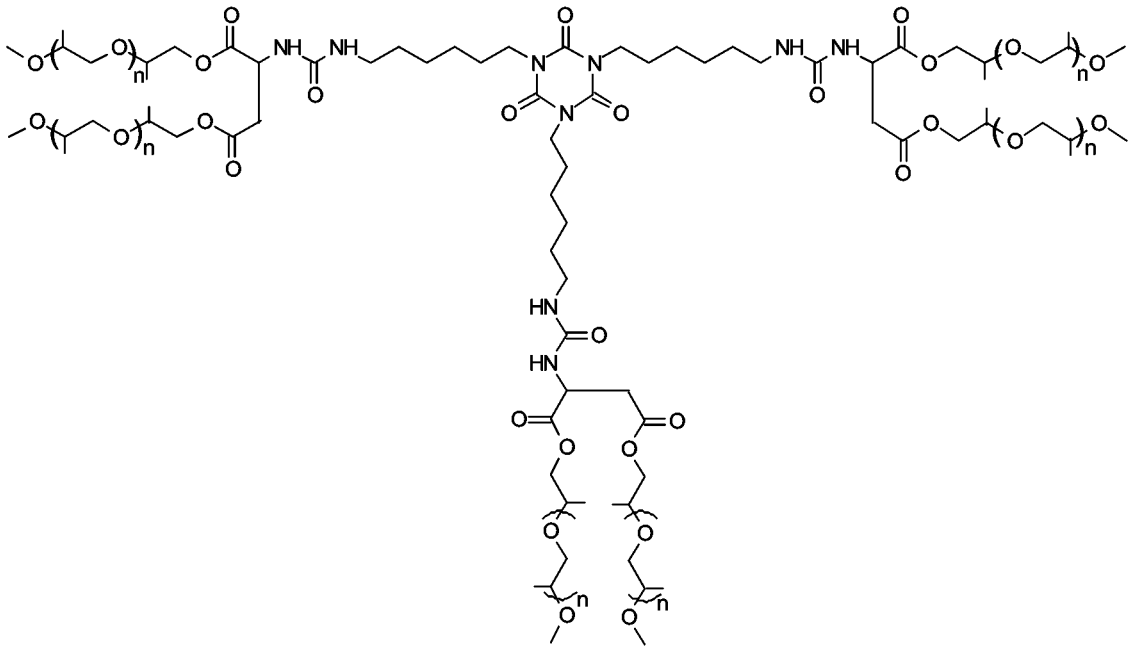

This triurea has poly(propylene glycol) (Mn=1200) as tails. The low molecular weight poly(propylene glycol) is a non-fluorous, CO_2-soluble polymer. Unfortunately, the triurea shown above does not dissolve in CO_2 at 100 °C and pressure of 7000 psi.

Chapter 6. The Effect of Spacer Length and Number of Aromatic Rings In The Copolymer of Aromatic Acrylates with Fluoroacrylate on CO_2-Solubility and Viscosity Enhancement

Unpublished PhD Proposal of

Sevgi Kilic;

Data Not Yet Published

1. Carbon Dioxide as a Flooding Agent in Enhanced Oil Recovery

After application of primary (drilling under natural reservoir pressure) and secondary production (recovery by artificial maintenance of pressure by water, called waterflooding) of petroleum oil, much of the oil still remains behind in place due to inefficiency of these recovery processes. With the increasing demand for petroleum oil versus limited petroleum beds, it became unavoidable the discovery of more advanced techniques. Newly developed techniques fall under the broad heading of Enhanced Oil Recovery (EOR). The aim in EOR is to increase the production of crude oil beyond the limit recoverable by primary and secondary production methods. CO_2, being as the second expensive flooding fluid after water, has been used in Enhanced Oil Recovery for many years. CO_2 is non-flammable, low toxic, completely miscible with crude oil and classified as non-VOC. As well as above features, its low cost, availability in large quantities and environmentally benign nature render it as the potential flooding agent for EOR. Advantageously, it is in gaseous state at atmospheric conditions. It means CO_2 can be separated from the oil by simply releasing the pressure after the recovery.

In CO_2 flooding (also called CO_2 miscible displacement), Carbon dioxide is injected into the oil-bearing porous media at reservoir temperature, which is usually between 80 ^{o}F and 250 ^{o}F. The pressure of CO_2 is maintained above the minimum miscibility pressure to ensure its solvency with oil. Thus, unlike water flooding in secondary oil recovery, CO_2 can dynamically develop effective miscibility with petroleum oil and therefore displace the oil left behind by waterflooding.

2. Statement of Problem

The foremost disadvantage of CO_2 as an oil-displacing agent is its low viscosity, 0.03-0.10 cP at reservoir conditions (Fig. 2.1) while the oil to be displaced has viscosity of 0.1-50 cP. The low viscosity of CO_2 results its higher mobility (defined as permeability/viscosity of that fluid in porous media) compared to that of reservoir oil, causing mobility ratio to be greater than one. Mobility ratio is defined as the ratio of mobility of displacing fluid to the fluid which is being displaced. Much larger than one values of mobility ratio means that displacing fluid, i.e. CO_2, moves more easily than the displaced fluid. As a result, the carbon dioxide tends to "finger" towards production well without contacting much of the oil in the reservoir, resulting in low sweep efficiency (Fig. 2.2). Even if it is possible to achieve high displacement efficiency for the oil contacted, because of the fingering, efficiency of the process reduces. For maximum displacement efficiency, mobility ratio should be ≤ 1. Although mobility ratio can be made smaller, i.e. improved, by lowering the viscosity of oil, increasing the viscosity of the displacing fluid CO_2, increasing the effective permeability to oil, and decreasing the effective permeability to the displacing fluid CO_2, the most feasible way to lower the mobility ratio is to increase the viscosity of displacing fluid CO_2.

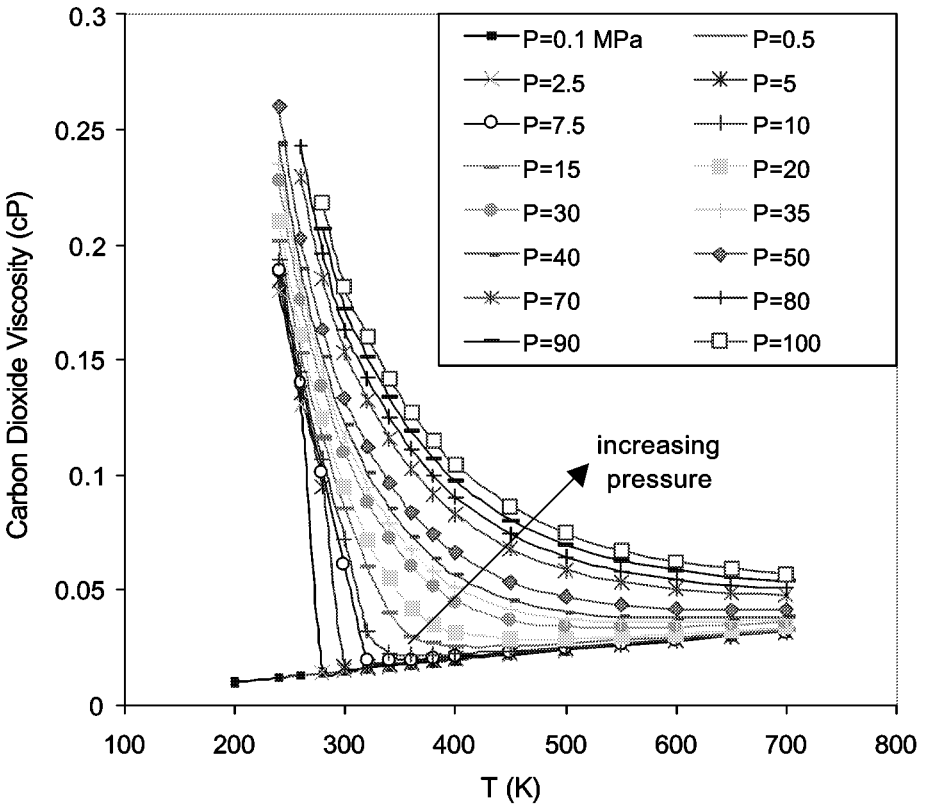

Figure 2.1. Change of viscosity of CO_2 with temperature at different pressures[v].

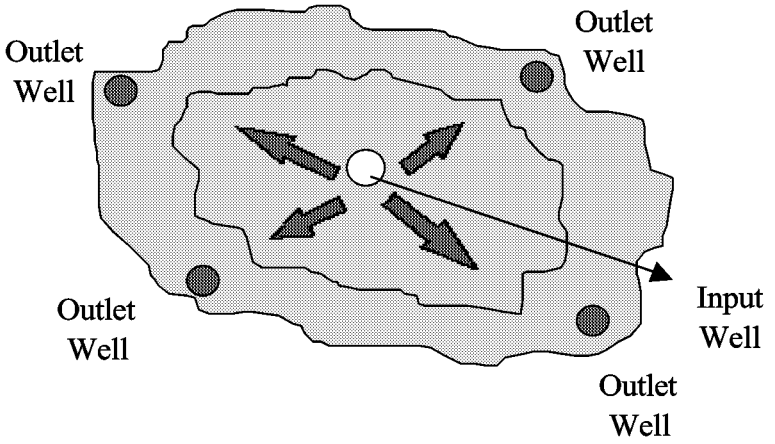

(a) CO_2 Flooding: Ideal Case

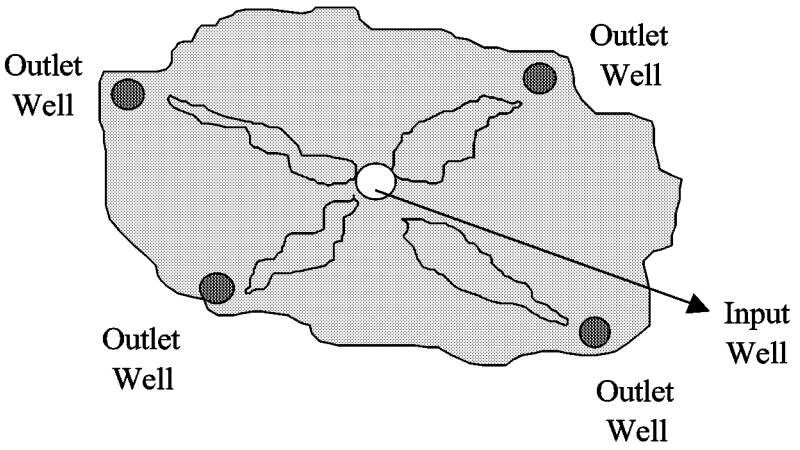

(b) CO_2 Flooding: Actual Behavior

Figure 2.2. CO_2 Flooding in EOR: (a) Ideal case, (b) Actual behavior[vi].

3. Previous Attempts to Decrease the Mobility of CO_2

In last two decades, a number of attempts have been made to identify a thickener for carbon dioxide to decrease its mobility and thus increase greatly the quantity of producible oil during EOR. A thickener that would be considered as a candidate for EOR should be inexpensive, safe and stable at reservoir conditions.

Heller et. al were the first group to study and report data on use of direct thickeners for dense CO_2. They evaluated the effect of viscosity increasing capability of commercially available polymers[vii,viii,ix]. None of the polymers that they tested was successful enough to induce viscosity enhancement in CO_2 due to extremely low solubility of these polymers. Despite of the unpromising results, based on their findings, they made some generalizations for features of polymers soluble in CO_2. In their study, they have found that for a polymer to be able to dissolve in CO_2, polymer should be amorphous, irregular in structure to maximize the entropy of mixing. Taking these findings into consideration; afterwards, they have synthesized polymers with various molecular weights in their laboratory. Although they were slightly more soluble, these polymers did not promote any significant increase in the viscosity. One important result that they reported, however, was that higher molecular weight polymers are much more effective in viscosifying CO_2.

Heller and co-workers also studied the possibility of using hydrocarbon based telechelic ionomers as an effective thickener for dense CO_2. Telechelic ionomers are the polymers with low molecular weight and having ionic groups at each end of the polymer chain. These compounds are known to have a thickening ability in light alkanes via

association of ionic groups forming pseudo-network structure. However, their effort to thicken CO_2 via sulfonated polyisobutylene concluded with failure due to the low solubility of alkyl based ionomers in dense CO_2, leading to no increase in viscosity[x].

Carbon dioxide shows good miscibility character with the light component of crude oil. Poor sweep efficiency of the process results from immiscibility of CO_2 with high molecular weight components due to unfavorable mobility of CO_2. For an effort to overcome this problem, Llave et. al brought the idea of adding an entrainer to CO_2[xi,xii]. The entrainer serves as a miscible additive (cosolvent) that modifies the phase behavior of carbon dioxide and enhances the solubility of crude oil components in the CO_2-rich phase, resulting in a thickened gas phase. The presence of the entrainer itself increases the density and viscosity of gas phase. Moreover, with the extraction of higher-molecular-weight hydrocarbons from the crude oil, further improvement in the mobility can be obtained. Although the viscosity increased substantially with the addition of entrainer, i.e. 1565 % at 44 mole % of 2-ethylhexanol, this much of cosolvent is not acceptable for EOR. The increase at low concentration of entrainer was very low; for example, 6 % viscosity increase with 0.5 mole % of 2-ethylhexanol.

Irani and co-workers succeeded considerable increase in viscosity of CO_2 by using commercially silicon polymers[xiii,xiv,xv]. But large amount of toluene had to be introduced as a cosolvent to enable the polymer to dissolve. For example, they reported hat the increase in viscosity is around 90-fold for neat CO_2 with a mixture of 6-wt% polymer, namely polydimethyl siloxane, 20 wt % toluene and 74 wt % CO_2 at 130 ^{o}F and 2500 psi. In their published work, they demonstrated that the use of viscous CO_2 in

corefloods accelerated oil recovery and delayed the early breakthrough of CO_2.

Normal micelles and microemulsions in aqueous solutions are known to be capable of increasing solution viscosity. Enick et. al extended this idea to CO_2 solutions and attempted to increase the viscosity by using commercially available surfactants[xvi,xvii,xviii,xix]. None of the commercially available surfactants were found soluble in CO_2. Therefore, no viscosity result could be attained.

In the literature, it was also reported that low molecular weight compounds could associate in solution via secondary forces to form pseudo polymer network structure, resulting in significant increase in the viscosity of the solvent. Dunn and Oldfield reported that tri-n-butyltin fluoride could increase the viscosity of light alkanes by forming linear polymer chains via dipole-dipole interactions between the fluorine and tin of adjacent molecules[xx]. Disappointedly, this compound was very slightly soluble in CO_2 (<2 wt.%) and it did not have any effect on viscosity. In order to enhance its solubility in CO_2, pentane was used as cosolvent. Several orders of magnitude CO_2-viscosity enhancement was obtained using 1 wt % tri-n-butyltin fluoride, but only using large amount (~50 mole %) of pentane[xvi].

Hydrocarbons are known to be insoluble in dense CO_2. Enick et. al showed that solubility can be improved by fluorination of an alkane or alkyl chain[xxi]. Semifluorinated alkanes were demonstrated to be good gelation agent for alkanes, forming microfibrillar morphology. Several CO_2/semifluorinated alkane systems were tested for gel formation. However, the resulting gel was not a single, viscous, transparent phase, but rather semifluorinated alkane microfibers interlocked forming a network, with the liquid filling the cavities. This type of gelling agent is not desirable for flow in porous media[xxi].

Heller and co-workers presented the gelation results of a variety of organic fluids and supercritical CO_2 with 12-hydroxystearic acid (HSA). In the absence of any cosolvent, HSA is indeed insoluble in dense CO_2. However, with the addition of a significant amount of cosolvent, such as 10-15 % ethanol, HSA was found to be completely soluble in CO_2, yet forming translucent or opaque gels[xxii].

Terry et. al attempted to increase the viscosity of CO_2 by in-situ polymerization of monomers miscible with CO_2. Authors polymerized the light olefins in an environment of supercritical CO_2 using commonly available initiators. However, due to insolubility of the resulting polymer in CO_2, this approach could not find application in EOR[xxiii]

In summary, from above review, it is clear that none of traditional hydrocarbon thickeners or commercially available compounds is a good candidate for CO_2 thickening. Success was hindered due to insolubility of these compounds in dense CO_2 or their requirement for a large amount of co-solvent to dissolve. However, economically and environmentally, it is desirable to have the thickener dissolved in dense CO_2 without a need for a cosolvent. Therefore, these results urged researchers to design and synthesize thickeners specifically for CO_2. For a polymer to be able to be a good candidate for thickening, its solubility in CO_2 is first needed.

In the last decade, with the identification of CO_2-philic functionalities, successful design of CO_2 thickeners became possible. DeSimone and coworkers reported that silicones and fluoropolymers exhibit higher degree of solubility in CO_2 at moderate pressures and temperatures than other hydrocarbon based polymers[xxiv,xxv,xxvi]. In a subsequent publication, they reported that solubility of a CO_2-phobic polymer could also be achieved if a certain amount of CO_2-philic character is introduced in the polymer

chain[xxvii]. Not a long ago, DeSimone published the first work in the literature for CO_2 direct thickener without a need for a cosolvent. They observed that approximately 5-10 wt % of fluoroacrylate polymer, namely poly (1,1-dihydroperfluorooctyl acrylate), caused 3-8 fold increase in CO_2-viscosity[xxviii]. In close past, Shi et. al synthesized CO_2-soluble fluorinated polyurethane telechelic disulfates with molecular weights up to 29,900 determined by titration experiments. Their result showed that a concentration of 4 wt % of aforementioned polymer increases the solution viscosity 2.7 fold relative to neat CO_2 at room temperature and 34.5 MPa. Above 4 wt %, the polymer, however, was found insoluble in CO_2[xxix]. That was the world record until it was shown that, in our group, Fluoroacrylate-Styrene random copolymers could cause a greater increase in CO_2-viscosity[xxx]. The increase in viscosity was attributed to stacking of aromatic rings in the styrene molecule (aromatic ring association). Increase in viscosity was found to be depended on the composition of the copolymer, and 29mole%Styrene-71mole%fluoroacrylate copolymer was found as optimum composition for maximum increase. Further increase in composition was resulted as decrease in viscosity due to more likely intramolecular interactions rather than intermolecular interactions. The maximum increase at this optimum composition was found as 250 fold at a concentration of 5-wt% of copolymer at room temperature and 34.5 MPa. However, 10-100 folds increase in viscosity at dilute polymer concentrations, which is our target, remains as a challenge to be investigated.

4. Design of CO_2-Direct Thickeners

4.1. Thermodynamics of Solubility of Polymers in CO_2

For successfully design and synthesis of CO_2-thickeners (polymers), first, solubility of the polymeric materials in CO_2 is essential. In order for a polymeric material to be dissolved in a given solvent, the Gibbs free energy of mixing, ΔG_{mix} must be negative. The Gibbs free energy of mixing is given by

$$\Delta G_{mix} = \Delta H_{mix} - T.\Delta S_{mix} \qquad (4.1)$$

where ΔH_{mix} and ΔS_{mix} are the change of enthalpy and entropy, respectively, on mixing. Enthalpic interactions depend predominately on solution density and on polymer segment-segment, solvent-solvent and polymer segment-solvent interaction energies. ΔS_{mix} depends on both the combinatorial (or configurational) and the noncombinatorial entropy of mixing. Although it is not possible to decouple the impact of entropic and enthalpic contributions to the Gibbs free energy of mixing, we need to consider the effect of each one separately by applying to the principle of molecular thermodynamics for successfully design of CO_2-soluble polymers.

For a dense CO_2 solution, ΔH_{mix} is expected to be approximately equal to the change in internal energy on mixing, ΔU_{mix}. Following expression is given for the internal energy of an isotropic, homogeneous mixture relative to an ideal gas mixture[xxxi]:

$$\Delta U_{mix} \approx \frac{2\pi\rho(P,T)}{kT}\sum x_1 x_2 \int \Gamma_{12}(r,T) g_{12}(r,\rho,T) r^2 dr \qquad (4.2)$$

where x_1 and x_2 are mole fractions of solvent CO_2 and polymer, respectively, Γ_{12} (r,T) is the intermolecular pair potential energy of the solvent and the polymer segments, g_{12} (r,ρ,T) is the radial distribution function, r is the distance between molecules, ρ(P,T) is

the solution density, and k is the Boltzman constant. Imbedded in the Eq. 4.2 is the radial distribution function that describes the spatial positioning of molecules or segments of molecules with respect to each other. Given that the internal energy of the mixture is roughly proportional to density, the solubility of a polymer is expected to improve by increasing the system pressure (hydrostatic pressure). However, the polymer will dissolve only if the energetics are weighted toward polymer segment-solvent interactions relative to polymer segment–segment or solvent-solvent interactions. For certain polymer-CO_2 mixtures, hydrostatic pressure alone will not overcome a mismatch in energetic between the polymer and CO_2.

Following expression is a rough approximation to the intermolecular potential energy between CO_2 and polymer segments, Γ_{12}, which depends on the physical properties of the solvent and polymer:

$$\Gamma_{12}(r,T) \approx -\left[C_1 \frac{\alpha_1 \alpha_2}{r^6} + C_2 \frac{\mu_1^2 \mu_2^2}{r^6 kT} + C_3 \frac{\mu_1^{\,2} Q_2^{\,2}}{r^8 kT} + C_4 \frac{\mu_2^{\,2} Q_1^{\,2}}{r^8 kT} + C_5 \frac{Q_1^2 Q_2^2}{r^{10} kT} + Complex \quad formation \right] \tag{4.3}$$

where α is the polarizability, μ is the dipole moment, Q is the quadrupole moment, $C_{1\text{-}5}$ are constants[xxxii]. Eq. 4.3 is not expected to predict an accurate value of the interaction of a polymer segment with another segment or with solvent molecules since restrictions due to chain segment continuity is not counted.

Not shown in the Eq. 4.3 is the induction interactions since the contribution of dispersion and polar interactions to the potential energy is much larger compared to induction interactions[xxxiii]. The first term in the equation counts for dispersion interactions, and

depends on only polarizability, not on temperature. However, dipolar and quadrupole interactions are inversely proportional to temperature so that the importance of these interactions increases significantly as the solution temperature is lowered. At elevated temperatures, thermal energy disrupts the configurational alignment of the polar moments of the molecules. Due to its structural symmetry, CO_2 has no dipole moment ($\mu=0$); it does have a quadrupole moment ($Q=-4.3x10^{-26}$ $erg^{1/2}cm^{5/2}$). The quadrupole nature of CO_2 works against it in solubilizing polymers that are predominantly comprised of nonpolar repeat units since CO_2's quadrupole interactions dominate, especially at low temperatures. Conversely, CO_2 is expected to be feeble solvent for polymers with repeat units that have a large dipole moments since, then, the interchange energy is dominated by polymer-polymer interactions rather than polymer-CO_2 interactions, especially at low temperatures where polar interactions are magnified. Therefore, the solubility of polymers in CO_2 strongly depends on degree of polarity of polymer from the energetic point of view. Partially fluorinated polymers exhibit high degree of solubility due to polar-quadrupole interactions with CO_2[xxxii,xxxiv,xxxv]. Specific interactions such as complex formation can also contribute to the attractive pair potential energy. Kazarian and co-workers have used spectroscopic techniques to characterize the interactions between CO_2 and polymers. They demonstrated that polymers possessing $\bar{e}$-donating functional groups (e.g. carbonyl groups) exhibit specific interactions with CO_2[xxxvi]. They argued that this complex formation is most probably of a Lewis acid-base nature, where the carbon atom of the CO_2 molecule acts as an $\bar{e}$-acceptor and the carbonyl oxygen in the polymer as an $\bar{e}$-donor.

To sum up, from the energetic viewpoint, the balance of intermolecular interactions in solution gives an idea about whether a polymer will dissolve in CO_2. By defining interchange energy as ω[xxxiii],

$$\omega = z\left[\Gamma_{12}(r,T) - \frac{1}{2}\left[\Gamma_{11}(r,T) + \Gamma_{22}(r,T)\right]\right] \qquad (4.4)$$

where z is the coordination number. Γ_{11} and Γ_{22} are calculated in a similar manner to Eq. 4.3 for the polymer and solvent. The positive value of the interchange energy suggests the solution is in its lower energy state, in other words, enthalpic energy of mixing favors dissolution of polymer in solvent CO_2.

Based on Flory-Huggins lattice theory for a mixture whose molecules differ greatly in size (like polymer solutions), the contribution of the combinatorial entropy on the Gibbs free energy of mixing is given by[xxxiii]

$$\frac{\Delta G^C}{RT} = N_1 \ln \Phi_1^* + N_2 \ln \Phi_2^* + \chi \Phi_1^* \Phi_2^* (N_1 + rN_2) \qquad (4.5)$$

in which

N_1 is the number of solvent molecules, and N_2 is that of polymer molecules, and r is the number of segments in a polymer chain. So the total number of lattice sites is (N_1+rN_2). Φ_1^* and Φ_2^* are the fractions of the sites occupied by the solvent and polymer, respectively, defined as

$$\Phi_1^* = \frac{N_1}{N_1 + rN_2} \qquad (4.6)$$

and

$$\Phi_2^* = \frac{rN_2}{N_1 + rN_2} \qquad (4.7)$$

Eq. 4.5 is a well-known Flory-Huggins relationship, and χ in the equation is the Flory-Huggins interaction parameter, determined by the energies which characterize the interactions between pairs of polymer segments, between pairs of solvent molecules, and between one polymer segment and one solvent molecule. A general form of Flory-Huggins interaction parameter is given by[xxxvii]

$$\chi = \chi_s + \frac{\chi_h}{T} \qquad (4.8)$$

in which χ_s counts for the entropic contribution and χ_h for enthalpic contribution.

The first two log terms in the equation account for combinatorial entropy of mixing, and are always negative. But, the negative contribution from combinatorial entropy decreases as the molecular weight of the polymer increases. The interaction parameter, χ, is generally restricted to values that are ≥ 0; but, it takes negative values only in the presence of specific interactions. Negative value of χ represents favorable contributions to the change in the free energy of mixing arising from the presence of specific intermolecular interactions (Lewis acid-base interactions as mentioned above). Therefore, in its most simple form, the energy of mixing essentially reduces to a balance between the combinatorial entropy part and the last term in the equation.

Here, we don't argue that the Flory-Huggins equation for real polymer solutions does provide an accurate description of the thermodynamics properties of polymer

solutions, but there is little doubt that this relatively simple theory contains most of the essential features for the polymers in solution. Indeed, Flory-Huggins theory is the basis of polymer thermodynamics in solution; and almost all theories derived to date are based

in someway on Flory-Huggins theory to enlighten further understanding of thermodynamics of polymeric solutions.

Entropic and Enthalpic contributions to interaction parameter in Eq. 4.8 are defined as[xxxvii,xxxviii]

$$\chi_s = \frac{1}{z}\left(1-\frac{1}{r}\right)^2 \qquad (4.9)$$

$$\chi_h = \frac{\upsilon_1}{R} A_{12} \qquad (4.10)$$

Imbedded in Eq. 4.9 is the r standing for number of segments in the polymer chain, and z for lattice coordination number which reflects the number of contacts that polymeric segments can make with neighboring segments. z may have a value between 6 and 12 depending on the type of packing, i.e. the way in which the molecules are arranged in three dimensional space[xxxiii]. In Eq. 4.10, υ_1 is the solvent molar volume, and A_{12} is the interchange energy density, defined as[xxxvi]

$$A_{12} = \left(c_{11} + c_{22} - 2c_{12}\right) \qquad (4.11)$$

where c_{ij}'s characterize the intermolecular forces acting between molecules (or molecular segments) i and j. For the pure components, c_{11} and c_{22} are the cohesive energy densities of the solvent and polymer[xxxviii]:

$$c_{11} = \frac{\Delta E_1^{\upsilon}}{\upsilon_1} = \lambda_1^2 + \tau_1^2$$

$$c_{22} = \frac{\Delta E_2^v}{\upsilon_2} = \lambda_2^2 + \tau_2^2 \qquad (4.12)$$

where ΔE_1^v and ΔE_2^v are, respectively, the energy of vaporization of solvent and polymer to a gas at zero pressure. λ_1 and λ_2 are defined, respectively, as the nonpolar solubility parameters of solvent and polymer, τ_1 and τ_2 as polar ones. Cohesive energy density is a measure of the strength of the intermolecular forces keeping the molecules together, or in other words, that is the energy needed to remove a molecule from its nearest neighbors. The quantity c_{12} represents the intermolecular forces acting between solvent and molecular segments of polymer in solution. c_{12} may include dispersion forces, dipole-dipole forces, dipole-induced dipole forces, and specific interactions (solvation) between solute and solvent[xxxiii,xxxviii]:

$$c_{12} = F_{disp}(\lambda_1, \lambda_2) + F_{di-di}(\tau_1, \tau_2) + F_{ind}(\lambda_1, \tau_1, \lambda_2, \tau_2) + F_{spec\cdot\text{int}} \qquad (4.13)$$

in which

$F_{disp}(\lambda_1, \lambda_2)$ represents the dispersion forces between nonpolar solvent and nonpolar polymer:

$$F_{disp}(\lambda_1, \lambda_2) = \lambda_1 \lambda_2 \qquad (4.14)$$

$F_{di-di}(\tau_1, \tau_2)$ represents the interactions between permanent dipoles and quadrupoles in the solute and solvent:

$$F_{di-di}(\tau_1, \tau_2) = \tau_1 \tau_2 \qquad (4.15)$$

$F_{ind}(\lambda_1, \tau_1, \lambda_2, \tau_2)$ counts for the induction forces between a permanent dipole (or quadrupole) and and induced dipole. It may be represented by $\Psi(\lambda_1\tau_1, \lambda_2\tau_2)$ where ψ is

an unspecified function. $F_{spec\cdot\text{int}}$ represents the contribution to the pair interaction energy from any solvation (association and complex formation) which may occur in solution[xxxviii]. One has to keep in mind that contribution of induction forces is very small relative to dispersion forces, even for strongly polar substances; therefore, they may be neglected most of the time[xxxiii].

For the special case where neither solvent nor solute is polar, A_{12} is defined as

$$A_{12} = (\delta_1 - \delta_2)^2 \qquad (4.16)$$

where $\lambda_1=\delta_1$ and $\lambda_2=\delta_2$ since τ_1, τ_2 =0. Any specific interactions occurring between solvent and polymer segments add a positive term to c_{12} and correspondingly decrease A_{12}. This means that χ_h also decreases and thus mutual solubility of the two species is enhanced. This qualitative result is intuitively correct, since any specific interaction, such as exist between a carbonyl group and CO_2, helps to "pull" the polymer into solution. The general form of interaction parameter for nonpolar systems, arising from only dispersive interactions, is given as

$$\chi = \frac{1}{z}\left(1-\frac{1}{r}\right)^2 + \frac{\upsilon_1}{RT}(\delta_1 - \delta_2)^2 \qquad (4.17)$$

From Eq. 4.5 above, we can conclude that for good solubility, χ should be small (if positive) or negative in order to render Gibbs free energy of mixing negative, and this occurs only when δ_1 approaches to δ_2 for nonpolar systems in which only dispersive interactions exist. A criterion of a good solvent for a given polymer is then

$$\delta_1 \cong \delta_2 \qquad (4.18)$$

Equation 4.18, most of the time, provides a useful practical guide in selection of polymer-solvent pair for nonpolar systems. However, as reported by Johnston et. al as

well[xxxix], solubility parameter approach does not apply to CO_2-polymer systems. In that work, they reported that, for example, hexane and CO_2, having solubility parameters very close to each other's in value, showed that different solubility behavior to different polymers. More specifically, they found that polypropylene and polybutadiene are quite soluble in hexane, although they are not in CO_2; contrariwise, poly(1,1-dihydroperfluorooctyl acrylate) is quite soluble in CO_2 although it is not in hexane. The main reason behind this results from large quadrupole moment of CO_2. In the creation of the solubility parameter approach above for nonpolar systems, it was assumed that attractive interactions between molecules are primarily due to dispersion forces. Since CO_2 has a large quadrupole moment, contributions to cohesive energy density from quadrupole forces should be also considered as well as dispersion force. In that case, the energy of vaporization is divided into two parts[xxxiii]

$$\Delta E = \Delta E_{disp} + \Delta E_{quad} \tag{4.19}$$

As a result, two cohesive energy densities can be computed, corresponding to the two types of intermolecular forces:

$$c_{disp} \equiv \frac{\Delta E_{disp}}{\upsilon} \tag{4.20}$$

$$c_{quad} \equiv \frac{\Delta E_{quad}}{\upsilon} \tag{4.21}$$

The cohesive energy density for solvent CO_2 becomes

$$c_{11_{total}} = c_{11_{disp}} + c_{11_{quad}} \tag{4.22}$$

where

$$c_{11_{quad}} = \frac{\beta Q_1^4}{kT\left(\frac{\upsilon_i}{N_A}\right)^{13/3}} \qquad (4.23)$$

where Q_1 is the quadrupole moment of CO_2, υ_1 the molar liquid volume, N_A is Avogadro's number, k is the Boltzmann's constant, T is the absolute temperature, and β is a numerical dimensionless constant[xl].

The interaction parameter, A_{12}, becomes

$$A_{12} = \left(c_{11_{disp}} + c_{11_{quad}} + c_{22} - 2c_{12_{disp}} - 2c_{12_{quad}}\right) \qquad (4.24)$$

Using the intermolecular forces theory, Myers showed that[xxxviii]

$$c_{12_{quad}} = \frac{\beta Q_1^2 Q_2^2}{kT\left(\frac{\upsilon_{12}}{N_A}\right)^{13/3}} \qquad (4.25)$$

For υ_{12} Myers used the combining rule

$$\upsilon_{12}^{1/3} = \frac{1}{2}\left(\upsilon_1^{1/3} - \upsilon_2^{1/3}\right) \qquad (4.26)$$

The term $c_{12_{quad}}$ might be negligible if the polymer doesn't have a quadrupole moment. From Eq. 4.24, we can arrive to the conclusion of that, since the solvent is a "constant" in our work, by lowering the cohesive energy density of the polymer, we can enhance the solubility of polymer in CO_2. Studies showed that certain polymers (such as fluoroethers, fluorinated acrylates, silicones) exhibit CO_2-philic character (i.e. tendency to dissolve in CO_2 at significantly lower pressures than their hydrocarbon analogs)[xxxix,xli,xlii,xliii]. These polymers have low surface tension, and thus low cohesive energy densities. Therefore, polymers with relatively weak self-interactions, and thus low cohesive energy densities, should exhibit enhanced solubility in CO_2.

Concerning the contributions from configurational entropy of mixing, one needs to design polymeric materials in such a way so as to provide high free volume and high chain flexibility. The increase in free volume and flexibility is reflected as a decrease in the glass transition temperature of the polymer (T_g). Flexibility of side chains is more pronounced on T_g than flexibility of the main chain[xliv]. Charlet et al. reported that branching increases the free volume of the polymer by simply reducing the intermolecular interactions between polymer segments that would arise due to short-range molecular orientation offered by a high content of linear segments without pendant groups[xlv]. Lepilleur et al also observed that number of shorter side chains grafted to polymer backbone has larger effect on the solubility than longer chains having the same concentration of side chains grafted to the backbone, but with less number. They argue that this effect is more likely due to free volume effect, and thus favorable entropy of mixing[xlvi].

In summary, as a rule of thumb, for a given polymer to dissolve in CO_2, the Gibbs free energy of mixing must be negative. From the energetic point of view, although solvent quality of CO_2 can be enhanced by changing the hydrostatic pressure, dissolution of the polymer is possible only if energy of cross-interactions between the polymer and CO_2 outweighs that of self-interactions. CO_2 has a large quadrupole moment. Strong quadrupole-quadrupole interactions between CO_2 molecules render it a feeble solvent for polymers. Therefore, polymer introduced into CO_2 should possess some polarity so that polar-quadrupole interactions between the polymer and CO_2 outweigh the quadrupole-quadrupole interactions between CO_2 molecules. Note that too much polarity can increase the polar-polar interactions between polymer chains, making them stay preferably

together. Presence of Lewis acid-base type interactions between carbonyl groups and CO_2 molecule favors dissolution by simply 'pulling' the polymer chains into CO_2 phase, enhancing the entropy of mixing. Those interactions are imperative from the point of view of overwhelming the strong quadrupole-quadrupole interactions between CO_2 molecules as well. Since the solvent is "constant" in this work, the weaker the interactions between polymer chains, the easier for the polymer to form single phase with CO_2. Degree of interactions between polymer chains is determined by cohesive energy density. Its lower value favors dissolution in CO_2. Indeed, certain polymers (fluoroacrylates and silicones) show relatively better solubility character in CO_2 mainly due to their low cohesive energy density as well as polar-quadrupole interactions between polymer and CO_2. Polymer configuration is another issue playing major role in solubility. Presence of side chains eases dissolution due to disrupted packing of chains. By incorporation of side chains, the free volume increases as well, which then, carbonyl group can be easily attacked by CO_2 molecules, promoting better mixing.

4.2. Stacking of Aromatic Rings

Stacking of aromatic rings is a matter of noncovalent interactions and known for many years[xlvii]. Application of these interactions to synthetic polymers allows the creation of higher order architecture[xlviii]. In stacking of the rings, equilibrium structure corresponds to a balance between attractive and repulsive forces.

The general accepted picture of stacking is the delocalization of electrons on the carbon atoms of benzene and slight residual positive charges on the hydrogen atoms. This inherent polarity of benzene, an electron-rich central core being surrounded by an electron-poor periphery of hydrogens, gives rise to T-shaped arrangement (Figure 4.1). In other words, this electrostatic description energetically favors the T-shaped (edge-to-face) arrangement[xlix,l,li,lii,liii]. The hydrogen atoms are attracted to the more electron rich carbon atoms to give a herring-bone arrangement of molecules. As the polycyclic aromatic hydrocarbon becomes larger, the carbon-to-hydrogen ratio increases. The result is that larger polycyclic aromatic hydrocarbon molecules stack one above the other more strongly[xlviii,lii,liv].

The energy of interaction between two stacking molecules in solution includes association of the two molecules and displacement of solvent. Hunter and Sanders declared that in nonpolar organic solvents, the electrostatic interactions with the solvent will be negligible, and so the dominant electrostatic interaction would come from the association energy[xlvii]. In addition, aromatic solvents are known to significantly disrupt stacking interactions because the solvent molecules effectively solvate the solute, opening up stacked conformations. So, carbon dioxide, being non-polar and a non-aromatic, favors attractive interaction of aromatic rings by stacking. Indeed, for any solute molecules to associate in solution to form higher order structure, solvent molecules

are required not to interfere with solute molecules so that a stable higher order architecture can be attained in the solution.

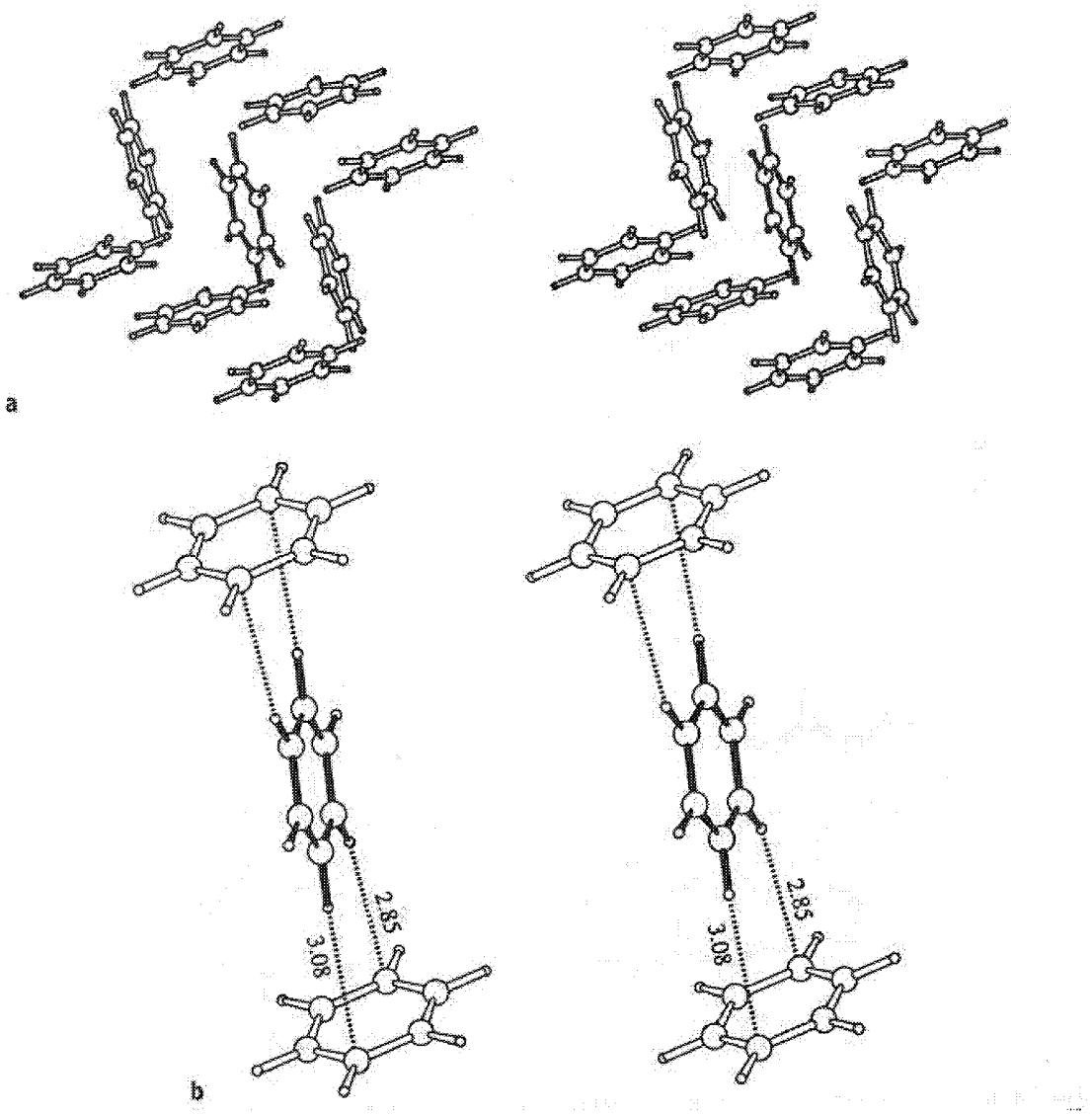

Figure 4.1. Packing of molecules in crystalline benzene, showing: **a.** a stereoview of the overall structure; **b.** the shortest C···H distances in A° (representative of an H···π interactions[lii]

5. Research Objectives and Approach

Our research objective is to lower the mobility ratio in CO_2-flooding by increasing the viscosity of CO_2 via dissolution of minimum amount of polymeric material in CO_2. Our goal is to increase the viscosity 10-100 fold at concentrations less than 1 wt % of polymer. The key to designing a thickener is to achieve, first, the solubility of polymer in CO_2. To date, polymers of fluoroacrylates (see Fig. 5.1) have proven to be highly CO_2-philic, their presence at sufficient amount in any molecular structure has the capability of "pulling" even highly CO_2-phobic groups into CO_2 phase. In our design strategy, we chose to include the fluoroacrylate moiety in our thickener, at least for the initial work.

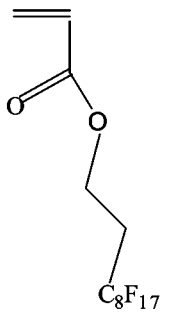

Figure 5.1. Structure of fluoroacrylate monomer used in our work.

Despite its highly CO_2-philic character, homopolymers of fluoroacrylate unfortunately, do not give rise to considerable increases in the viscosity of CO_2[lv]. This is due to lack of any associating group in the body of fluoroacrylate homopolymer. This result necessitates the incorporation of another group (a second monomer) to the backbone of fluoroacrylate

polymer, where the second monomer should impart an attractive intermolecular association among the polymer chains in CO_2, forming higher order architectures in order

to promote enhancement in viscosity of CO_2. Fluoroacrylate should still be in the body of final polymer (a copolymer) and its content should be at the level needed to maintain solubility in CO_2. From work previously reported by Huang et al.[xxx], we know that aromatic rings can associate by forming noncovalent bonds via stacking, and thus result in enhancement in viscosity. Consequently, we designed the second monomer to contain an aromatic ring. Noting that Lewis acid-base interactions between carbonyl groups and CO_2 are favorable, we also included a carbonyl group in the second monomer, leading to generation of an aromatic acrylate monomer. We hypothesize that, by separation of aromatic ring(s) from the rigid polymer backbone by a spacer unit, the aromatic group(s) can relax to optimum geometry to achieve the strongest interactions. In the stacking profile of aromatic rings, the hydrogen atoms are attracted to the more electron rich carbon atoms to give herring-bone arrangements of molecules. So, we also hypothesize that as the polycyclic aromatic hydrocarbons becomes larger, the-carbon-to-hydrogen ratio increases in the ring; thus, larger polycyclic aromatic hydrocarbon molecules stack one above the other more strongly, resulting in higher viscosity enhancement in CO_2. The generalized Aromatic Acrylate-Fluoroacrylate copolymer structure is given in Fig. 5.2.

Since stacking of aromatic rings is related to electronic structure of the ring(s), tuning of electronic structure may have a larger effect on the strength of stacking, and thus, viscosity. We hypothesize that, by substitution of electron-donating or -withdrawing

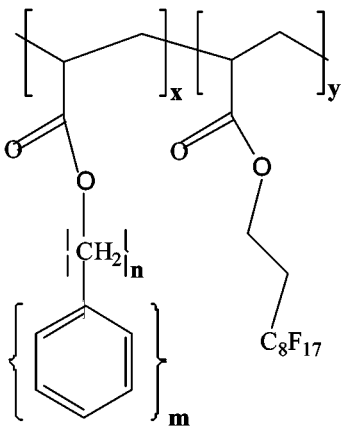

Figure 5.2. General Structure of Aromatic Acrylate-Fluoroacrylate Copolymers

groups to the ring, we can enhance the association strength of ring(s), and thus viscosity. In the selection of substituents, we are aware of that bulky groups may prevent the rings from optimum alignment for maximum stacking strength.

This research is basically focused on enhancement of viscosity of CO_2 by means of stacking of aromatic rings in solution. One can arise the question of what would be the effect if there were a non-aromatic unit in the second monomer instead of aromatic one. To answer this question, we will also investigate the effect of copolymers of fluoroacrylate with non-aromatic acrylates on viscosity, in which, they are analogous to fluoracrylate-aromatic acrylate copolymers, but only the aromatic moiety is replaced with cycloaliphatic unit.

Solution viscosity strongly depends on the size, molecular weight and polymer-solvent interactions. We hypothesize that by measuring these parameters by static light scattering, we can have a more comprehensive understanding on chain conformation in solution, size and polymer-solvent interactions, and their effects on viscosity.

Based on above hypothesis, we plan to do followings:

1. **Spacer Length:** We will synthesize copolymers at varying compositions by chancing the spacer length, but keeping the aromatic ring(s) constant. We will evaluate solubility and viscosity of these copolymers in CO_2 using variable-volume, high- pressure windowed cell.
2. **Surface Area of Overlap:** We will synthesize copolymers at varying compositions by chancing the number of aromatic rings, but keeping the spacer length constant. Different lengths of spacer unit will be investigated. These copolymers will be tested for their solubility and viscosity as well.
3. **Substitution:** After we find out the optimum spacer length and number of aromatic rings in the copolymer promoting maximum increase in viscosity, we will modify aromatic rings by substitution. We will evaluate solubility and viscosity of the copolymers with substituted rings using our high-pressure equipment and find out the effect of substituent on stacking strength of aromatic rings, and in consequence, viscosity.
4. **Copolymers with Cycloaliphatic Acrylates**: In order to compare association strength of aromatic rings by stacking, we will synthesize a copolymer with an alkyl acrylate; in addition, we will do series of control experiments with various compositions of cycloaliphatic acrylate-fluoroacrylate copolymers. In the copolymers, spacer length will be kept the same as the corresponding aromatic acrylate, but aromatic rings will be replaced by cycloaliphatic one. These

copolymers will be evaluated their solubility and viscosity enhancement as well, and their association strength will be compared with their aromatic analogous.

5. **Chain Conformation and Size** : The effect of chain conformation and the size on viscosity will be investigated using static light scattering technique. From the measurable parameters from this technique, namely radius of gyration (R_g), molecular weight and second virial coefficient, we will examine the factors contributing viscosity enhancement.

6. Experimental Protocol
6.1. Synthesis of Copolymers

Copolymerization was carried out by bulk free radical polymerization of monomers in the presence of initiator AIBN. Details of the synthesis procedure are given in Appendix A. General structure of the copolymers is given in Table 6.1.

6.2. Phase Behavior Measurements

The phase behavior and viscosity measurements were performed at room temperature (~295 K) using a high pressure, variable-volume, windowed cell, with a cylindrical sample volume, Scheme 6.2. Isothermal compressions and expansions of mixtures of specified overall composition were used to determine the two-phase boundary Scheme 6.3.(a). A known amount of polymer was introduced to the sample volume, together with stainless steel mixing balls. High-pressure liquid carbon dioxide was then metered via a positive displacement pump into the sample volume, a hollow cylinder. Addition of carbon dioxide was done isothermally and isobarically by withdrawing the overburden fluid at the same time. The CO_2-polymer mixture was pressurized and mixed until a transparent single phase resulted. The system was then slowly depressurized by withdrawing the overburden fluid and thus expanding the sample volume. The pressure at which visual appearance of a second phase starts was taken as the cloud point pressure of that mixture at that concentration. Measurements were repeated by repressurizing until a single phase was observed and then de-pressurizing the system again.

Table 6.1. General Structure of the Copolymers

Copolymers	General Structure
(a) Hexyl Acrylate-Fluoroacrylate	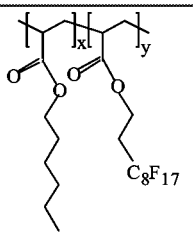
(b) Styrene-Fluoroacrylate	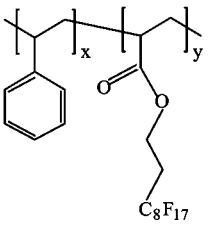
(c) Partially sulfonated Styrene-Fluoroacrylate	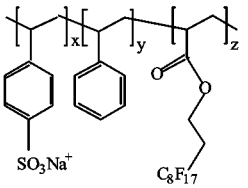
(d) Aromatic acrylate-Fluoroacrylate	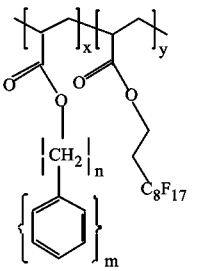
(e) Cyclic Acrylate-Fluoroacrylate	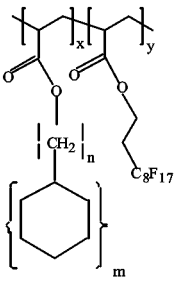

The average of 5 measurements was recorded as the cloud point pressure. Experiments were conducted over a range of compositions, thus two-phase boundary of P-x diagram was established.

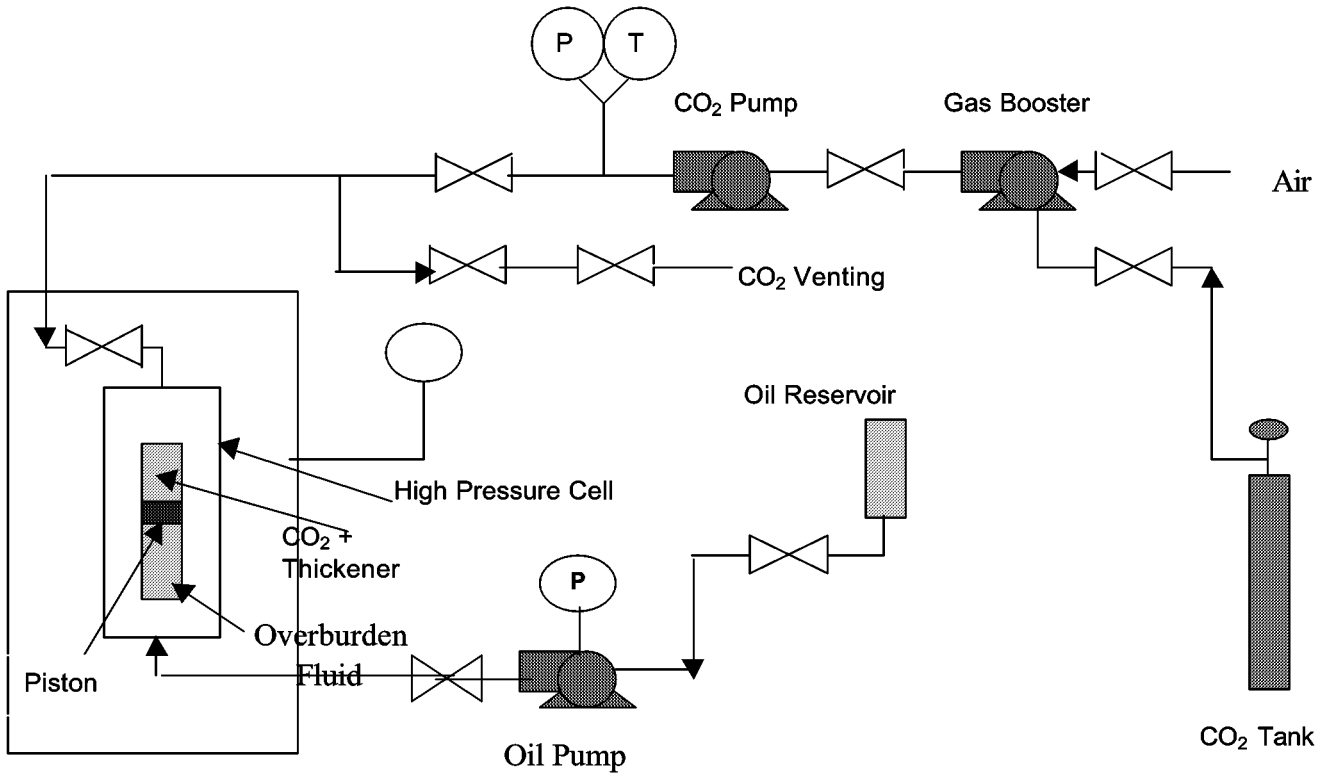

Scheme 6.2. High Pressure, Variable Volume, Windowed Cell (D. B. Robinson Cell)

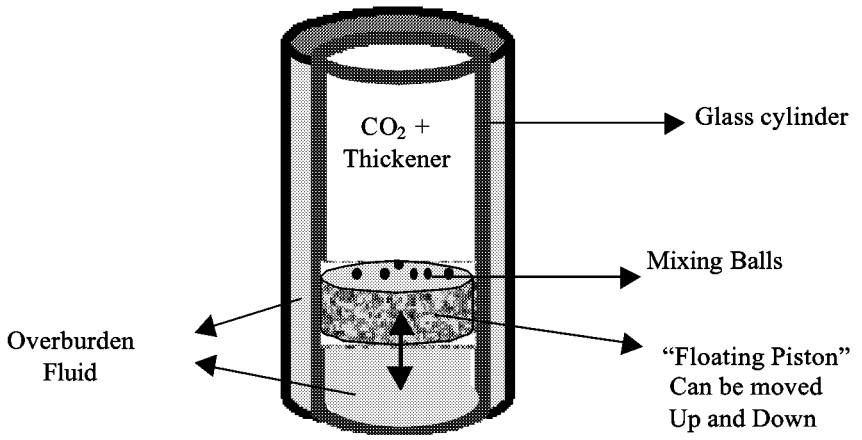

(a) Solubility Measurement

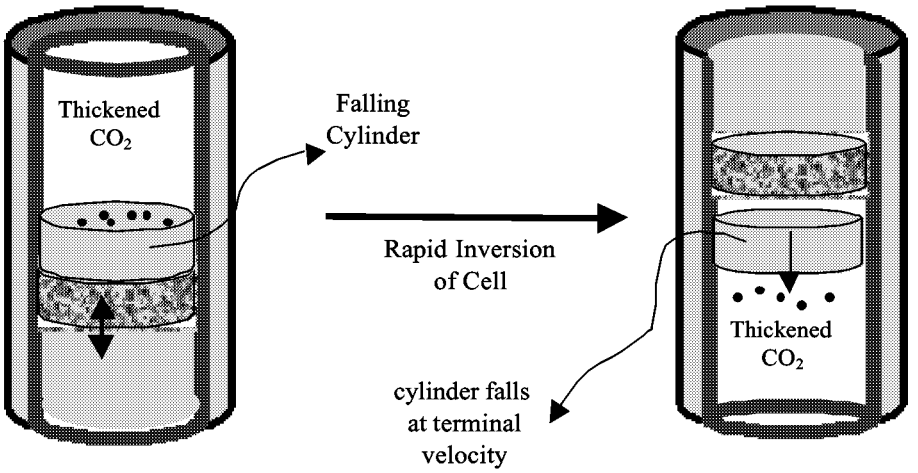

(b) Viscosity Measurement

Scheme 6.3. Sample volume of the cell used for phase behavior and viscosity measurements.

6.3. Solution Relative Viscosity Measurements

The relative viscosity of CO_2-polymer solutions was determined using the same high-pressure equipment used for phase behavior experiments. The viscosity of transparent, single-phase thickener-CO_2 solutions was determined using falling cylinder viscometer. This method relates the viscosity of the fluid to the density difference between the solid and the fluid, the terminal velocity of the cylinder, and a viscometer constant which depends on the geometry of the system. The governing equation for the system can be expressed as

$$\eta = \kappa \frac{(\rho_c - \rho_f)}{u_t} \qquad (6.1)$$

where ρ_c and ρ_f are, respectively, density of the cylinder and the fluid, and u_t is the terminal velocity of the falling cylinder. The viscometer constant is usually determined by calibration in a fluid of known density and viscosity. Although Eq. 6.1 was derived for Newtonian fluids, it can also be used for estimating the viscosity of non-Newtonian fluids provided that the shear rate is low and shear dependence of the viscosity is not considered[lvi,lvii].

Although other viscosity measurements, (e.g. capillary viscometry and flow through porous media) provide more comprehensive and precise assessments of viscosity as a function of shear rate, the falling cylinder viscometer technique is useful for the determination of significant viscosity changes in CO_2-thickener solutions. In the present work, relative viscosity of the thickened CO_2 solutions (the ratio of viscosity of thickened to that of neat CO_2) was reported because of its convenience. Assuming that the change

in density of the fluid is small upon the addition of the thickener, from the Eq. 6.1 above, it becomes clear that ratio of the viscosities is inversely equal to the ratio of terminal velocities. Using the basic relationship (velocity=distance/time):

$$\frac{\eta_{solution}}{\eta_{CO_2}} = \frac{u_{c,CO_2}}{u_{c,solution}} = \frac{t_{solution}}{t_{CO_2}} \qquad (6.2)$$

In a typical measurement of fluid viscosity, a finely machined aluminum cylinder was placed into the cylindrical sample volume before the polymer sample and the mixing balls were added. Upon equilibration of the system resulting in a single, transparent phase, the cell was rapidly inverted. It was visually ensured that cylinder falls coaxially through the cell. Measurements taken at different position of the glass cylinder indicated that the falling cylinder reaches its terminal velocity within the first 1/10 of the length of its fall, even earlier for very viscous fluids. The fall time of the aluminum cylinder was recorded over a fixed distance at constant temperature and pressure Scheme 6.3.(b). Measurements were repeated at least 5 times at each concentration and the average was taken. The same experiment was conducted using neat CO_2, and average relative viscosity is calculated from the ratio of fall times, as indicated in Eq. 6.2.

7. Results and Discussion

In previous attempts[vii,viii,ix,xii,xiii,xv,xvi,xxiii], success in designing a CO_2-thickener was hindered by low solubility of hydrocarbon-based polymers. With the identification of CO_2-philic moieties (fluoroacrylates), design of a CO_2-thickener became possible. As shown in this research also, solubility of even highly CO_2-phobic materials can be achieved with the incorporation of sufficient amount of fluoroacrylate in the final polymer. Unfortunately, a homopolymer of fluoroacrylate does not enhance the viscosity of CO_2 due to lack of associating groups in the fluoroacrylate unit[lv]. A series of aromatic acrylate-fluoroacrylate copolymers was designed and tested for their solubility and viscosity enhancing ability. The change in the series was created by changing either spacer length (number of CH_2 units indicated by "n") or number of aromatic rings (indicated by "m") or both in the aromatic acrylate unit in the copolymer. All of the copolymers were found to be soluble in CO_2 at room temperature, and increased the solution viscosity to some degree depending its type and molar composition. General structure of all the copolymers is given in Table 6.1.

7.1. Phase Behavior of Polymers in Dense CO_2

All of the polymers reported here are soluble in CO_2 at room temperature. Figure 1 shows experimental cloud point curves for one of the compositions of Styrene-Fluoroacrylate Copolymers and its partially sulfonated analogue. Although it was expected that partial sulfonation of styrene could make dissolution of the copolymer more difficult, experimental result showed that at this particular composition, location of

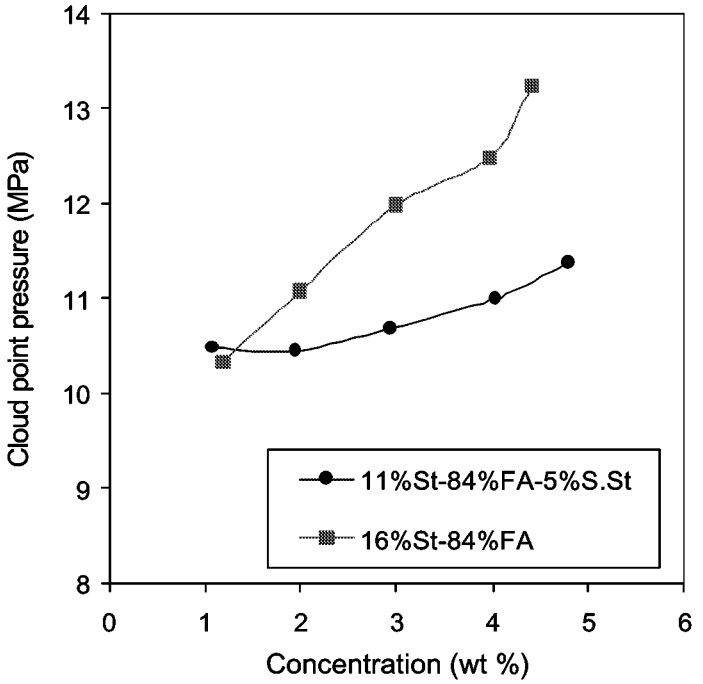

Figure 7.1. Phase Behavior of Sulfonated and Unsulfonated Styrene-Fluoroacrylate Copolymer in CO_2 at room temperature (St: Styrene, FA: Fluoroacrylate, S.St: Sulfonated Styrene)

phase boundary is lower for sulfonated copolymer than its unsulfonated analogue. This might be explained by the tendency of sulfonate group to withdraw electrons from the electron-rich aromatic ring[lviii], and thus, favorable Lewis acid-base type interactions between CO_2 and e-rich sulfonate group.

Our work is mostly focused on copolymers of fluoroacrylate and various aromatic acrylates. In this proposal, behavior of two different types of aromatic acrylate copolymers was reported. Phase behavior of Phenyl Acrylate-Fluoroacrylate copolymers is illustrated in Fig. 7.2 and that of Benzyl Acrylate-Fluoroacrylate copolymers in Fig. 7.3 as a function of concentration at various copolymer compositions. In both figures, as the aromatic acrylate content increases, solubility of the copolymer requires higher

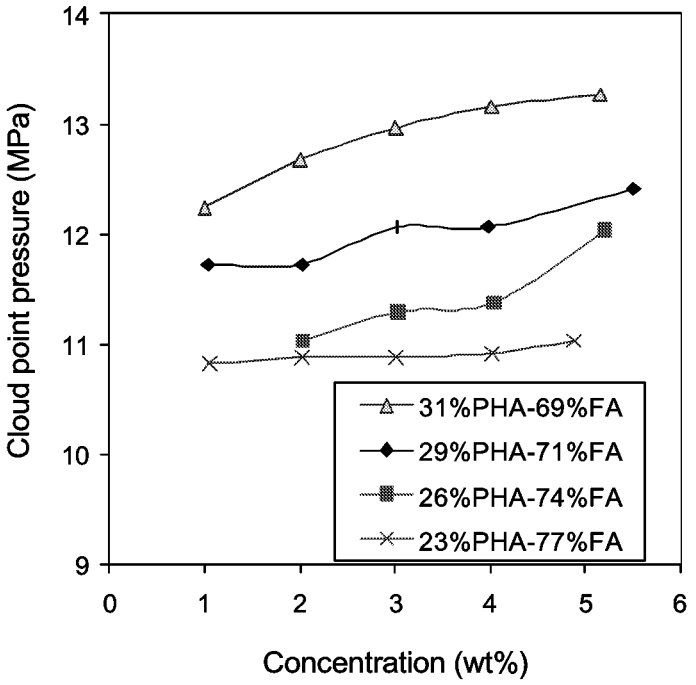

Figure 7.2. Phase Behavior of Phenyl Acrylate-Fluoroacrylate Copolymer in CO_2 at room temperature (PHA: Phenyl Acrylate, n=0, m=1; FA: Fluoroacrylate)

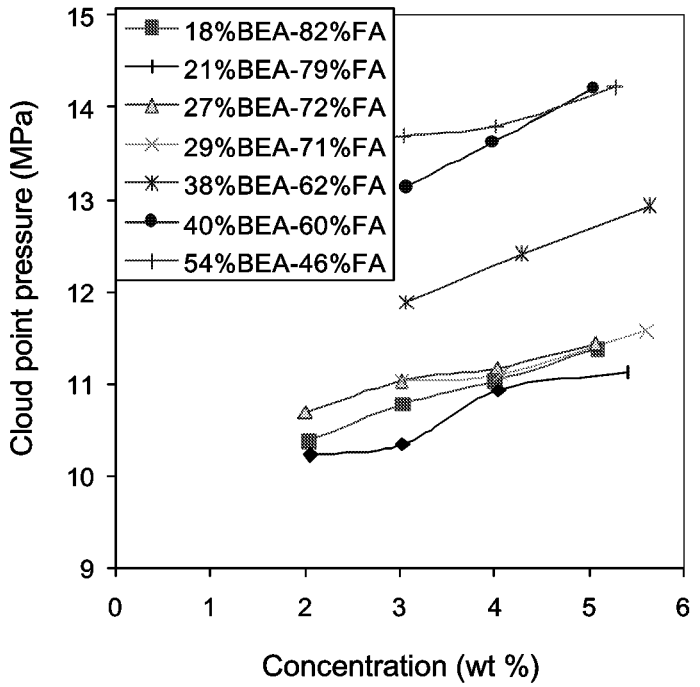

Figure 7.3. Phase Behavior of Benzyl Acrylate-Fluoroacrylate Copolymer in CO_2 at room temperature (BEA: Phenyl Acrylate, n=1, m=1; FA: Fluoroacrylate)

pressures due to highly CO_2-phobic character of aromatic acrylate component. Note that solubility of aromatic acrylate-fluoroacrylate copolymers is slightly better for the same aromatic acrylate content in the copolymer when the length of spacer unit increases in the aromatic acrylate unit. This might be due to easy access of CO_2 molecules to carbonyl group hidden by bulky aromatic ring and lowered cohesive energy density of aromatic acrylates due to increased number of CH_2 units.

Because of their viscosity enhancing ability, our attention is currently focused on copolymers of aromatic acrylates with fluoroacrylate. We have been also testing the behavior of non-aromatic acrylates in the copolymer to verify association strength of aromatics by stacking. In Figure 7.4, the phase behavior of 26%Hexyl acrylate-74%Fluoroacrylate and 16%CHA-84%FA copolymers are given. From the comparison of Fig. 7.2, 7.3 and 7.4, it can be concluded that, for the same mol percent of fluoroacrylate, polymer-polymer interactions in HA-FA copolymer is much favorable owing to highly CO_2-phobic long alkyl chain (six CH_2 units) in the copolymer, resulting in phase behavior curve to be shifted upward for the copolymer. The increased solubility with aromatic acrylate-fluoracrylate copolymers may be a consequence of the strong quadrupole moment of aromatic ring that interacts favorably with the quadrupole of CO_2[xxxii]. In this work, series of cycloaliphatic acrylate copolymers has been tested for their behavior in CO_2, in which the aromatic ring is replaced with cycloaliphatic (non-aromatic, cyclic ring) keeping the spacer length and number of rings same as parent aromatic acrylates, to verify the influence of aromatic rings on the association.

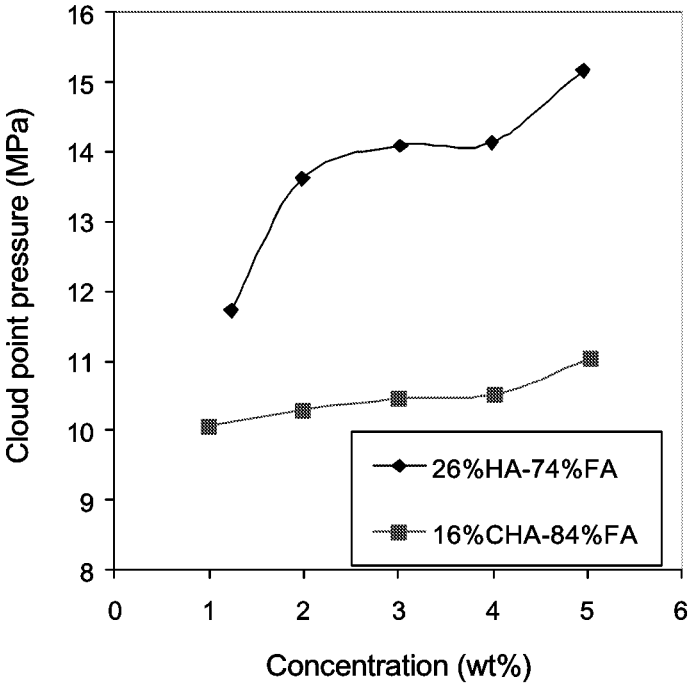

Figure 7.4. Phase Behavior of Copolymers of Fluoroacrylate with Non-Aromatic Acrylates in CO_2 at room temperature (HA: Hexyl Acrylate; CHA: Cyclohexyl Acrylate, n=0, m=1; FA: Fluoroacrylate)

The aromatic and cycloaliphatic acrylates appeared to dissolve at similar pressures. Overall, when compared styrene copolymer to aromatic acrylate copolymers (Fig. 7.1, 7.2 and 7.3), Styrene-Fluoroacrylate copolymer dissolves at much higher pressure. This results from lack of carbonyl group in the styrene molecule. Favorable Lewis acid-base type interactions between CO_2 and carbonyl group help the acrylate polymers dissolve at lower pressures.

In summary, it can be said that solubility of CO_2-phobic polymers can be attained in CO_2 by incorporation of CO_2-philic fluoroacrylate monomer. Presence of a carbonyl group in the body of CO_2-phobic monomer affects the solubility in a positive manner.

Although they both are CO_2-phobic, presence of aromatic rings instead of alkyl chain favors dissolution due to their strong quadrupole-quadrupole interactions with CO_2. Furthermore, location of phase behavior curve is strong function of content of CO_2-phobic unit in the copolymer.

7.2.Viscosity Behavior of Polymers in Dense CO_2

The power of polymers to influence fluid rheology arises from the greater volume of a macromolecule and chain entanglements in solution, unlike small molecules. Additional influence can be achieved by means of intermolecular associations. These associations should be strong enough to give rise to stable higher order macromolecular architectures, yet not form crosslinks to attain the solubility of polymer chains in the solvent. Stacking of aromatic rings in the copolymer is considered to be the primary force in this work for intermolecular association needed to raise the viscosity of CO_2. Effect of styrene-fluoroacrylate copolymer and its partially sulfonated analogue on viscosity is shown in Fig. 7.5.

Not surprisingly, the viscosity enhancement decreases as the concentration of polymer in the solution decreases. The effect on viscosity is more pronounced with sulfonated copolymer solution of CO_2 compared to unsulfonated one, especially at higher wt % of the polymer in solution. This might be explained by additional contribution from the attractive interaction between partially positive charge of Na^+ and π-face of aromatic ring[lix] as well as stacking of aromatic rings or stronger stacking tendency of the rings due the change in their electronic structure by substitution of electron withdrawing sulfonation group.

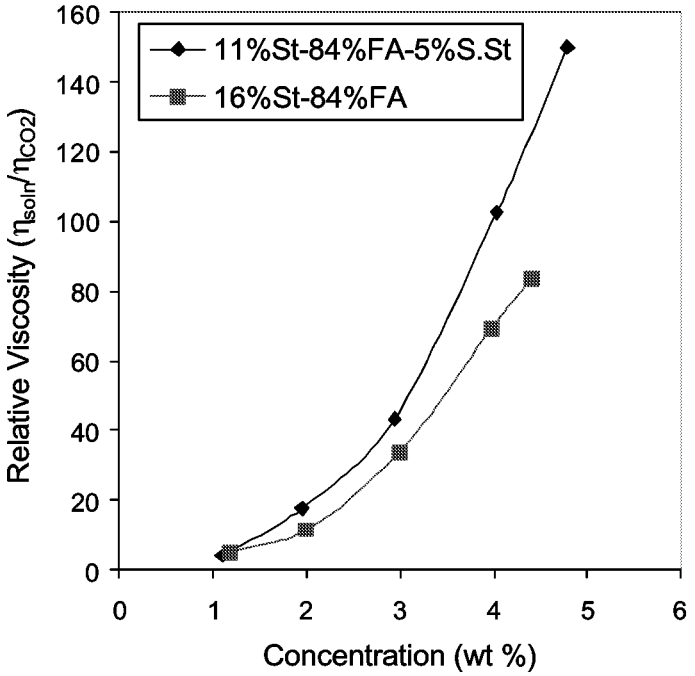

Figure 7.5. Relative viscosity of Sulfonated and Unsulfonated Styrene-Fluoroacrylate Copolymer Solutions in CO_2 as a function of concentration at room temperature at 41.37 MPa (St: Styrene, FA: Fluoroacrylate, S.St: Sulfonated Styrene)

Similar to styrene, aromatic acrylates in the copolymers have also the ability to increase the viscosity of neat CO_2. Degree of increase in viscosity depends on the structure of aromatic acrylate and its content in the copolymer as seen in Fig. 7.6 and Fig.7.7. In both figures, viscosity increases with the addition of aromatic moiety; but after a certain composition, additional increase in the content of aromatic acrylate in the copolymer causes viscosity enhancement to drop down. This result indicates that there is an optimum composition for each type of copolymer. The same effect was observed with Styrene-Fluoroacrylate copolymer previously[xxx].

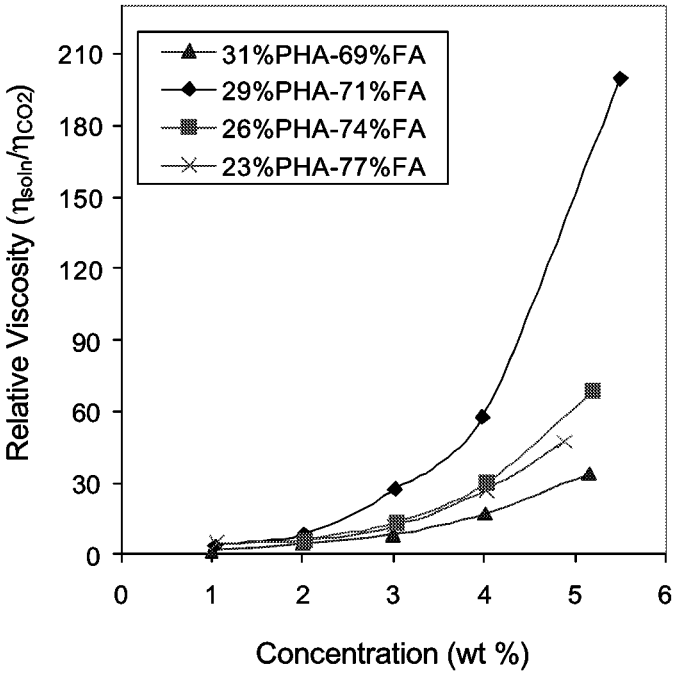

Figure 7.6. Relative viscosity of x%PHA-y%FA copolymer solutions in CO_2 as a function of concentration at room temperature at varying copolymer composition (PHA: Phenyl Acrylate, n=0, m=1; FA: Fluoroacrylate)

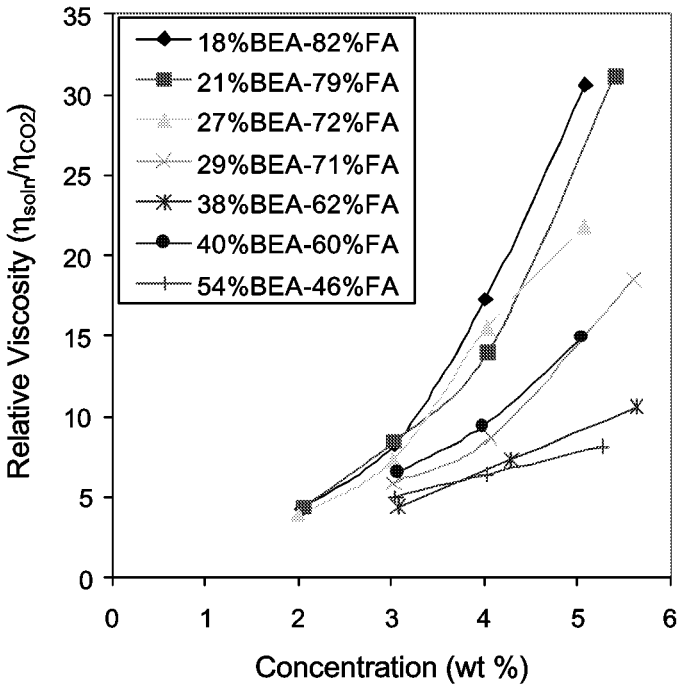

Figure 7.7. Relative viscosity of x%BEA-y%FA copolymer solutions in CO_2 as a function of concentration at room temperature at varying copolymer composition (BEA: Benzyl Acrylate, n=1, m=1; FA: Fluoroacrylate)

Although one can expect that, with increasing content of aromatic acrylates, number of crosslink points increases; however, after this optimum composition, due to CO_2-phobic nature aromatic acrylates, hydrodynamic volume of chains decreases, resulting in intrachain attractive interactions dominate. Then, interaction type becomes mostly intramolecular rather than intermolecular, resulting in lower viscosity enhancement. 29%PHA-71%FA and 18%BEA-82%FA were found as the optimum compositions one can achieve maximum viscosity increment for the corresponding copolymers.

Although we initially thought that by increasing length of spacer unit (number of n), aromatic rings could relax to optimum position to achieve the most proper stacking position, resulting higher increase in viscosity, it was experimentally observed that increasing spacer unit has a reverse effect on viscosity with the copolymers possessing only single aromatic ring (Fig. 7.6, 7.7). We surmise that the difference between anticipated and the actual behavior results from the short range interactions along the chain as a consequence of stretching out of the rings from the main backbone chain by increasing spacer length to make mostly intramolecular association rather than intermolecular. As seen in Figure 7.8, for the same content of fluoroacrylate, the enhancement in viscosity is much superior with the copolymer possessing shorter spacer length.

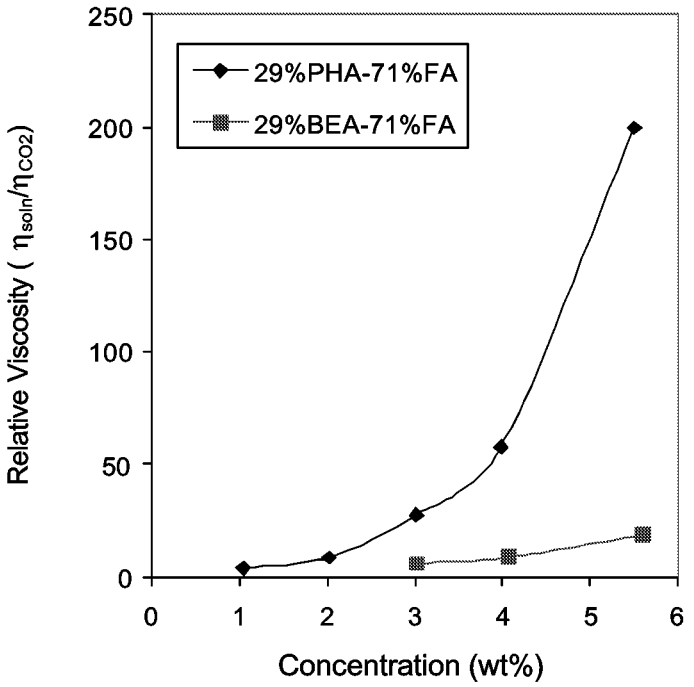

Figure 7.8. Relative viscosity of 29%BEA-71%FA and 29%PHA-71%FA copolymer solutions in CO_2 as a function of concentration at room temperature (BEA: Benzyl Acrylate, n=1, m=1; PHA: Phenyl acrylate, n=0, m=1; FA: Fluoroacrylate)

Hydrodynamic volume of the polymer chain in CO_2 solution is an important parameter determining viscosity enhancement. Increased hydrodynamic volume is an indication of polymer chains are extended out into the solution with the solvent filling the cavities among the chains. At this position, it is much easier for the polymer chains to acquire intermolecular interactions rather than intramolecular. A number of studies have been done investigating the change in polymer conformation driven by solvent density in supercritical fluids[lx,lxi]. Those works indicated that the polymer chains expand as the density of supercritical fluid increases, screening attractive intrachain forces. In other words, solvent quality of CO_2 improves with pressure. This outcome was also reflected in

our results as higher viscosity enhancement at higher system pressures (Fig.7.9 and Fig. 7.10). This result suggests that due to the chain expansion induced by pressure (higher hydrodynamic volume), aromatic rings can do association through more intermolecular way than intramolecular one.

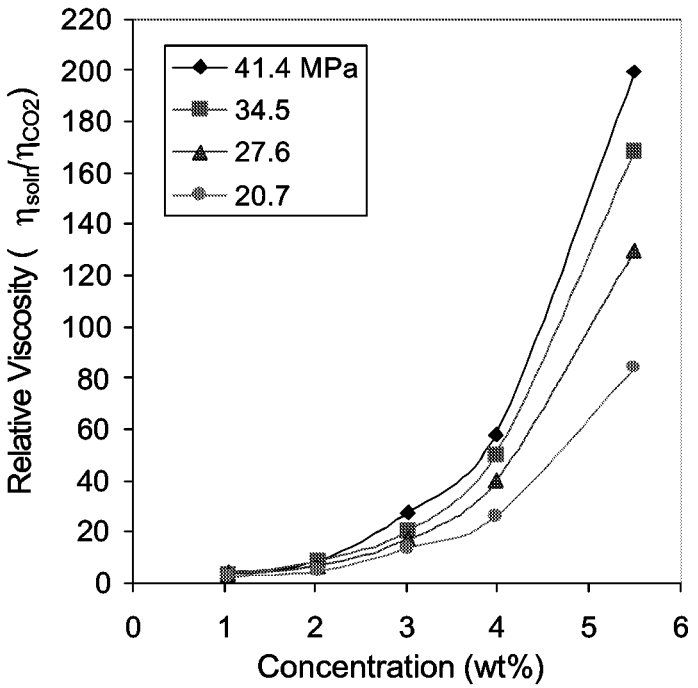

Figure 7.9. Relative viscosity of 29%PHA-71%FA copolymer solutions in CO_2 as a function of concentration at room temperature at varying pressures (PHA: Phenyl Acrylate, n=0, m=1; FA: Fluoroacrylate)

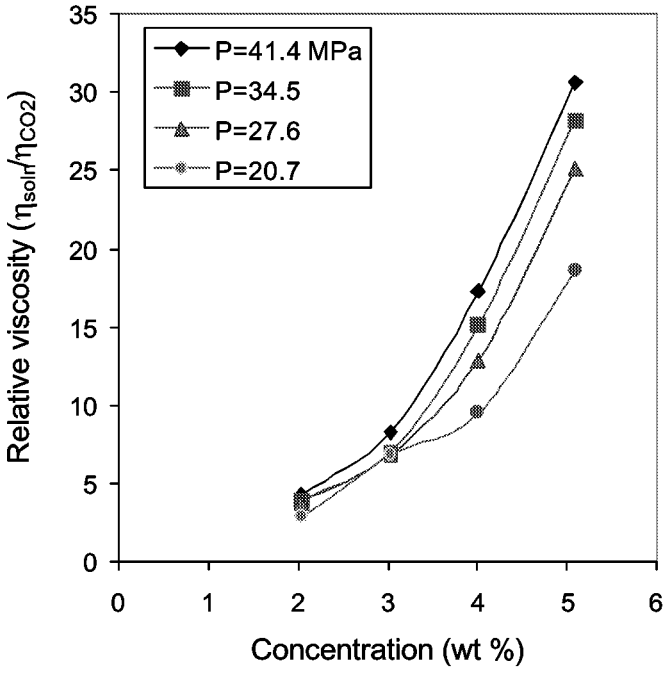

Figure 7.10. Relative viscosity of 18%BEA-82%FA copolymer solutions in CO_2 as a function of concentration at room temperature at varying pressures (BEA: Benzyl Acrylate, n=1, m=1; FA: Fluoroacrylate)

Success in designing effective CO_2 thickeners in our work was arisen from discovering suitable polymer groups that have the ability to associate in CO_2 without being disturbed by the presence of CO_2 molecules, rather forming stable supramolecular structures. As mentioned before, some studies have also been done with the copolymer of fluoroacrylate with non-aromatic acrylates to verify the strength of association of aromatic rings by stacking. Results designated that some sorts of associations also exist between non-aromatic units, but with the results we have at this point, we are unable to draw the general conclusion.

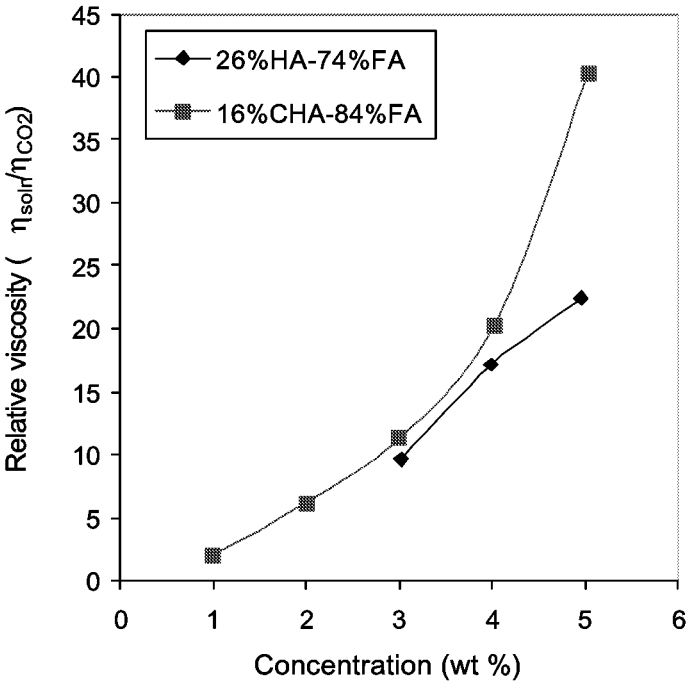

Figure 7.11. Relative viscosity of Copolymers of Fluoroacrylate with Non-Aromatic Acrylates in CO_2 at room temperature as function of concentration (HA: Phenyl Acrylate; CHA: Cyclohexyl Acrylate, n=0, m=1; FA: Fluoroacrylate)

8. Future Work

Present research basically focused on investigation of the effect of copolymers of aromatic acrylate-fluoroacrylate on viscosity of neat CO_2. We proposed to synthesize a series of aromatic acrylate-fluoroacrylate copolymers and evaluate their solubility and viscosity enhancement ability using high-pressure, windowed cell. The change in the series was planned to be created in the aromatic acrylate unit by either changing the spacer length but keeping the aromatic ring(s) constant, or changing the aromatic ring(s) but keeping the spacer length constant.

To date, we investigated the effect of spacer length in the copolymer with a single aromatic ring on solubility and viscosity, and found that spacer length has a reverse effect on viscosity for the copolymers possessing single ring. This result was attributed to short range interaction of the rings along the chain with increasing spacer length to give mostly intramolecular type of association rather than intermolecular. Our aim is specifically to find the copolymer structure (in terms of spacer length and number of aromatic rings) resulting maximum increase in viscosity at minimum concentration in CO_2. Following route (Scheme 8.1) is being suggested for the synthesis of aromatic acrylate monomers to be copolymerized with fluoroacrylate in our succeeding study:

In a typical experiment, a mixture of (THF), alcohol and triethylamine (Et_3N) is put a round bottom flask equipped with a stir-bar. The mixture is maintained at 0 ^{o}C in an ice/water bath under an argon atmosphere.

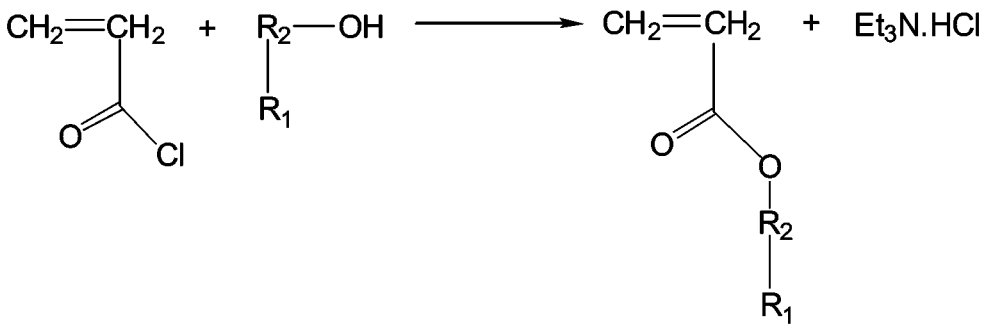

where

R_1: $(Ar)_m$

R_2: $(CH_2)_n$

Scheme 8.1. Reaction route for the synthesis of acrylate monomer.

Acryloyl chloride dissolved in THF is added in a drop-wise fashion to the mixture of alcohol and Et_3N in THF. Upon completion of reaction, product is washed with $NaHCO_3$ to remove the inhibitor in the acryloyl chloride. The product is concentrated on rota-vapor to remove the solvent and excess of reactants. Finally, it is dried over $NaSO_4$.

Above route enables us to synthesize a variety of aromatic acrylate monomers at desired spacer length and having desired number of aromatic rings. To complete this research, a series of aromatic acrylates at varying number of aromatic rings at chosen spacer lengths will be synthesized according to above route, and they will be copolymerized with fluoroacrylate at various compositions. Association strength of aromatic rings by stacking will be verified by synthesizing copolymers analogous to aromatic acrylate-fluoroacrylate copolymers, but in which aromatic unit is only replaced by cycloaliphatic one. At this moment, we believe that stacking of aromatic rings in

solution is a result of delocalization of electrons in the ring structure, and thus electrostatic attractive interactions between the rings. Substitution of the rings with electron-donating or -withdrawing group, and thus change in the electronic structure of the rings would give a new insight to better understanding of stacking process. All synthesized copolymers will be tested in CO_2 for solubility and viscosity using a high-pressure, windowed cell. We also plan to dig out some information about the chain conformation and measure the size using static light scattering technique to evaluate the factors contributing to viscosity enhancement more comprehensively.

In summary, followings are left to complete this research:

1. The effect of number of aromatic rings at chosen spacer lengths on viscosity will be investigated. Different lengths of spacer unit will be examined.
2. Association strength of aromatic rings in the copolymers will be verified with their cycloaliphatic acrylate analogous, in which spacer length and number of rings are kept same as parent aromatic acrylates.
3. The effect of substitution on the electronic structure of the aromatic rings, and thus viscosity will be examined for better understanding of stacking process
4. The effect of polymer chain conformation, size and interactions with the solvent on viscosity will be investigated using static light scattering technique.

Appendix A. Synthesis of Copolymers

A.1. Synthesis of Random Copolymer of Hexyl acrylate with Fluoroacrylate:

3,3,4,4,5,5,6,6,7,7,8,8,9,9,10,10,10-heptadecafluorodecyl acrylate (FA) (97%), and Hexyl acrylate (HA) (98%) were obtained from Aldrich and both monomers were washed with 5% NaOH aqueous solution before use in order to remove inhibitors. The initiator, 2,2'-Azobisisobutyronitrile (AIBN, 98%, Aldrich) was recrystallized from methanol. Solvents, 1,1,2-trichlorotrifluoroethane (TCTFE, 99.8%, Aldrich) and methanol (anhydrous, Aldrich) were used as received.

Copolymerization was carried out by bulk free radical polymerization of fluoroacrylate and hexyl acrylate in the presence of AIBN. A mixture of AIBN (0.0053 g, 0.032 mmol, 0.38 mol % of monomers), HA (0.52 g, 3.33 mmol) and FA (4.11 g, 7.93 mmol) was placed in an ampule. The mixture was purged with N_2 and then, the ampule was flame-sealed. The reaction mixture was kept at 65-70 ^{o}C overnight. The resulted semi-transparent sticky solid polymer was dissolved in TCTFE and precipitated into methanol. The product was purified twice by dissolution in TCTFE and reprecipitation in methanol. After vacuum-oven-dry overnight, copolymer was obtained with 90-95 % yield. General structure of hexyl acrylate-fluoroacrylate copolymer is given in Table 6.1. (a).

A.2. Synthesis of Random Copolymers of Styrene with Fluoroacrylate and its Sulfonation

All reagents, except 95 % sulfuric acid and NaOH pellets (J. T. Baker), were purchased from Aldrich. FA was purified by washing 5% NaOH solution and Styrene (St) was distilled under reduced pressure to remove the inhibitors. AIBN were purified via crystallization from methanol. TCTFE, Methanol (anhydrous), 1,2 dichloroethane, and acetic anhydride (99+%) were used as received.

A random copolymer of fluoroacrylate, styrene, and partially sulfonated styrene is synthesized via a three-step procedure:

a) *Random Copolymerization of Styrene with Fluoroacrylate*

In a typical experiment, styrene (0.49 g, 4.7 mmol), FA (20.44 g, 39.45 mmol) and AIBN (0.0153 g, 0.093 mmol, 0.2 mol % of monomers) were charged to an ampule. The mixture was purged with N_2 and then the ampule was flame-sealed. A white waxy solid was resulted in after overnight polymerization reaction at ~65-70 ^{o}C. Polymer was purified by dissolving in TCTFE and precipitating in a large excess of methanol. After vacuum oven dry overnight, a white polymer was obtained with 95% yield. General structure of styrene-fluoroacrylate copolymer is given in Table 6.1. (b).

b) Sulfonation of Styrene-Fluoroacrylate Copolymer

Partial sulfonation of the phenyl group was performed using acetyl sulfate, prepared according to the procedure reported in literature[lxii,lxiii,lxiv]. For sulfonation, 2.77 g copolymer prepared in the previous step was dissolved in 38 ml TCTFE. The solution

was heated to reflux, after which 0.6 ml of the pre-prepared acetyl sulfate solution was added. When acetyl sulfate was added to the polymer solution, solution acquired a dark green/brown tint. The reaction was allowed to proceed 2 hours under reflux and then terminated by the addition of large amount of methanol. To facilitate the complete removal of residual sulfonating agent from the functionalized polymer, the sulfonated polymer was redissolved in TCTFE and reprecipitated in methanol twice. Then, sample was dried in a vacuum oven overnight.

c) Neutralization of Sulfonated Styrene-Fluoroacrylate Copolymer

To the solution of sulfonated copolymer in TCTFE, added approximately 10 drops of 1 wt % phenolphthalein (indicator). Solution was titrated by 1.0 N NaOH until the end point indicated by a change from colorless to pink. Resulting functionalized ionomer was precipitated in methanol. Polymer was purified several times by dissolving in TCTFE and precipitating in methanol. After drying in vacuum oven overnight, slightly brown tint polymer was obtained. General structure of sulfonated styrene-fluoroacrylate copolymer is given in Table 6.1. (c)

A.3. Synthesis of Random Copolymers of Aromatic Acrylates with Fluoroacrylate

Benzyl acrylate (BEA) and cyclohexyl acrylate (CHA) were obtained from Scientific Polymer Products, Inc., Phenyl acrylate (PHA) was obtained from Lancaster, Inc. and 2-phenylethyl acrylate (PEA) was from Polysciences. Inhibitor in monomers was removed prior to use via inhibitor remover column supplied by the manufacturer.

Polymerization of aromatic acrylates with fluoroacrylate was done by bulk free radical polymerization technique similarly to styrene-fluoroacrylate copolymer.

However, when we run polymerization overnight, we observed that resulting copolymers are insoluble in TCTFE. We applied heat, but it did not help dissolution of the copolymers in TCTFE. We tried to dissolve in various mixtures of organic solvents (tetrahydrofuran, ethyl acetate, dichloromethane, benzene, toluene, cyclohexane, petroleum ether, 3M-perfluorinated ethers, perfluoromethyl cyclohexane, acetone, chloroform) with TCTFE. We also applied heated to these solutions. All our efforts with the hope of acquiring solubility of the copolymers resulted with frustration. We surmise that these overnight-synthesized copolymers are cross-linked. Indeed, bulk free radical polymerization of acrylates does not happen in a fashion to give linear polymer chains, but rather it happens to give branched chains early in the polymerization, crosslinked polymeric structures at higher conversions due to H-abstraction reactions. As stated by several authors, H-abstraction process is not avoidable in any acrylate polymerization at any conversion[lxv,lxvi,lxvii,lxviii]. With the decrease in the concentration of monomer during polymerization, intramolecular H-abstraction reaction starts and goes along with the propagation, and subsequently, with increasing polymer concentration at higher conversions, H-abstraction reaction occurs more intermolecularly. At low conversions, intramolecular H-abstraction causes branching in the polymer chain. At high conversions, propagating branches resulting from intermolecular H-abstraction terminate by combination reaction, causing formation of crosslinked polymer chains. As a consequence of our efforts, we found that polymerization should be stopped prior to a "critical conversion"; otherwise, polymerization results in insoluble, crosslinked gels. What we mean by "critical conversion" is the conversion at which viscosity of polymer solution increases suddenly, and gel effect is observed.

In a typical experiment, say for 18%BEA-72%FA Copolymer, an ampule equipped with stir-bar was flashed with Argon. A known amount of FA (4.5 g, 8.7 mmol), BEA (0.25 g, 1.5 mmol) and AIBN (0.0052 g, 0.11 wt% of monomers) was added. Ampule was flame-sealed and placed in a large oil bath at T=62±1 °C. Polymerization was monitored at all times. At the conversion where gel effect was observed, reaction was stopped by simply quenching the ampule in liquid N_2. Higher conversions yielded insoluble gels. General structure of aromatic acrylate-fluoroacrylate copolymers is given in Table 6.1. (d).

A.4. Synthesis of Random Copolymers of Cyclic Acrylates with Fluoroacrylate

Polymerization was done according to the procedure explained in Section A.3. General Structure of copolymers is given in Table 6.1. (e).

Appendix B. Polymer Characterization

Chemical characterization of the resulting products was accomplished via ^{1}H NMR using Bruker 300 MHz spectrometer. NMR spectroscopy was carried out by dissolving sample in TCTFE in an 8 mm O.D. inner tube, which is then placed in an 10 mm O.D. outer tube containing deuterated chloroform and tetramethylsilane.

References

[i] Fan, E.; Arman, S.A.; Kincaid, S.; Hamilton, A.D. *J.Am. Chem.Soc.* **1993, *115*,** 369.

[ii] Norwick,J.S.; Holmes, D.L.; Noronha, G.; Smith, E.M.; Nguyen, T.M.; Huang, S.-L. *J. Org. Chem.* **1996**, *61*, 3929.

[iii] Andreeti, G.D.; Ori, O.; Ugozzoli, F.; Alfrieri, C., Pochini, A.; Ungaro, R. *J. Inclusion Phenomenon.* **1988**, *6*, 523.

[iv] Carr, A.J.; *Hydrogenbonding Molecules in Medicinal chemistry and material Science.* University of Pittsburgh: Pittusburgh, 1998, pp 205.

[v] Vesovic et. al, *J. Phys. Chem. Ref. Data*, vol. 19, p. 765 (1990)

[vi] Beckman, E. J., Unpublished

[vii] Heller, J. P., Donaruma, L. G., Dandge, D. K., *Poly. Preprints*, vol. 22, p. 59 (1981)

[viii] Heller, J. P., Dandge, D. K. Card, R. J., Donaruma, L. G., *SPE J.*, p. 679, (Oct. 1985)

[ix] Heller, J. P., Dandge, D. K., Card, R. J., Donaruma, L. G., *SPE J.* 11789, p. 173 (1983).

[x] Martin, F., Heller, J. P., PRRC 90-34, Sept. 1990

[xi] Llave, F. M., Chung, F. T. H., Burchfield, T. E., *SPE Reservoir Eng.*, p. 47, Feb. 1990

[xii] Llave, F. M., Chung, F. T. H., Burchfield, T. E., *SPE/DOE* 17344

[xiii] Bae, J. H., Irani, C. A., *SPE J.* 20467, p. 73, Sept. 1990

[xiv] Harris, T., Irani, C., Pretzer, W., US Patent 4,913,235 (1990)

[xv] Irani, C., Harris, T., Pretzer, W., US Patent 4,945,990 (1990)

[xvi] Iezzi, A., Enick. R., Brady, J., *Supercritical Fluid. Sci. Tech., ACS Symp. Series*, p.122 (1989)

[xvii] Hoefling, T. A., Stofesky, D., Reid, M., Beckman, E., Enick, R. M., *J. Supercritical Fl.*, vol. 5, p. 237 (1992)

[xviii] Vikramanayake, R., Turberg, M., Enick, R., Fl. Phase Equil. vol. 70, p. 107 (1991)

[xix] Enick, M., *SPE J.*, 21016, p. 149 (1991)

[xx] Dunn, P., Oldfield, D. J., *J. Macromol. Sci. Chem.,* vol. A4(5), p. 1157 (1970)

[xxi] Iezzi, A., Bendale, P., Enick, R., Turberg, M., Brady, J., *Fluid Phase Equil.* vol. 52, p 307 (1989)

[xxii] Gullapalli, P., Tsau, J., Heller, J. P., *SPE J.* 28979, p. 349 (1995)

[xxiii] Terry, R. E., Zaid, A., Angelos, C., Whitman, D. L., *SPE J.* 16270, p. 289 (1987)

[xxiv] DeSimone, J., Guan, Z., Combes, J., Menceloglu, Y., *Macromolecules*, vol. 26, p. 2663 (1993)

[xxv] DeSimone, J., U.S. Patent 5,496,901 (1996)

[xxvi] DeSimone, J. M. et. al, *Science*, vol. 257, p. 945 (1992)

[xxvii] Guan, Z., DeSimone, J. M., *Macromolecules,* vol. 27, p. 5527 (1994)

[xxviii] McClain, J. B., Betts, D. E., DeSimone, J. M., *Poly. Preprints,* vol. 74, p. 234 (1996)

[xxix] Enick, R. M.; Beckman, E. J.; Shi, C.; Karmana, E., *J. Supercrit. Fl.*, vol. 13, p. 127 (1998)

[xxx] Huang, Z., Shi, C., Xu, J., Kilic, S., Enick, R. M., Beckman, E. J., *Macromolecules*, vol. 33, p. 5437 (2000)

[xxxi] Lee, L. L., *Mol. Thermo. of Nonideal Fluids*, Butterworth Publishers: Stoneham, MA, (1988)

[xxxii] Kirby, C. F., McHugh, M. A., *Chem. Rev.*, vol. 99, p. 565 (1999).

[xxxiii] Prausnitz, J. M., Lichtenthaler, R. N., Azevedo, E. G, *Molecular Thermodynamics of Fluid-Phase Equilibria*, Prentice Hall, Inc. Englewood Cliffs, New Jersey, (1986)
[xxxiv] Guan, Z., DeSimone, J. M., *Macromolecules*, vol. 27, p. 5527 (1994)
[xxxv] Rindfleisch, F., DiNoia, T. P., McHugh, M. A., *J. Phys. Chem.*, vol. 100, p. 15581 (1996)
[xxxvi] Kazarian, S. G. et al., *J. Am. Chem. Soc.*, vol. 118, p. 1729 (1996).
[xxxvii] Van Dijk, M., Wakker, A., *Concepts of Polymer Thermodynamics*, Technomic Publishing Co., Inc., 1997.
[xxxviii] Blanks, R. F., Prausnitz, J. M., *Ind. Eng. Chem. Fundam.*, vol. 3, p. 1 (1964).
[xxxix] O'Neil, M. L., Cao, Q., Fang, M., Johnston, K. P. et. al, *Ind. Eng. Chem., Res.,* vol. 37, p. 3067 (1998)
[xl] Myers, A. L., Prausnitz, J. M., *Ind. Eng. Chem. Fundam.*, vol. 4, p. 209 (1965).
[xli] Luna-Barcenas, G., Mawson, S., DeSimone, J. M., Sanchez, I. C., Johnston, K. P., *Fluid Phase Equil.,* vol. 146, p. 325 (1998)
[xlii] Canelas, D. A., Betts, D. E., DeSimone, J. M., *Macromolecules*, vol. 29, p. 2818 (1996)
[xliii] McClain, J. B., Londono, D., Samulski, E. T., DeSimone, J. M. et. al, *J. Am. Chem. Soc.*, vol. 118, p.917 (1996)
[xliv] Chen, Y., Mays, J., Hadjichristidis, *J. Poly. Sci. Part B: Poly. Phys.,* vol. 32, p. 715 (1994)
[xlv] Charlet, G., Ducasse, R., Delmas, G, Polymer, vol. 22, p. 1190 (1981).
[xlvi] Lepilleur, C., Beckman, E.J., Schonemann, H., Krukonis, V. J., *Fluid Phase Equil.,* vol. 134, p. 285 (1997)
[xlvii] Hunter, C. A., Sanders, J. K. M., *J. Am. Chem. Soc.*, vol. 112, p.5525 (1990)
[xlviii] Desiraju, G. R., *The Crystal as a Supramolecular Entity*, John Wiley & Sons: Chichester, 1995.
[xlix] Cozzi, F., Cinquini, M., Annuziata, R., Siegel, J. S., *J. Am. Chem. Soc.*, vol. 115, p.5330 (1993)
[l] Petsko, G. A., Burley, S. K., *J. Am. Chem. Soc.*, vol. 108, p.7995 (1986)
[li] Gould, R. O., Gray, A. M., Taylor, P., Walkinshaw, M. D., *J. Am. Chem. Soc.*, vol. 107, p.5921 (1985)
[lii] Weber, E., Topics in Current Chemistry: Design of Organic Solids, Springer: Germany, 1998.
[liii] Cozzi, F., Siegel, J. S., *Pure & Appl. Chem.,* vol. 67, p. 683 (1995)
[liv] Kool, E. T. et al., *J. Am. Chem. Soc.*, vol. 118, p. 8182 (1996)
[lv] McClain, J. B., Betts, D. E., Canelas, D. A., Samulski, D. A., DeSimone, J. M., *Poly. Preprints*, vol. 74, p. 234 (1996)
[lvi] Sen, Y. L.; Kiran, E. J.; *J. Supercrit. Fluids*, vol. 3, p. 91 (1990)
[lvii] Sutterby, J. L., *AIChE*, vol. 12, p. 63 (1966)
[lviii] Storey, R. F., Lee, Y., *J. Poly. Sci. Part A: Poly. Chem.,* vol. 31, p. 35 (1993)
[lix] Dougherty, D. A., *Science*, vol. 271, p. 163 (1996)
[lx] Buhler. E., Dobrynin, A. V., DeSimone, J. M., Rubinstein, M., *Macromolecules*, vol. 31, p.7347 (1998)
[lxi] Barcenas, G., Meredit, J. C., Sanchez, I. C., Johnston, K. P., et. al, *J. Chem. Phys.*, vol. 107, p. 10782 (1997)
[lxii] Makowski, H. S., Lundberg, R. D., Singhal, G. H., US Patent 3,870,841

[lxiii] Storey, R. F., Lee, Y., *J. Polym. Sci.: Part A: Poly. Chem*., vol. 31, p. 31 (1993)
[lxiv] Orler, E. B., Yontz, D. J., Moore, R. B., *Macromolecules*, vol. 26, p. 5157 (1993)
[lxv] Azukizawa, M., Yamada, B., Hill, D. J. T., Pomery, P. J., *Macromol. Chem. Phys.*, vol. 201, p.774 (2000)
[lxvi] Yamada, B., Azukizawa, M., Yamazoe, H., Hill, D. J. T., Pomery, P. J., *Polymer*, vol. 41, p.5611 (2000)
[lxvii] Ahmad, N. M., Heatley, F., Lovell, P. A., *Macromol*, vol. 31, p. 2822 (1998)
[lxviii] Britton, D., Heatley, F., Lovell, P. A., *Macromol*, vol. 31, p. 2828 (1998)